Report No. 144

epaResearch
Climate - Water - Sustainability
Identifying pressures • Informing policy • Developing solutions

The Protection of Water Resources: Developing Novel Sensor Materials

Authors: Bernadette Alcock-Earley, Lynn Garry, Conor McCarthy, Carmel Breslin, Denise Rooney

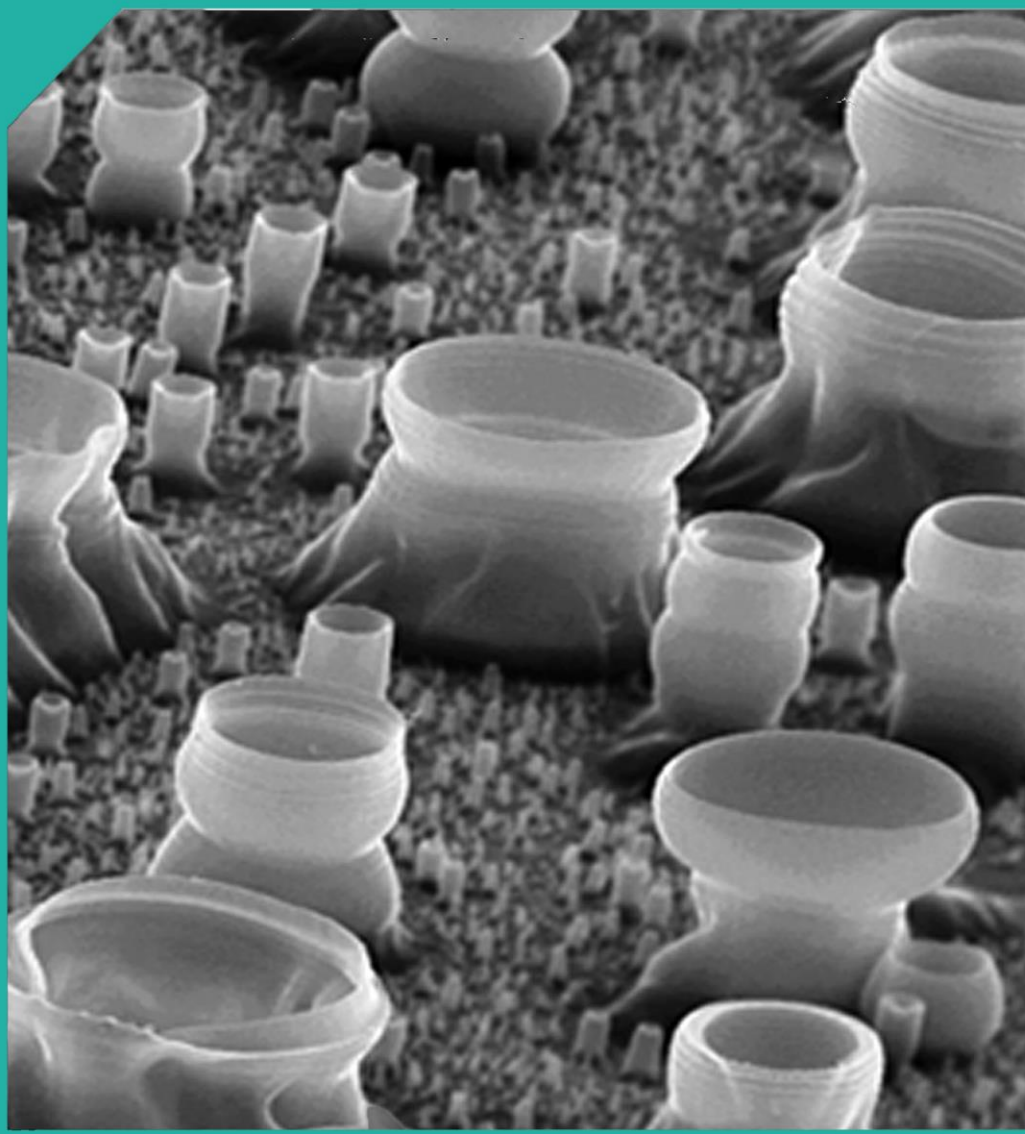

Comhshaol, Pobal agus Rialtas Áitiúil
Environment, Community and Local Government

www.epa.ie

Environmental Protection Agency

The Environmental Protection Agency (EPA) is a statutory body responsible for protecting the environment in Ireland. We regulate and police activities that might otherwise cause pollution. We ensure there is solid information on environmental trends so that necessary actions are taken. Our priorities are protecting the Irish environment and ensuring that development is sustainable.

The EPA is an independent public body established in July 1993 under the Environmental Protection Agency Act, 1992. Its sponsor in Government is the Department of the Environment, Community and Local Government.

OUR RESPONSIBILITIES

LICENSING

We license the following to ensure that their emissions do not endanger human health or harm the environment:

- waste facilities (e.g., landfills, incinerators, waste transfer stations);
- large scale industrial activities (e.g., pharmaceutical manufacturing, cement manufacturing, power plants);
- intensive agriculture;
- the contained use and controlled release of Genetically Modified Organisms (GMOs);
- large petrol storage facilities;
- waste water discharges;
- dumping at sea.

NATIONAL ENVIRONMENTAL ENFORCEMENT

- Conducting over 1200 audits and inspections of EPA licensed facilities every year.
- Overseeing local authorities' environmental protection responsibilities in the areas of - air, noise, waste, waste-water and water quality.
- Working with local authorities and the Gardaí to stamp out illegal waste activity by co-ordinating a national enforcement network, targeting offenders, conducting investigations and overseeing remediation.
- Prosecuting those who flout environmental law and damage the environment as a result of their actions.

MONITORING, ANALYSING AND REPORTING ON THE ENVIRONMENT

- Monitoring air quality and the quality of rivers, lakes, tidal waters and ground waters; measuring water levels and river flows.
- Independent reporting to inform decision making by national and local government.

REGULATING IRELAND'S GREENHOUSE GAS EMISSIONS

- Quantifying Ireland's emissions of greenhouse gases in the context of our Kyoto commitments
- Implementing the Emissions Trading Directive, involving over 100 companies who are major generators of carbon dioxide in Ireland.

ENVIRONMENTAL RESEARCH AND DEVELOPMENT

- Co-ordinating research on environmental issues (including air and water quality, climate change, biodiversity, environmental technologies).

STRATEGIC ENVIRONMENTAL ASSESSMENT

- Assessing the impact of plans and programmes on the Irish environment (such as waste management and development plans).

ENVIRONMENTAL PLANNING, EDUCATION AND GUIDANCE

- Providing guidance to the public and to industry on various environmental topics (including licence applications, waste prevention and environmental regulations).
- Generating greater environmental awareness (through environmental television programmes and primary and secondary schools' resource packs).

PROACTIVE WASTE MANAGEMENT

- Promoting waste prevention and minimisation projects through the co-ordination of the National Waste Prevention Programme, including input into the implementation of Producer Responsibility Initiatives.
- Enforcing Regulations such as Waste Electrical and Electronic Equipment (WEEE) and Restriction of Hazardous Substances (RoHS) and substances that deplete the ozone layer.
- Developing a National Hazardous Waste Management Plan to prevent and manage hazardous waste.

MANAGEMENT AND STRUCTURE OF THE EPA

The organisation is managed by a full time Board, consisting of a Director General and four Directors.

The work of the EPA is carried out across four offices:

- Office of Climate, Licensing and Resource Use
- Office of Environmental Enforcement
- Office of Environmental Assessment
- Office of Communications and Corporate Services

The EPA is assisted by an Advisory Committee of twelve members who meet several times a year to discuss issues of concern and offer advice to the Board.

EPA Research Programme 2014-2020

The Protection of Water Resources: Developing Novel Sensor Materials

2007-DRP-1-S5

EPA Research Report 144

Prepared for the Environmental Protection Agency

by

National University of Ireland Maynooth

Authors:

Bernadette Alcock-Earley, Lynn Garry, Conor McCarthy, Carmel Breslin, Denise Rooney

ENVIRONMENTAL PROTECTION AGENCY
An Ghníomhaireacht um Chaomhnú Comhshaoil
PO Box 3000, Johnstown Castle, Co.Wexford, Ireland

Telephone: +353 53 916 0600 Fax: +353 53 916 0699
Email: info@epa.ie Website: www.epa.ie

ACKNOWLEDGEMENTS

This report is published as part of the EPA Research Programme 2014-2020. The programme is financed by the Irish Government. It is administered on behalf of the Department of the Environment, Community and Local Government by the Environmental Protection Agency which has the statutory function of co-ordinating and promoting environmental research.

EPA RESEARCH PROGRAMME 2014-2020

Published by the Environmental Protection Agency, Ireland

Front page image - Scanning Electron Microscopy micrograph of polymer microtubule

ISBN: 978-1-84095-581-1

Details of Project Partners

Bernadette Alcock-Earley
Research carried out at:
Department of Chemistry,
National University of Ireland Maynooth,
Maynooth,
Co. Kildare

Current contact details
Tel.: +353 86 845 3660
E-mail: Ber.AlcockEarley@gmail.com

Lynn Garry
Department of Chemistry,
National University of Ireland Maynooth,
Maynooth,
Co. Kildare
Tel.: +353 1 708 6856
E-mail: Lynn.Nifhearraigh@nuim.ie

Conor McCarthy
Department of Chemistry,
National University of Ireland Maynooth,
Maynooth,
Co. Kildare
Tel.: +353 1 708 6856
E-mail: Conor.McCarthy@nuim.ie

Carmel Breslin
Department of Chemistry,
National University of Ireland Maynooth,
Maynooth,
Co. Kildare
Tel.: +353 1 708 3677
E-mail: Carmel.Breslin@nuim.ie

Denise Rooney
Department of Chemistry,
National University of Ireland Maynooth,
Maynooth,
Co. Kildare
Tel.: +353 1 708 3616
E-mail: Denise.Rooney@nuim.ie

Table of Contents

Executive Summary

One of the more pressing challenges in the 21st Century is the provision of an adequate clean water supply that is free from pollutants and suitable for a diversity of uses. Although the quality of water in Ireland is generally good, the protection of water resources in Ireland is becoming increasingly important and will be a major challenge in the next few years and into the future, as an ever-increasing population will need a continuous supply of clean drinking water. The protection of the quality of water resources and the sustainability of these resources are key environmental goals in the Environmental Protection Agency 2020 Vision (EPA, 2000) strategy document, and are also in line with the Flagship initiative of the Europe Union Commission (European Commission, 2011) strategy for a resource-efficient Europe. The research described herein sets out to develop polymer-coated, membrane-based technologies that could be used to detect organic contaminants, nitrates or heavy metals, namely chromium and copper, in aqueous systems. The membranes were modified so as to investigate their potential in the required sensing capacity.

In recent years, there has been considerable concern about the level of nitrate in water. This is highlighted by the Nitrates Directive (1991/676/EEC), the EU Water Framework Directive (2000/60/EC) and related legislation.

The novel electrochemical deposition of poly[N-(2-cyanoethyl)pyrrole] (PPyEtCN) into nanowire and microtube morphologies was investigated and is reported here. Cyclic and pulsed electrochemical techniques were employed to electrodeposit copper micro and nano particles at PPyEtCN and polypyrrole (PPy) surfaces. A PPy nanowire/copper-modified electrode was investigated for its effectiveness as an electrochemical sensor for the detection of the nitrate ion. PPy nanowire films were successfully electrochemically synthesised and modified with copper, with good reproducibility. These nanocomposites were then tested for use in the detection of nitrate through electroreduction of the ion. It was found that the sensitivity of the nanocomposite was not as low as required, however, its stability allowed for slower degradation of the nitrate reduction signal, suggesting that these electrodes may be suitable for long-term sensing systems, where longevity rather than sensitivity is required.

The Water Framework Directive clearly outlined a requirement that the levels of Cr(VI) and Cu(II) in Irish water be monitored. Electrochemical sensors were designed and investigated for their potential use in the detection of metal ions in aqueous solutions. Chromium commonly exists in either its hexavalent (Cr(VI)) or trivalent (Cr(III)) form. Chromium (VI) is a highly toxic metal ion that is well known for its contribution to a variety of health problems, such as cancers and chronic dermatitis. It is widely used in industries, such as tanning, stainless steel production and metal finishing, and may be leached into groundwater. Chromium can readily be transported in soil, and leached into water bodies far from the original sites of contamination, so its removal from industrial waste to within the regulatory limits is vital. Copper is generally found in its divalent or monovalent form. Ingested in relatively high concentrations, it can induce symptoms of severe food poisoning; long-term exposure can result in damage to the liver and kidneys, and is also linked to Alzheimer's disease. It is toxic to fish and aquatic life with high levels of bioaccumulation. Copper is often used in electrical and plumbing systems and is known to

corrode under certain circumstances, resulting in leaching into soils and water sources. Copper is also a waste product of a number of industries, such as electroplating. The European Communities (Drinking Water) (No. 2) Regulations 2007 set out a mandatory limit in drinking water of 50 μg L^{-1} chromium and 2 mg L^{-1} copper.

Glassy carbon electrodes (GCEs) were modified with graphene or multi-walled carbon nanotubes (MWCNTs) and their ability to detect the electrochemical reduction of Cr(VI) was investigated. It was found that a MWCNTs modified glassy carbon electrode could be used. Although it would appear that simple modification of an electrode with MWCNTs can be used to detect Cr(VI), there are problems with its limit of detection (LOD). By modifying the MWCNTs with gold nanoparticles (AuNPs), enhanced detection of Cr(VI) was observed.

A platinum (Pt) mesh was modified with the diethyl-dithiocarbamate (DDC) ligand and immobilised in a Nafion film, and its oxidation to DSF was investigated as a possible copper (Cu) sensor. The resulting modified electrode could be used as a simple sensor for the detection of Cu(II) ions in solution, and a detection limit of 5.40×10^{-5} M was determined using cyclic voltammetry. Preliminary investigations suggested that the sensitivity of the electrode may be enhanced by introducing MWCNTs into the film. However, there were problems with the reproducibility of this modified electrode, as variable amounts of MWCNTs incorporated into each DDC/Nafion film formed.

The investigation and development of an electrochemical system to remediate organic contaminants was carried out using a working electrode modified with polypyrrole (PPy) doped with sulfonated β-cyclodextrin (sβ-CD). The aim of the research was to form an inclusion complex between the cyclodextrin immobilised in the polypyrrole film and the organic contaminant. This would allow for detection and the possible subsequent remediation of the targeted organic contaminant.

Initial studies were carried out on phenol and chlorophenols. However, as there was no evidence of an inclusion complex being formed, further investigation into the possible use of PPy-sβCD was carried out. Atrazine was chosen as a sample herbicide as, although it was banned in the EU in 2004, it is still widely used in the US and Australia, and is strongly persistent in the aqueous environment. It was therefore chosen as a model herbicide for this study. Unfortunately, there was no evidence of detection of atrazine and therefore it is unlikely that an inclusion complex is being formed.

Acetaminophen or paracetamol is a widely-used, over-the-counter analgesic and antipyretic. Cyclic voltammetry measurements indicated good stability of both the film and the interaction of the acetaminophen and cyclodextrin. Complexation between acetaminophen and sβ-CD was determined using UV-vis spectroscopy and cyclic voltammetry, while the Job's method was employed to distinguish the stoichiometric value of the complex, with evidence that a 1:1 acetaminophen:sβ-CD complex stoichiometry exists. When the influence of concentration of acetaminophen was investigated, it was found that there was no clear linear relationship between concentration and the oxidation peak current, especially at higher concentrations. This may be due to the formation of phenoxy radicals during oxidation of acetaminophen. These radicals can then polymerise and cause faster passivation of the electrode surface.

1. Introduction

It is reported in the fifth 'State of Environment' EPA report Ireland's Environment 2012 – An Assessment (O'Lehane and O'Leary, 2012), that Ireland has better-than-average water quality in comparison to other EU member states. However, it is evident that Ireland faces major challenges in meeting targets set for 2015, 2021 and 2027, as required by the Water Framework Directive. A key priority of the Strategic Plan 2013–2015 (EPA, 2013) is to maintain a relevant environmental research programme to influence policy, identify pressures and develop solutions to key environmental challenges. The EU Joint Programming Initiative 'Water Challenges for a Changing World' is a strategic initiative to pool national research resources of member states in this important area. In addition, the support of research into nanotechnologies will enable Ireland to benefit from the growth forecasted for the economic impact of these technologies, as highlighted by the report Ireland's Nanotechnology Commercialisation Framework 2010–2014 (Forfás, 2010).

The three projects involved in this research were concerned with the formation of new materials that could possibly be used in environmental sensing applications and/or have potential applications in environmental remediation. These novel materials consisted of modified conducting polymer films. Conducting polymers have attracted much interest because of their electronic, electrochemical and optical properties. These polymers were used in all three projects and served as a platform technology. The polymers were synthesised as nanostructures and/or modified with metallic nanoparticles, carbon nanotubes or macrocyclic cages, so that the materials were capable of sensing and/or remediation of nitrates, heavy metals and organic contaminants. These modifications were carefully selected to ensure that the final materials will have the required sensing or remediation capacity. Initially, polypyrrole films were used, as polypyrrole is one of the most important conducting polymers because of its facile preparation and good stability. Other conducting polymers, such as Nafion and poly(N-(2-cyanoethyl)pyrrole), were also employed.

The research topic dealing with the design of nanomaterials by employing electrochemical techniques has developed rapidly in the last decade (Bedioui et al., 2012; Jiao et al., 2012; Singh et al., 2013). This is due to a strong understanding of the electrochemical processes that occur at electrode surfaces, which enables fabrication of a range of nanomaterials (Paunovic and Schlesinger, 2006). These materials have wide technological importance, as the various compositions and morphologies have applications in areas such as solar cells, memory, and sensor devices (Dong et al., 2013; Kois et al., 2013; Kumar et al., 2012; Veloso et al., 2012). Furthermore, employing nanostructured materials has led to increases in efficiencies compared to the typical 'bulk' materials (Oja et al., 2013). In the field of polymer science, nanomaterials have proven to be attractive candidates as electrochemical sensors, due to the higher sensitivities and faster redox chemistry they can achieve (Oja et al., 2013). For this reason, the development of novel, facile and template-free methods to produce polymeric and metallic nanomaterials is a research goal with strong merit and importance. The fundamental processes involved in electrodepositing polypyrrole (PPy) are discussed, in terms of the structural and

electronic characteristics. This is followed by analysis of the most relevant and up-to-date literature accounts relating to PPy nanostructuring, particularly focusing on nanowires and hollow microtubes/containers. Similarly, the latest developments within the fields of substituted PPy and copper electrodeposition are discussed, with reference to the most significant work in the literature. The objectives of this research was to firstly develop a means of fabricating novel morphologies of the functionalised poly[*N*-(2-cyanoethyl)pyrrole] (PyEtCN) monomer. The growth of PPyEtCN nanowires is investigated, with the aim of controlling the morphology by a template-free method. This work is extended to developing an emulsion polymerisation solution to grow various hollow morphologies of PPyEtCN. Secondly, pulsed and cyclic electrochemical techniques were investigated for their ability to control the electrodeposition of copper microparticles at polypyrrole (PPy) surfaces for nitrate sensing. These electrodeposition techniques were also attempted at the novel PPyEtCN polymers.

2. Results and Discussion

2.1 Development of Macrocyclic Cages Encapsulated in Conducting Polymer Matrices for the Detection of Organic Contaminants

2.1.1 Introduction

The goal of the project outlined in this report was to investigate and develop new environmental technologies suitable for pollution detection and possible remediation, based on the formation of an electrochemical sensor consisting of polypyrrole (PPy) doped with sulfonated β-cyclodextrin (sβ-CD). Among the various conducting polymers, polypyrrole is one of the most frequently investigated (Maksymiuk, 2006). This is due to its ease of preparation by electropolymerisation, relative stability compared to other conducting polymers, and the ready commercial availability of many of its derivatives. Polypyrrole (PPy) is synthesised from the monomer pyrrole (Py). As with other organic molecules, polymerisation occurs upon oxidation of the monomer. A conjugated polymer chain with overlapping π-orbitals and a positive charge along the backbone forms as a result of oxidation. The use of PPy has many advantages, including its large surface area owing to its fibrous structure and, thus, is a high-capacity electrode material. Furthermore, the ease of preparation, inherent electrical conductivity, high stability in air and aqueous media make PPy a promising interfacial material. Cyclodextrins are naturally occurring macrocyclic oligosaccharides built from α-1,4-linked D-glucopyranose units. The most common and readily available cyclodextrins are the α, β and γ-cyclodextrins. These cyclodextrins are composed of six, seven and eight glucopyranose units respectively. Cyclodextrins are well known to bind with suitable guest molecules in aqueous solutions to form inclusion complexes. The formation of such inclusion complexes occurs without the formation of any covalent bonds, nor are any covalent bonds broken (Valle, 2004). In general, the inclusion complex formed between a cyclodextrin (CD) and a guest molecule (D) is a 1:1 association. The formation of cyclodextrin complexes in aqueous solutions has been studied intensively using a variety of electrochemical and spectroscopic techniques, including nuclear magnetic resonance (NMR) (Bernini et al., 2004), UV-vis spectroscopy (Dang et al., 1998), cyclic voltammetry (CV) (Ibrahim et al., 2002) and rotating disc voltammetry (Coutouli-Argyropoulou et al., 1999). Cyclodextrins will alter the electrochemical and spectral behaviour of the guest molecule if an inclusion complex is formed. Initially, compounds were tested for detection by PPy-sβCD and, if this proved successful, then further studies into remediation would be carried out.

2.1.2 Development and Characterisation of the Polypyrrole Sulfonated β-Cyclodextrin Modified Electrode

Experiments were carried out to investigate how the growth of the PPy-sβCD films were affected, by varying the concentration of the pyrrole monomer, the concentration of sulfonated β-cyclodextrin, the applied potential and the working electrode. In addition, the presence of a supporting electrolyte in the monomer solution was also explored to see the effect it had on the growth of the PPy-sβCD film. Initially, studies looked at the effect of varying the applied polymerisation potential on the polymer growth. The concentration of pyrrole and sβ-CD were kept constant at 0.2 and 0.01 M respectively and polymerisation took place at the platinum working electrode. As expected, the time taken for the polymer to reach the required film thickness decreases significantly with increasing

polymerisation potential, from 0.6 to 0.8 V (Figure 1a). These data are in good agreement with literature reports on other dopants, indicating that the sβ-CD to some extent acts in the same manner as more traditional dopants used during electropolymerisation. All further polymerisations were carried out at 0.6 V in the presence of 0.2 M pyrrole and 0.01 M sβ-CD, unless otherwise stated. As can be seen in Figure 1b, polymerisation under these conditions was very reproducible.

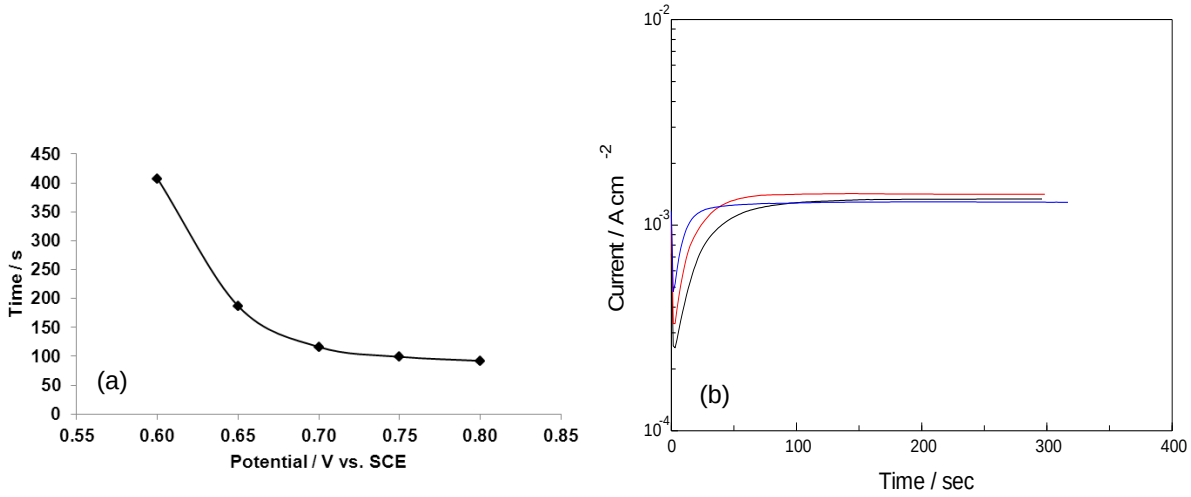

Figure 1. (a) Electropolymerisation time required to reach the required film thickness as a function of the applied potential. The PPy-sβCD films were grown from a monomer solution containing 0.20 M pyrrole and 0.01 M sulfonated β-cyclodextrin. (b) Current time transient for the deposition of PPy-sβCD at 0.6 V from a monomer solution containing 0.20 M pyrrole and 0.01 M sulfonated β-cyclodextrin.

SEM measurements (Figure 2a) showed that the PPy-sβCD film exhibits a 'cauliflower' morphology typically seen for PPy films. However, its morphology seems to be more structured and organised and this is not normally observed with a characteristic PPy film. Energy dispersive X-ray (EDX) measurements (Figure 2b) were subsequently performed and confirmed the presence of sulphur, which can only correspond to the incorporation of the sβ-CD anions during electrochemical synthesis, as no other supporting electrolyte was used.

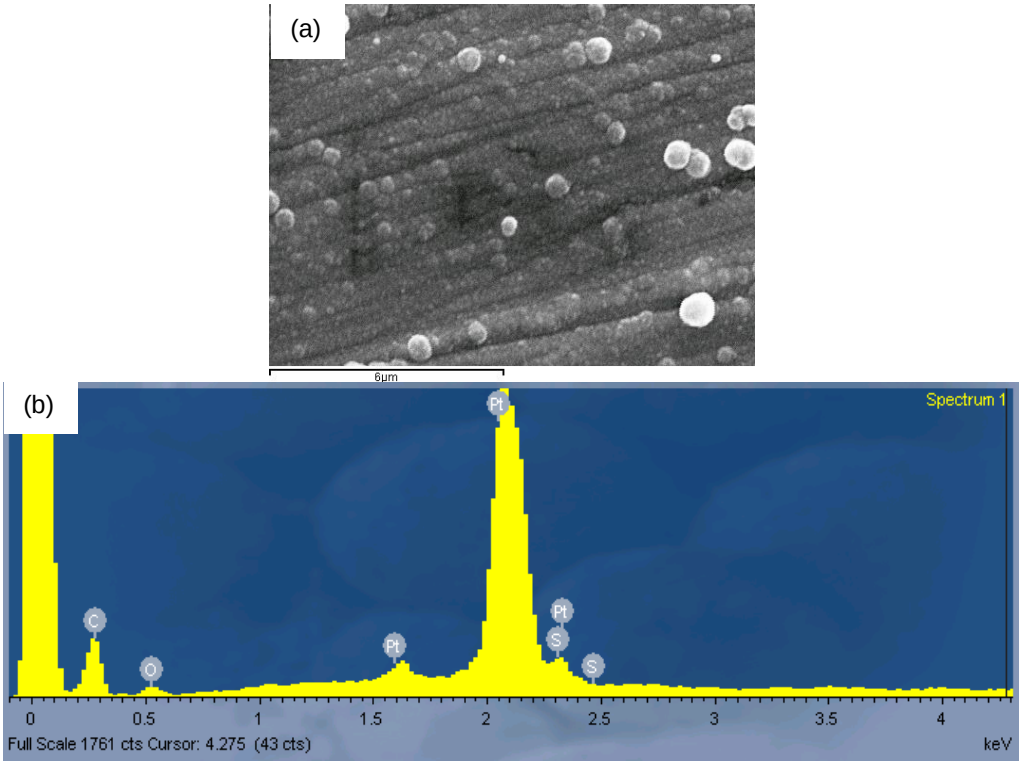

Figure 2. (a) SEM micrograph of a PPy-βSCD film electrosynthesised at 0.6 V from a monomer solution containing 0.2 M pyrrole and 0.01 M sulfonated β-cyclodextrin. (b) EDX spectra of PPy-sβCD film.

By assuming that the sβ-CD are doping the PPy film at the electroactive centres, then the surface coverage will result in an estimation of the number of sβ-CD molecules distributed within the PPy film. An estimation of the surface coverage of the electrode was made using Equation 1, where Γ is the surface coverage of electroactive centres (mol cm^{-2}), n represents the number of electrons involved in the reaction, F is the Faraday constant (C mol^{-1}), A is the surface area of the electrode (cm^2) and Q is the total amount of charge calculated from the integration of the oxidation peak of PPy-sβCD recorded using cyclic voltammetry. By using the oxidation peak charge calculated by integration, the surface coverage was estimated at 2 x 10^{-9} mol cm^{-2}.

$$\Gamma = \frac{Q}{nFA} \qquad \text{Equation 1}$$

A large background current was observed in the cyclic voltammograms, indicating that the polymer was exhibiting a high charging capacitance. By using Equation 2, the capacitance was calculated for the PPy-sβCD film and compared to that calculated for a PPy film doped with Cl$^-$ ions (PPy-Cl). Both films were polymerised under the same conditions.

$$C = \frac{I}{dV/vt} \qquad \text{Equation 2}$$

C is the capacitance (F cm^{-2}), I is the current density (A cm^{-2}) and dV/vt is the scan rate (V s^{-1}) (Patake et al.. 2009). The capacitance of the PPy-sβCD film was found to be 1.84 x 10^{-3} F cm^{-2}, while it was 1.3 x 10^{-4} F cm^{-4} for PPy-Cl. These high values are typical of the capacitance recorded for conducting polymers. The fact that the capacitance of the PPy-sβCD film is higher than that of the PPy-Cl film indicates that considerably more negative charge is being stored in the film and, as a result, more cations will be attracted to the film surface.

2.1.3 Phenol and 3-Chlorophenol

Phenol is produced on a large scale from petroleum. It is an important commodity as a

precursor to many materials and compounds. The primary use of phenol is in the production of phenolic resins used in plywood. Along with its derivatives, it is widely distributed in the environment and can be found as components of detergents, herbicides and numerous pharmaceutical drugs. Chlorophenols are used as herbicides and pesticides. Their chemical stability and high resistances to biological degradation cause them to be a serious risk to the environment.

In order to determine the most stable working electrode substrate, the oxidation of phenol and 3-chlorophenol was carried out at unmodified, gold, platinum and glassy carbon electrodes. All three substrates gave a similar response, with an oxidation peak centred at approximately 1.0 V (Figures 3a and 3b). As can be seen in Figures 3c and 3d, all three substrates showed a large initial drop in peak current between cycles 1 and 2, with the peak current observed at the platinum substrate remaining stable in subsequent cycles. The gold and glassy carbon substrates also showed a marked decrease in peak current between the first two cycles, however, unlike platinum, the peak currents continued to decrease.

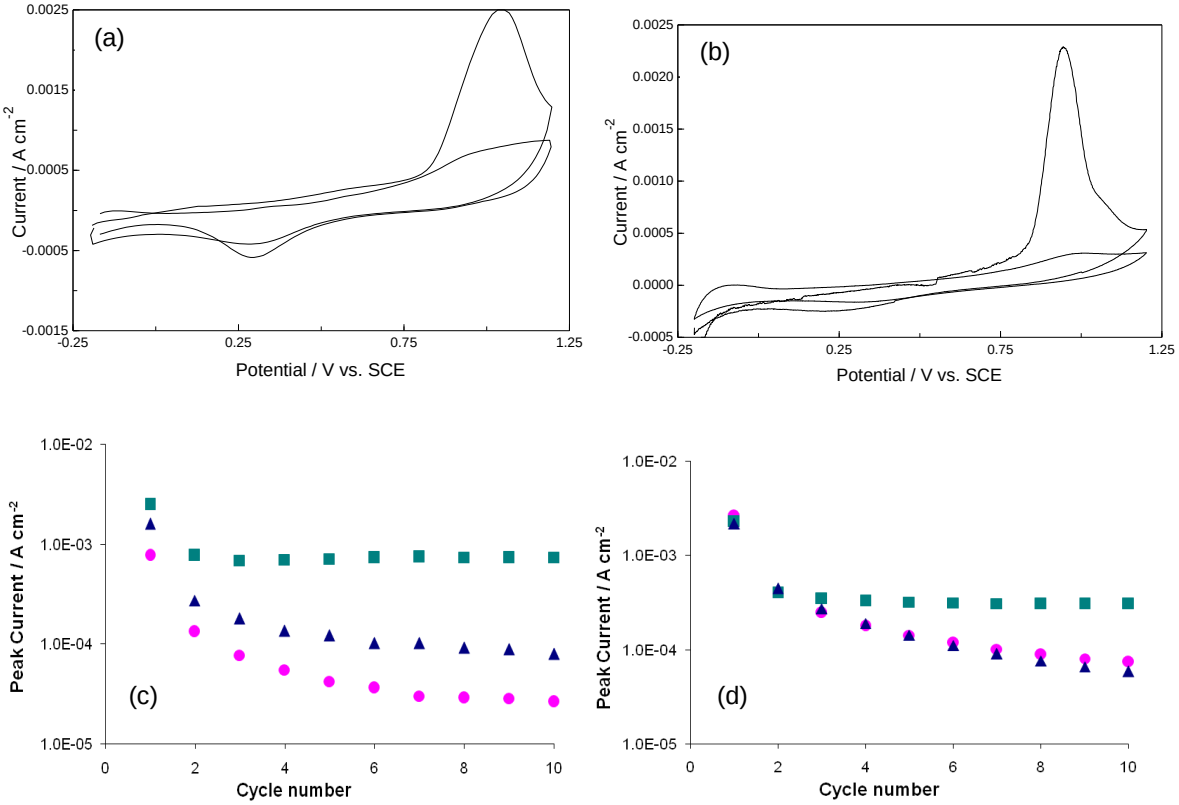

Figure 3. Cyclic voltammograms of the oxidation of (a) 0.0125 M Phenol and (b) 0.0125 M 3-Chlorophenol at an unmodified platinum working electrode, showing cycles 1 and 10. The effects of cycle number on peak current at unmodified ■ platinum, ● gold and ▲ glassy carbon for the oxidation of (c) 0.0125 M Phenol (d) 0.0125 M 3-Chlorophenol.

The observed decreases in peak current are indicative of fouling of the electrode surface. This may be due to the fact that higher phenol concentrations allow for the formation of greater amounts of phenoxy radicals, which then polymerise and cause faster passivation of the electrode surface. In the first step in the oxidation of phenols, phenoxy radicals are formed. These can then either be oxidised further or be coupled forming ether and quinone type oligomeric and

polymeric compounds. Formation of the insoluble polyphenol results in deactivation of the electrode surface (Gattrell and Kirk, 1993). It was hoped that by modifying the more stable platinum substrate with PPy-sβCD, this fouling and deactivation of the electrode would be minimised. The PPy-sβCD was polymerised, as previously described in Section 2.1.2, at a platinum working electrode. The modified electrode was then transferred to a phenol solution. Oxidation of 0.0125 M phenol was carried out in 0.1 M H_2SO_4 by cycling the potential between -0.2 and 1.2 V. Oxidation of 3-chlorophenol was carried out under similar conditions but the electrolyte was changed from sulphuric acid to Britton-Robinsons buffer, in order to increase the reproducibility. In order to reduce the possibility of fouling of the electrodes surface, 0.1% w/v of the surfactant sodium dodecylsulfate (SDS) was added. As can be seen in Figures 4a and 4b, oxidation of phenol and 3-chlorophenol at PPy-sβCD was observed, with a peak centred at approximately 1.0 V. Again, the stability of the electrode was monitored by observing the oxidation peak current over continued cycling (Figures 4c and 4d). While the peak currents remained higher than those observed at the unmodified electrode, there was still a significant decrease in oxidation current, suggesting instability and continued, although lower, fouling of the electrode.

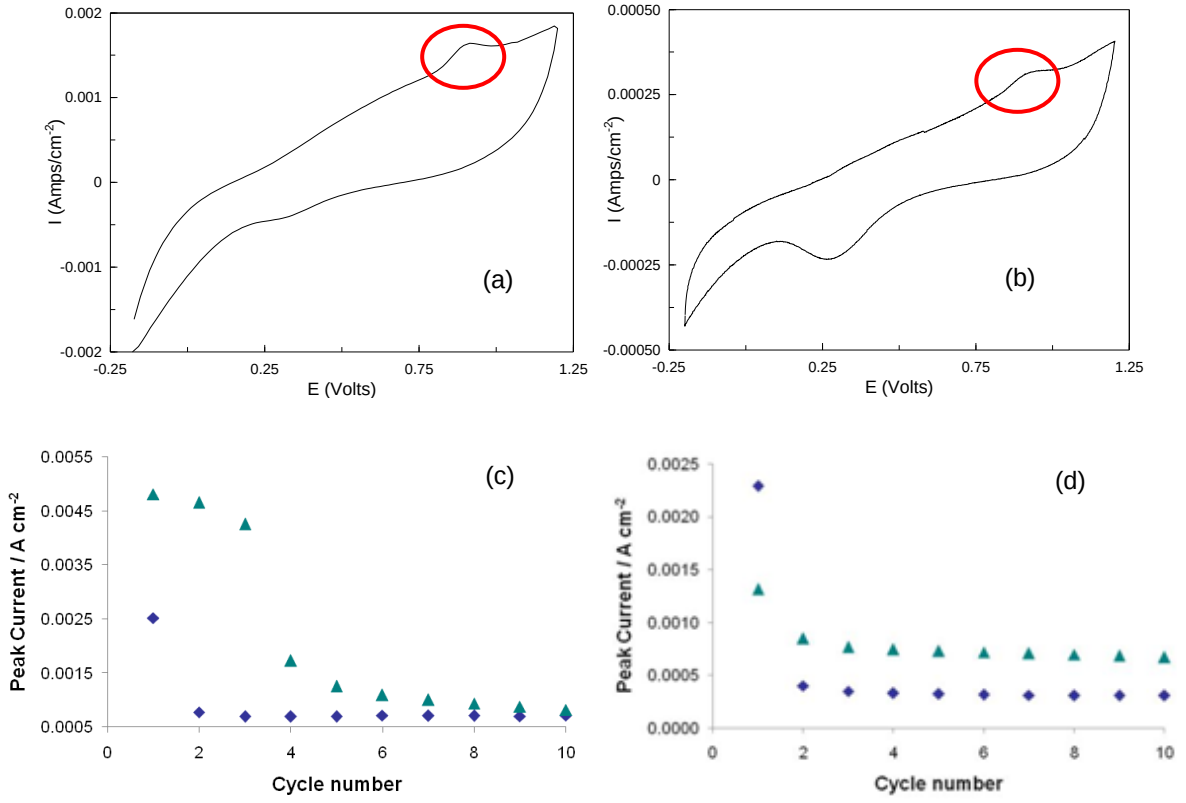

Figure 4. (a) Oxidation of 0.0125 M Phenol in 0.1 M H_2SO_4 with 0.1% w/v sodium dodecylsulfate and (b) Oxidation of 0.0125 M 3-chlorophenol in 0.04 M pH 2 Britton-Robinsons Buffer with 0.1% w/v sodium dodecylsulfate. The effects of cycle number on peak for the oxidation of (c) 0.0125 M Phenol (d) 0.0125 M 3-chlorophenol at ▲ PPy-sβCD and ♦ unmodified platinum.

Unfortunately, when the influence of phenol or 3-chlorophenol concentration was investigated, it was found that there was no clear linear relationship between concentration and the oxidation peak current (Figures 5a and 5b). This was particularly evident at higher concentrations, possibly due to the presence of higher phenol concentrations allowing the formation of greater amounts of phenoxy radicals which polymerise and cause faster passivation of the electrode surface. It was found that the lowest concentration that could comfortably be observed using cyclic voltammetry was 0.01 M phenol or 3-chlorophenol.

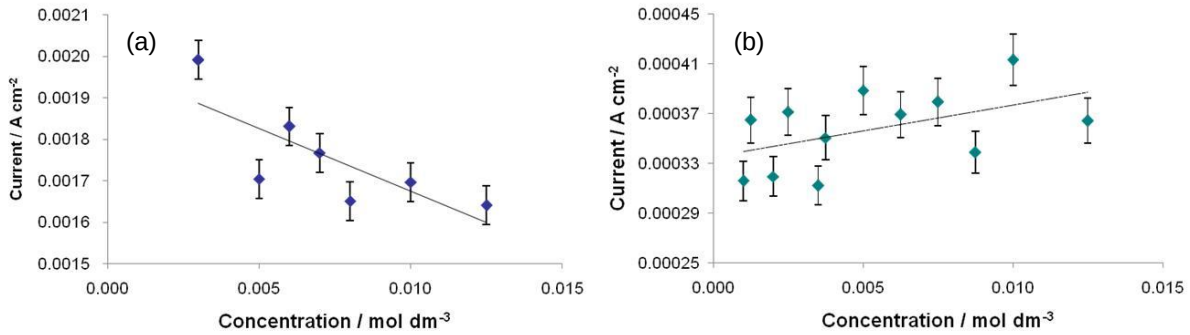

Figure 5. Influence of concentration on the oxidation of (a) phenol and (b) 3-chlorophenol at PPy-sβCD.

When the influence of dopant was investigated, it was found the phenol or 3-chlorophenol were only oxidised in the presence of the sβ-CD dopant. This would suggest that there was some interaction between the phenol or 3-chlorophenol and the sβ-CD. In order to determine if an inclusion complex is being formed, ^{1}H nmr was carried out. ^{1}H NMR spectroscopy is one of the most powerful techniques for examining host-guest chemistry in solution. It can provide complete information on the stoichiometry, binding constant, orientation and geometry of a host-guest interaction. Here, ^{1}H NMR was used to investigate the manner in which the phenol or 3-chlorophenol was included inside the cavity of the sβ-CD. This was achieved by monitoring the environment of the individual atoms and the complex. The samples were prepared by dissolving 5.0 x10^{-3} M phenol or 3-chlorophenol in the presence or absence of 2.0 x 10^{-2} M sβ-CD in 0.5 mL of D_2O (99.72%) / 0.10 M NaCl. The NaCl was employed to maintain a near-constant ionic strength. Figures 6a and 6b show the ^{1}H NMR of phenol and 3-chlorophenol in the presence and absence of the sβ-CD. The shift in the signal observed upon addition of the β-CD is tiny, and while it suggests that there is some interaction between the phenols and the β-CD, this interaction is most probably due to phenols being in weak steric interactions and not evidence of a strong inclusion complex being formed.

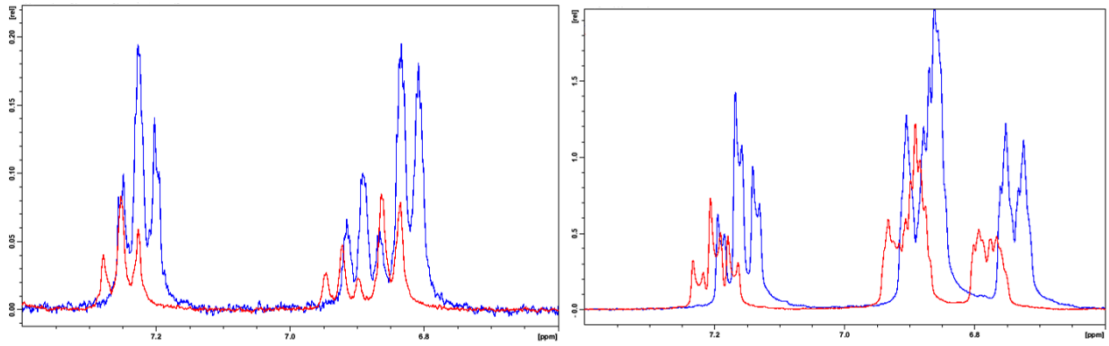

Figure 6. ^{1}H NMR of (a) phenol and (b) 3-chlorophenol in the presence of ——NaCl and —— NaCl and sβ-CD.

Due to the poor reproducibility of these results and no evidence of an inclusion complex being formed, further investigation into the possible use of PPy-sβCD in the remediation of phenol and phenol derivatives was not carried out.

2.1.4 Atrazine

Atrazine is a triazine herbicide used to stop pre- and post-emergence broadleaf and grassy weeds in major crops by binding to the plastoquinone-binding protein in photosystem II, inhibiting electron transport. While it was banned in the EU in 2004, it is still widely used in the US and Australia and is strongly persistent in the aqueous environment, and was therefore chosen as a model herbicide for this study. Although the toxicological effect of atrazine on humans is lower than that of other pesticides, such as organophosphates, severe environmental problems result from its persistence in soils and sediments as well as from run-off to surface and ground water. It is highly toxic to phytoplankton and freshwater algae and, as it is soluble in water, it can easily contaminate aquifers. It is a potential endocrine disruptor and has been shown to alter the natural hormonal system in animals.

According to Pospíšil et al. (1995), a reduction wave corresponding to a diffusion-controlled, two-electron process is observed in cyclic voltammograms of atrazine carried out in acid solutions of pH 2 to 1. As can be seen from the reaction mechanism in Figure 7, a cationic species (circled) is formed at low pH during reduction. As the cyclodextrin incorporated into the polypyrrole film is anionic, in order to ensure electrostatic interactions, it is necessary for the species, which are to be detected by the cyclodextrin, to be cationic or neutral. This mechanism proposed suggests that if the PPy-sβCD is employed in the reduction of atrazine, the cationic species may form an inclusion complex with the cyclodextrin and, hence, be detected.

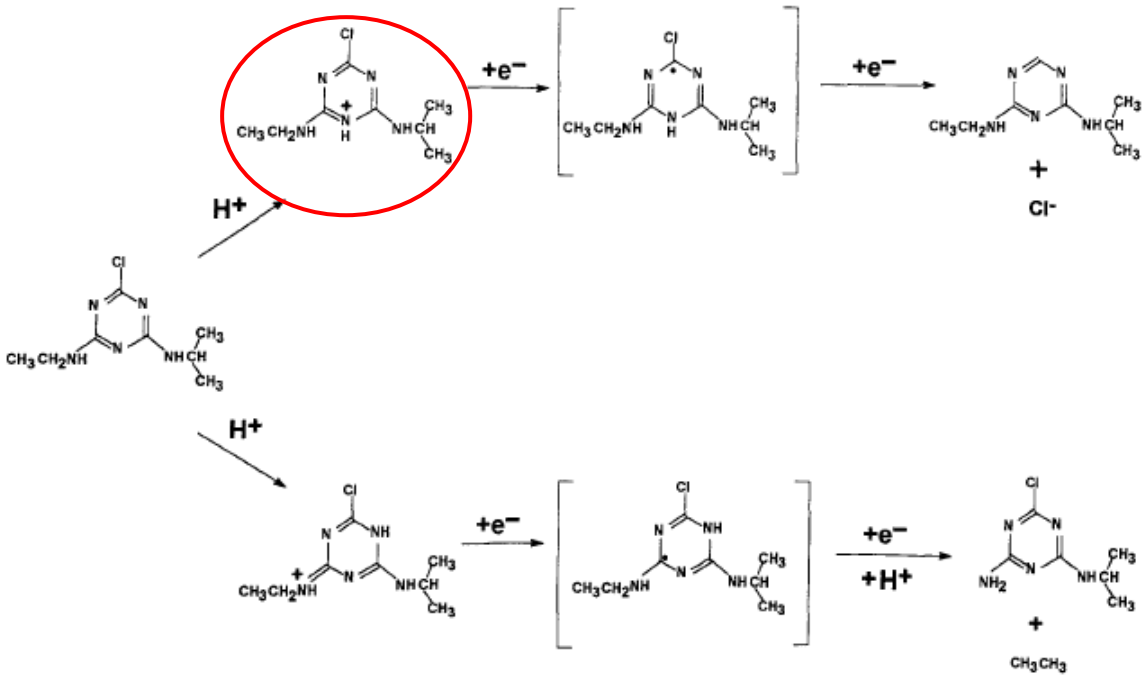

Figure 7. Reaction mechanism for the reduction of atrazine as outlined by Pospíšil et al. (1995). Cationic species for detection circled.

A polypyrrole film doped with sβ-CD was polymerised, as previously described. This film was then employed to detect atrazine. Several different acidic electrolytes were used, including Britton-Robinson buffer and sulphuric acid, however, atrazine was not successfully detected using the polypyrrole encapsulated cyclodextrin. Cyclic voltammograms in a cathodic direction (Figure 8a), and in an anionic direction (Figure 8b), showed no significant difference in voltammogram shape between the background scan (without atrazine) and those in the presence of atrazine.

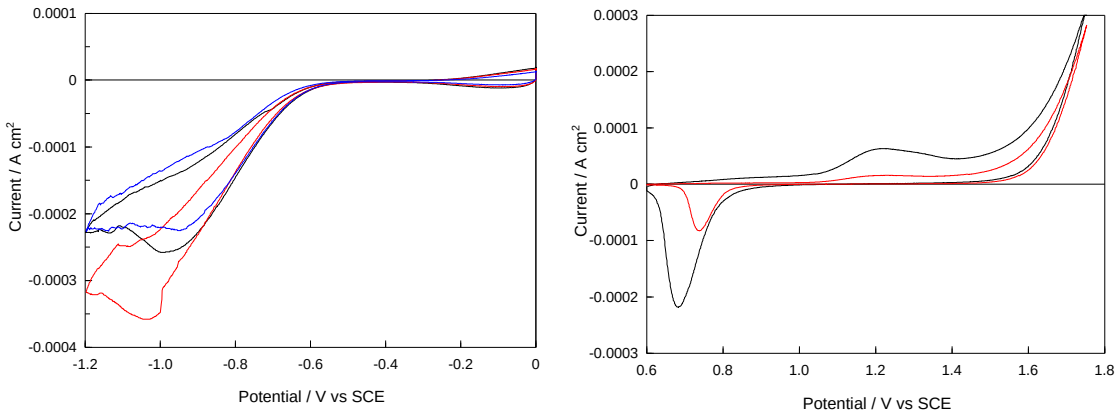

Figure 8. (a) Cyclic voltammogram of — 0.04 M Britton-Robinson buffer, — 2 mM atrazine and — 5 mM atrazine Britton-Robinson buffer at PPy-sβCD and (b) cyclic voltammogram of — 0.04 M Britton-Robinson buffer and — 2 mM atrazine in Britton-Robinson buffer at PPy-sβCD.

Again, due to no evidence of detection of atrazine and therefore it being unlikely that an inclusion complex is being formed, further investigation into the possible use of PPy-sβCD in the remediation of atrazine and atrazine derivatives was not carried out.

2.1.5 Acetaminophen

Acetaminophen or paracetamol is a widely-used, over-the-counter analgesic and antipyretic. It is most commonly used for the relief of headaches and other minor aches and pains, as well as being a major ingredient of numerous cold and flu remedies. In combination with opiod analgesics, such as codeine, acetaminophen is used in the management of more severe pain, such as post-surgical pain. Though it is used to treat inflammatory pain, it is not classified as a non-steroidal anti-inflammatory drug (NSAID), as it exhibits only weak anti-inflammatory activity.

PPy film fabrication was carried out using an electro-synthesis method, which deposited the polymer film at the working electrode (glassy carbon). PPy-sβCD films were prepared, as previously described, in electrolyte solutions containing 0.2 M pyrrole and 0.02 M sulfonated β-cyclodextrin at a constant potential of 0.65 V, and this was found to be reproducible. This polymer film was then transferred to 0.05 M PBS and 0.1 M KCl and cycled between 0.00 and 0.75 V to obtain a background measurement before 0.05 M acetaminophen was added. As can be seen in Figure 9, the background measurement showed no electroactivity or redox behaviour. However, upon the addition of acetaminophen, a redox couple centred around 0.40 V could be seen, indicating some interaction between the cyclodextrin and the acetaminophen. These peaks (I and II) were observed at scan rates of both 50 and 100 mV/s. Both peaks I and II maintained current over several cycles, indicating good stability of both the film and the interaction of the acetaminophen and cyclodextrin.

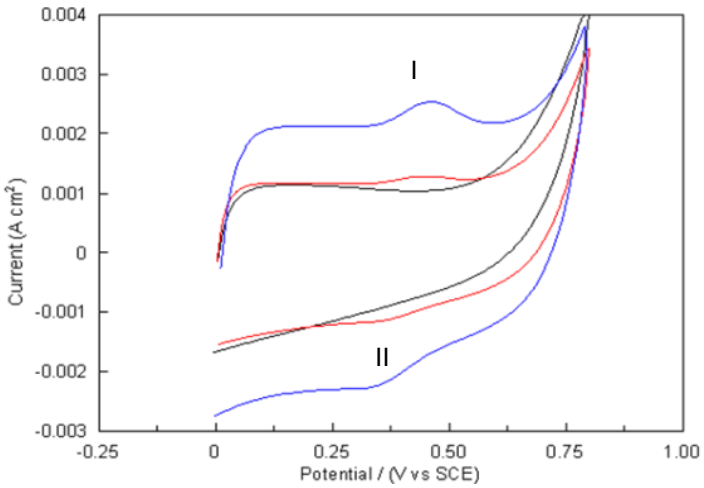

Figure 9. Cyclic voltammograms of PPy-sβCD in — 0.05 M PBS and 0.1 M KCl and in 0.05 M acetaminophen in 0.05 M PBS and 0.1 M KCl at a scan rate of — 50 mV/s and — 100 mV/s.

The appearance of the voltammogram during the electrooxidation reaction can yield information about the reaction kinetics occurring during electrocatalysis, such as diffusion and adsorption effects (Monk, 2001). For example, a linear relationship between current and the square root

of scan rate is evidence that the electrochemical reaction is under diffusion control. This relationship is described by the Randles-Sevcik equation, Equation 3.

$$I_p = Kn^{3/2}AD^{1/2}cv^{1/2} \qquad \text{Equation 3}$$

*I*p is the peak current (A), *K* is a constant (2.69 × 10^5), *A* is the surface area (cm^2), *c* is the concentration of the redox species (mol cm^{-3}), *D* is the diffusion coefficient (cm^2 s^{-1}) and *v* is the scan rate (V s^{-1}). The data represented in Figure 10 represents the oxidation peak current (peak I, Figure 9). As can be seen the square root of the scan, rate was plotted against the peak current. As expected, there was a slight shift in peak potentials towards more anodic potentials with increasing scan rate, which can be attributed to slow kinetics at the electrode. The diffusion co-efficient for the reaction was calculated to be 3.4 x 10^{-6} cm^2 s^{-1}. This suggests that the system is not completely under diffusion control. In fact, the system may be under a mix of diffusion and adsorption control, particularly at lower scan rates. A shift in peak potential with increasing scan rate towards more anodic potentials was also observed and this is attributed to slow reaction kinetics.

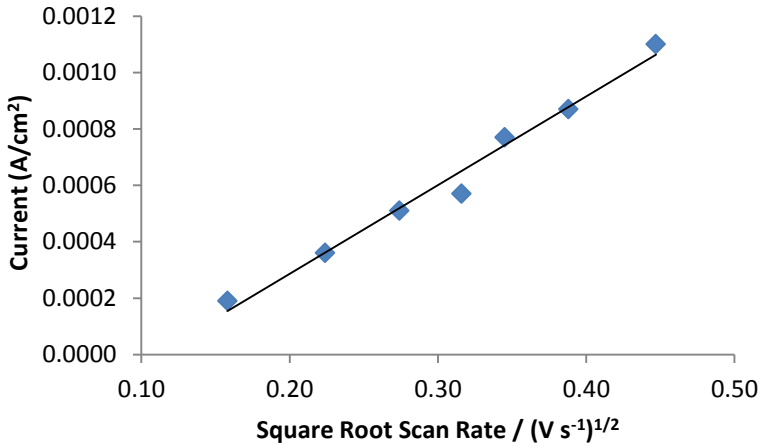

Figure 10. Plot of the square root of scan rate against the peak current for the detection of 0.05 M acetaminophen in 0.05 M PBS and 0.1 M KCl at PPy-sβCD.

The window for the cyclic voltammetry measurements was also varied and it was found that, as the switching potential was increased to more positive potentials, the oxidation and reduction peaks (I and II) reduced significantly. This may be due to the over-oxidation of the polypyrrole film.

Complexation between acetaminophen and sβ-CD was determined using UV-vis spectroscopy and cyclic voltammetry, while the Job's method was employed to distinguish the stoichiometric value of the complex. Job's method (Gibaud et al., 2005) or continuous variation is a common way to confirm this stoichiometric value. A series of solutions, where the sum of the guest (acetaminophen) and host (sβ-CD) concentrations was kept constant while changing the mole fraction, were prepared. These solutions were then analysed using UV-vis spectroscopy and cyclic voltammetry. The data for the Job's plot was generated by taking the

product of the mole fraction with the change of the property from that of an equal concentration of free guest (ΔA). This product was then plotted as a function of the mole fraction. The stoichiometry was determined from the x-co-ordinate at a maximum value of the Job's curve. Figure 11a below shows the Job's plot obtained from UV analysis. The maximum absorbance value was achieved at the 0.5 mole fraction and this is evidence that there exists a 1:1 acetaminophen:sβ-CD complex stoichiometry. To generate the Job's plot for the CV analysis, the changes in the current for peak I in Figure 9, in the presence and absence of CD (ΔI_p), was monitored. The Job's plot generated from the data (Figure 11b) reached a maximum value at 0.5 mole fraction, confirming the formation of a 1:1 acetaminophen:sβ-CD complex.

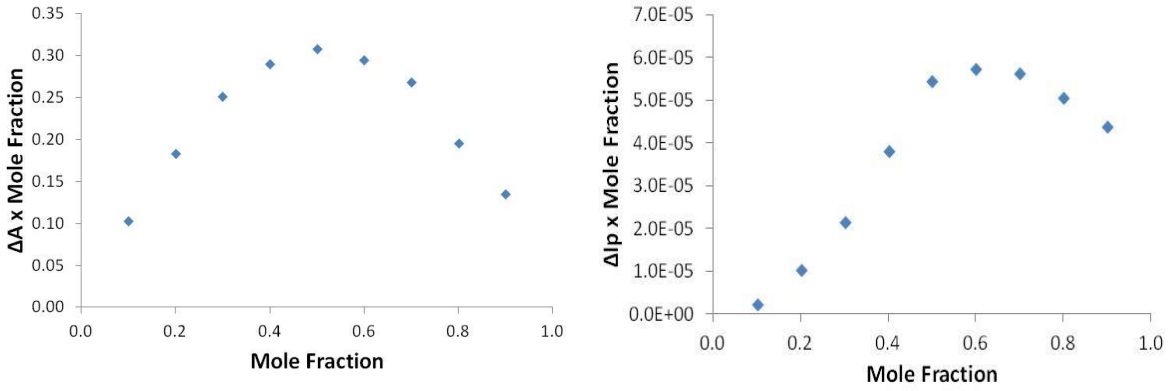

Figure 11. Job's plot curve of (a) change of UV-vis absorbance of acetaminophen upon the addition of sβ-CD and (b) change of peak current of acetaminophen upon the addition of sβ-CD.

The influence of acetaminophen concentration on the oxidation reaction was monitored by varying the acetaminophen concentration between 0.05 and 0.1 M. This range was chosen, as there was no clear resolution of oxidation peak I at concentrations below 0.05 M. It was found that there was no clear linear relationship between concentration and the oxidation peak current, especially at higher concentration. This may be due to the formation of phenoxy radicals during oxidation of acetaminophen. These radicals can then polymerise and cause faster passivation of the electrode surface. At higher concentrations of acetaminophen, this passivation is more pronounced.

Due to poor reproducibility, further investigation into the possible use of PPy-sβCD in the remediation of acetaminophen was not carried out.

2.2 Development of Novel Methodologies for the Electrodeposition of Polypyrrole-based Films in Controlled Morphologies with Potential Application in Nitrate Sensing

2.2.1 Introduction

Polypyrrole (PPy) is one of the most extensively studied conducting polymers (CP) due to its facile preparation and its attractive range of properties, including redox activity (Johanson et al., 2005), ion exchange capabilities (Dziewonski and Grzeszczuk, 2010) and biocompatibility (George et al., 2005). However, there is currently much interest in using functionalised monomers to generate conducting polymers as novel

materials, in particular as biosensors (Hafaid et al., 2010; Nie et al., 2009). When the functional group on the substituted pyrrole contains a terminal cyano group, supramolecular interactions between that group and other molecules are possible. The reason for investigation of these polymers was to employ them as possible candidates to enhance the electrochemical reduction of the nitrate ion. Developing them into the nanowire morphology would increase the sensor response significantly. In recent years, a number of authors have reported template-free electrochemical methods for the formation of PPy nanowires (Debiemme-Chouvy, 2009; Zang et al., 2008). These nanowires possess a higher surface area and shorter diffusion lengths than the analogous bulk materials, providing the wires with more attractive properties (Long et al., 2011). Although *N*-substituted PPy has been employed for sensor applications, there are few studies on the preparation of these polymers in the nanowire morphology. Moreover, these studies have utilised either a template approach or coated already grown PPy nanowires with the functionalised PPy (Roy et al., 2011).

2.2.2. Template-Free Electrochemical Polymerisation of Poly[N-(2-cyanoethyl)pyrrole] Nanowires

In a typical experiment, the 75 mM N-(2-cyanoethyl)pyrrole was dissolved in 3 ml EtOH, while both 20 mM $LiClO_4$ and 0.3 M $(NH_4)H_2PO_4$ were dissolved in 7 ml H_2O. The two solutions were mixed, stirred for 10 minutes and finally a potential of 0.85 V vs. SCE was applied. Due to the different solubilities of the reagents used, the nanowires were electropolymerised from a 70:30 H_2O/EtOH mixture. In accordance with previous studies, nanowire formation was highly dependent on the growth conditions (Wang et al., 2011). Their growth was only observed in the potential range of 0.8 to 1.0 V. If polymerisation was carried out using a low dopant concentration, microwires which were tapered towards the tip were formed. However, if dopant concentrations were increased, vertical wires were formed but these possessed a wide distribution of sizes. Once growth conditions were optimised, it was possible to consistently form a homogenous and adherent film of nanowires at the glassy carbon substrate, as can be seen in Figure 12(a).

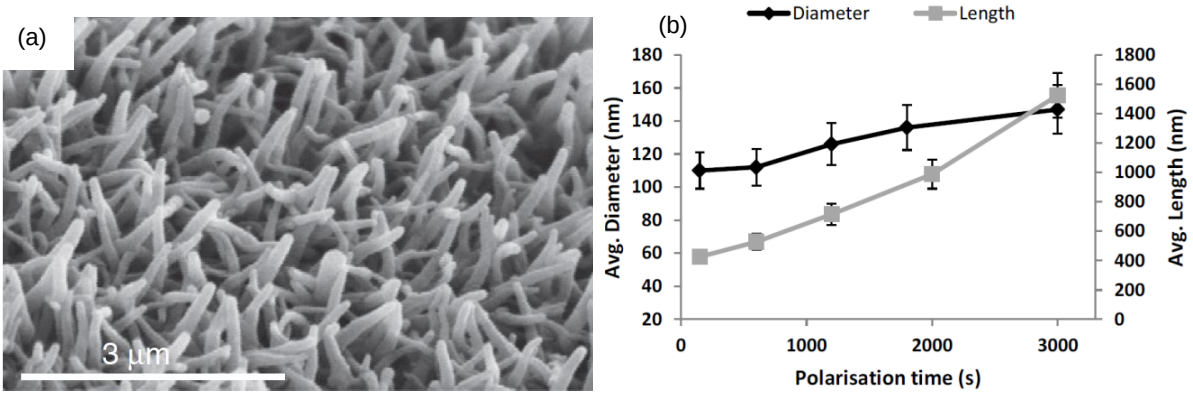

Figure 12. (a) SEM micrograph PPyEtCN nanowires. (b) Polarisation time vs. Average diameter and average length for PPyEtCN nanowires. Nanowires were grown under optimised conditions - 75 mM N-(2-cyanoethyl)pyrrole, 20 mM $LiClO_4$ and 0.3 M $(NH_4)H_2PO_4$ in 3:7 ethanol: water held at 0.85 V for 60 minutes.

In order to observe how the growth of the wires could be controlled, FE-SEM micrographs were recorded at various time intervals. It was found that only nodules were evident after one minute electropolymerisation, however, after five minutes, nanowire formation was observed and long tapered wires, as shown in Figure 11, were seen after 60 minutes. An obvious relationship between electropolymerisation time and wire diameter and length was established, allowing for controlled and reproducible growth of the PPyEtCN nanowires (Figure 12(b)).

Previous studies have shown that the initial stages of electropolymerisation of conducting polymers occurs via diffusion-controlled growth at nucleation sites (Asavapiriyanont et al., 1984). By using the Sharifiker and Hills models (Scharifker et al., 1983), the nucleation of the nanowires can be identified as either instantaneous or progressive in a 2-D or 3-D manner. A typical current-time transient recorded during the electropolymerisation period is shown in Figure 13(a). From these data, dimensionless $(I/I_{max})^2$ vs. (t/t_{max}) and (I/I_{max}) vs. (t/t_{max}) plots were produced from and compared to the theoretical 2-D and 3-D progressive and instantaneous models. From the resulting plots, as shown in Figures 13(b) and (c), it is clear that for the early stages of growth, the experimental data are consistent with the 3-D instantaneous phase of growth. Further experimentation found that uniform nanowire films were only formed when the early stages of polymer growth followed the 3-D instantaneous growth model.

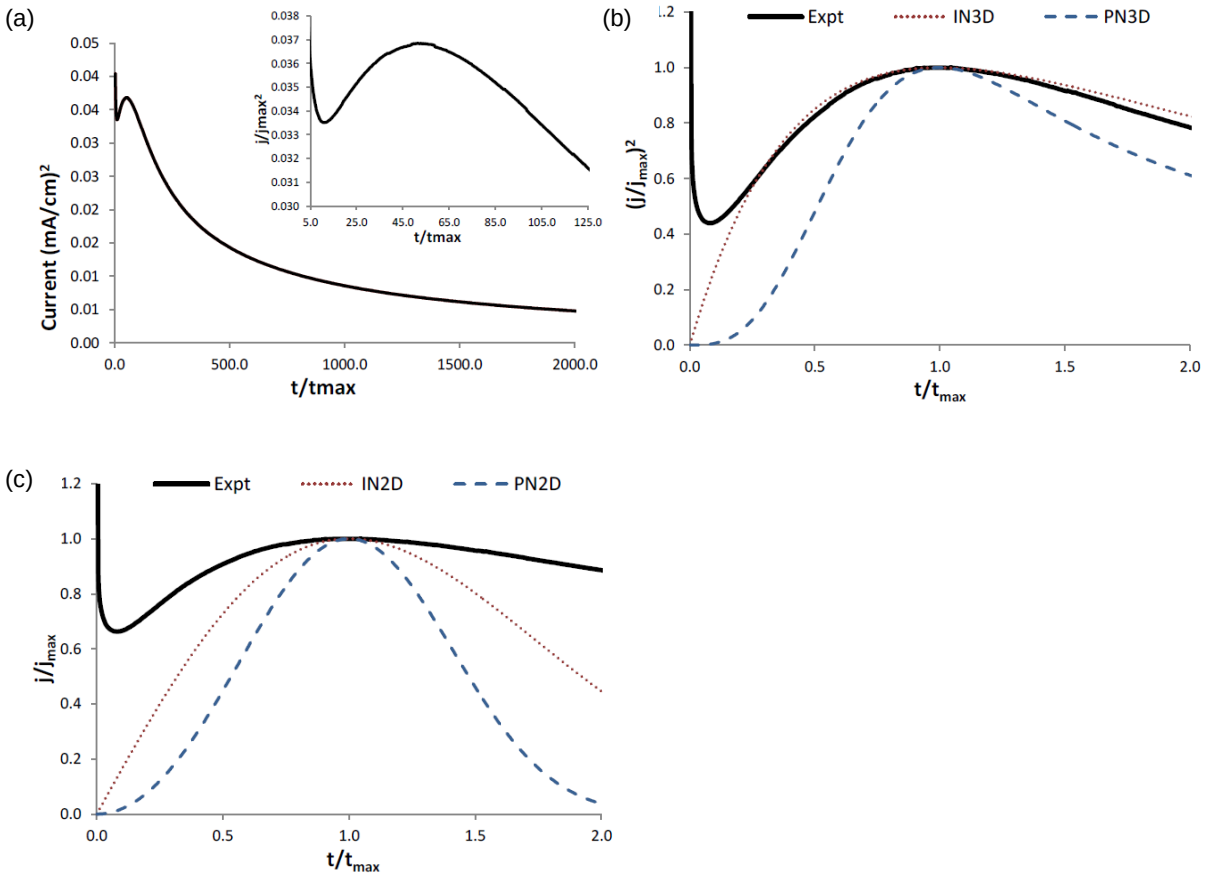

Figure 13. A typical current transient for the growth of PPyEtCN nanowires (a) with magnification of the I_p inset. Dimensionless plots of (a) $(j/j_{max})^2$ or (j/j_{max}) vs t/t_{max} compared with (b) 3-D instantaneous nucleation (IN3-D) and progressive nucleation (PN3-D) and (c) 2-D instantaneous nucleation (IN2-D) and progressive nucleation (PN2-D).

Cross sections of the PPyEtCN films were obtained in order to characterise the structure of the nanowires. As can be seen in Figure 14(a), the wires were attached together at the base by a layer of bulk polymer. It appears that the polymer is firstly nucleated on the surface in 3-D growth phase, followed by 1-D growth along the z-axis, giving the wires extended lengths perpendicular to the substrate. A transition electron microscopy (TEM) micrograph, as shown in Figure 14(b) shows that the contrast is uniform along the entire length of the wires, signifying a uniform density and a solid interior.

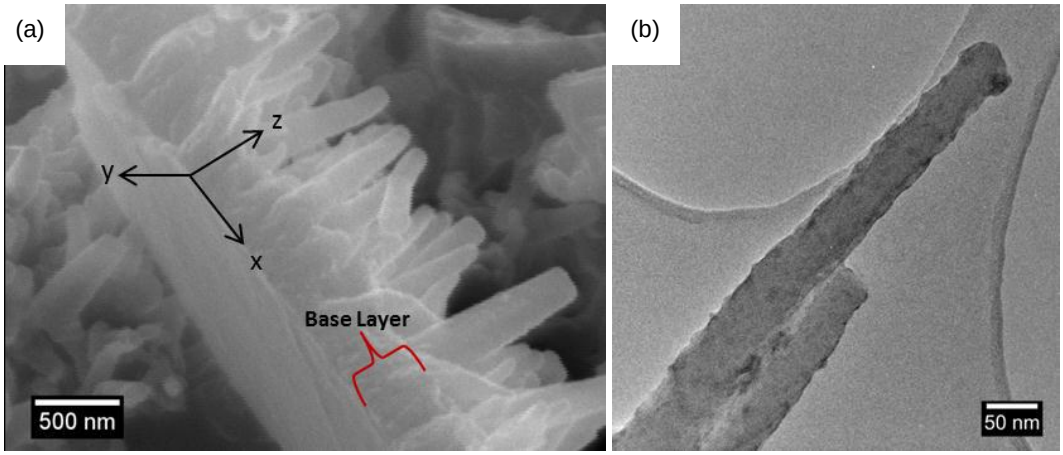

Figure 14. (a) SEM micrograph of a cross-section of a nanowire film showing the base layer, (b) TEM micrograph of PPyEtCN nanonwires.

Direct evidence of the presence of the cyano group was obtained using fourier transformation infra-red (FTIR) spectroscopy. A typical FTIR spectrum for a PPyEtCN nanowire film, as well as for the PPyEtCN monomer, is shown in Figure 15. The characteristic ν(C≡N) band at 2246 cm^{-1} can be clearly observed in both the monomer and polymer spectra. This signifies that the cyano moiety has remained intact after polymerisation. Raman spectra were obtained for the PPyEtCN nanowires and compared to the bulk PPy films (see Figure 15).

The PPyEtCN nanowires retained the characteristic bands associated with the Py monomer. A new band appeared at 1149 cm^{-1}, which was only present in the spectra for PPyEtCN, and is most likely associated with the ethyl chain from the cyano moiety (Teixeira-Dias et al., 2011). The most intense band in the PPy spectrum at 1595 cm^{-1} from the ν(C=C) has shifted to 1582 cm^{-1} for the PPyEtCN nanowires. This shift is indicative of a reduction in the amount of oxidised units in the nanowires compared to the bulk PPy. While PPy exhibits bands due to the bipolaron and polaron species at 940 and 980 cm^{-1}, only the latter is visible in the PPyEtCN spectrum. The ratio of the intensity of the ν (C=C) band to that of the skeletal band at 1503 cm^{-1} gives a measurement of the relative amounts of conjugation in the two polymers (Gupta, 2008), and was determined to be approximately 2.7 and 2.0 for the PPy and PPyEtCN systems respectively, indicating the lower degree of conjugation in the PPyEtCN film. This is consistent with the presence of a band at approximately 1705 cm^{-1} in both the Raman and FTIR spectra indicative of a carbonyl stretching mode.

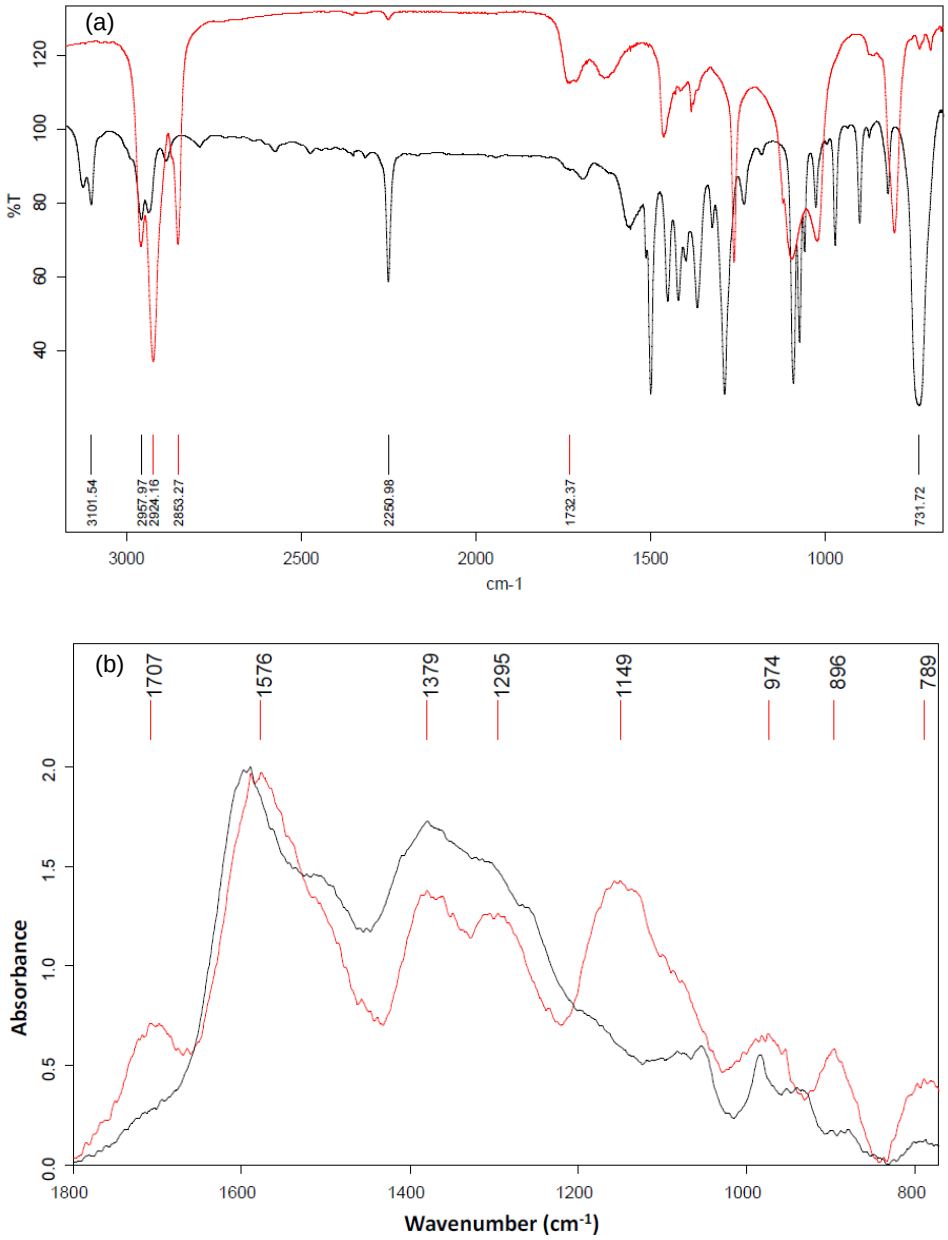

Figure 15. (a) FTIR spectrum of PyEtCN monomer (black trace) and PPyEtCN nanowire polymer (red trace) in KBr. (b) Raman spectrum at 660 nm of a PPy bulk polymer grown using at 0.85 V with 0.10 M $LiClO_4$ (black trace) and PPyEtCN nanowire polymer grown using 0.2 M $LiClO_4$, 0.3 M $(NH_4)H_2PO_4$ with 0.075 M PyEtCN (red trace) in a water/ethanol solution.

2.2.3. Electrodeposition of Poly[N-(2-cyanoethyl)pyrrole] Microtubes and Microcontainers from an Accoustically Formed Emulsion

When forming the PPyEtCN nanowires, it was observed that in certain experiments large, circular-shaped PPyEtCN microtubes were produced in a vertically aligned but random fashion across the electrode. These microtubes were produced with either a smooth or rippled exterior. The rippling effect was related to their size, as it was only observed for the larger diameter tubes. The PPyEtCN microtubes were produced in either large condensed groups over the electrode or in an irregular dispersed pattern. Therefore, it was not possible to control or predict their formation. Comparison of the growth

profiles of the randomly-formed microtube films and the nanowire films previously formed showed no major difference in the magnitude of the current response over the entire growth. However, examination of the very early stages of the growth corresponding to the nucleation phase, revealed a sharp increase in the recorded current transient. This narrow 'pre-peak' was only present for the films possessing microtubes, indicating that they were formed at the beginning of the nucleation phase. It was probable that insoluble monomer droplets had adsorbed on the electrode surface, which would also contain the dopant $LiClO_4$, since it is soluble in organic media. Having both monomer and dopant in close vicinity to the electrode would produce an increase in polymerisation rate at early times, leading to the increase in the current recorded. Although this observation does not provide much information about the mechanism of microtube growth, it does indicate they are formed at the beginning of nucleation under abnormal conditions. This was supported by EDX analyses of the interior cavity and exterior walls of the tubes. Results suggested that surface adsorbed monomer droplets, with a high concentration of ClO_4^-, are responsible for creating the microtubes. A similar observation was reported by Huang et al. (2008), as they successfully developed a PPy nano morphology employing undissolved monomer droplets, while Asami et al. (2005); Asami et al. (2006) also reported stable nano and microdroplets of monomer when insoluble monomer/electrolytes were used. Based on these reports, the monomer droplet hypothesis for the formation of the PPyEtCN microtubes has reasonable credibility.

Using adsorbed toluene droplets as soft templates, in conjunction with the mixed electrolyte system used for the template-free electrodeposition of PPyEtCN nanowires, it was possible to electrochemically synthesise PPyEtCN microtubes and microcontainers. When sufficient energy was applied to the toluene/water/ethanol system, through ultrasonication, it was possible to create a homogeneous dispersion of toluene microdroplets within the continuous phase. This turbidity could be maintained for several hours without the need for any surfactants or stabilisers. This was found to be a key factor in utilising this system as a soft template method, as the absence of stabilising agents leaves the toluene microdroplets available to adsorb to solid surfaces (Mazur, 2008). The electrochemical polymerisation mixture of 20 mM $LiClO_4$, 100 mM $(NH_4)H_2PO_4$, 56 mM PyEtCN and 80 µL toluene in 10 mL of water/ethanol (7:3) was emulsified by either being shaken vigorously and then sonicated for one minute using an ultrasonic probe, or stirred vigorously for five minutes and then sonicated for one minute using an ultrasonic bath. Both methods resulted in the solution forming an opaque emulsion. It was found that the emulsion formed using the ultrasonic probe was much more opaque and possessed a longer period of stability than that formed employing the ultrasonic bath. Emulsion produced using the ultrasonic probe was therefore used for further polymerisation experiments. Microtubes were formed by applying oxidation potentials between 0.85 and 1.30 V. While the tubular morphology was solely influenced by the adsorbed toluene droplets, the rate at which the tubes were formed and the shape of the hollow tube structure were found to be determined by the applied potential. Plate-like structures with very little vertical growth were formed at the lower range of applied potentials, while higher potentials resulted in a more bowl-like morphology (Figure 16). At higher oxidation potentials, the tubes had increased substantially in height but also an increase in diameter at their openings was observed. Scanning electron microscopy (SEM)

micrographs showed that the areas immediately surrounding the microtubes showed very little polymerisation. The microtubes formed preferentially in large numbers over the electrode surface as the main structures. However, away from these sites a thin layer of bulk polymer was observed.

This observation suggests that a proportion of the PyEtCN monomer was contained within the toluene droplets, with some monomer remaining free in solution. As the duration of sonication time was increased, the average diameter of the tubes decreased.

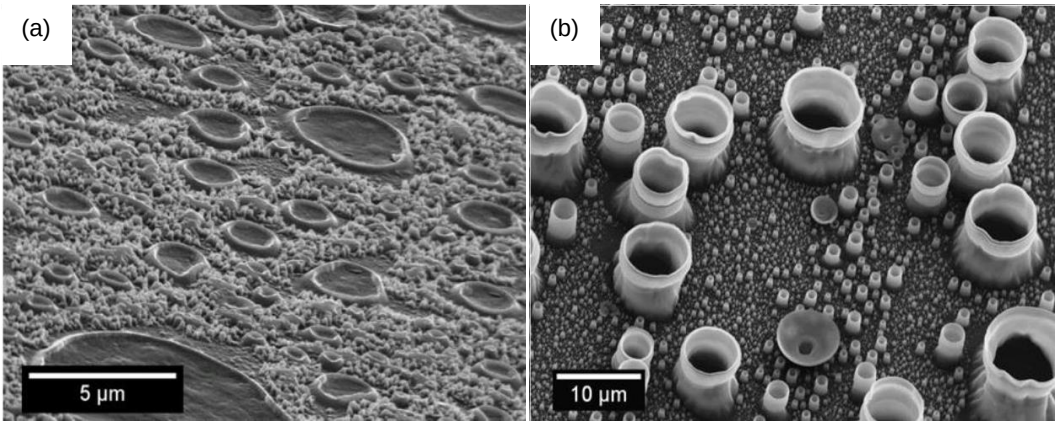

Figure 16. SEM micrographs of microstructures deposited at (a) 0.85 and (b) 1.20 V.

During prolonged periods of growth (30 minutes), a second stage of microtube nucleation was observed, resulting in smaller tubes developing within the larger tubes (Figure 17). These smaller microtubes evolved only from the inner walls of the bigger microtubes and were never observed forming from the base centre. This suggested that the toluene droplets had adhered strongly to the substrate throughout the polymerisation process, preventing further growth at these sites.

By using a mixed $LiClO_4$ / $(NH_4)H_2PO_4$ electrolyte system, the rate of polymerisation could be controlled. This control of kinetics during polymerisation allows for the growth of conducting polymers in an ordered morphology (Huang et al., 2008). In the researchers' system, it was found that the initial stage of polymerisation is rapid, however, this growth rate is not maintained due to the presence of $H_2PO_4^-$, which is believed to prevent an increase in H+ ion concentration at the polymer surface, thus regulating the polymerisation rate.

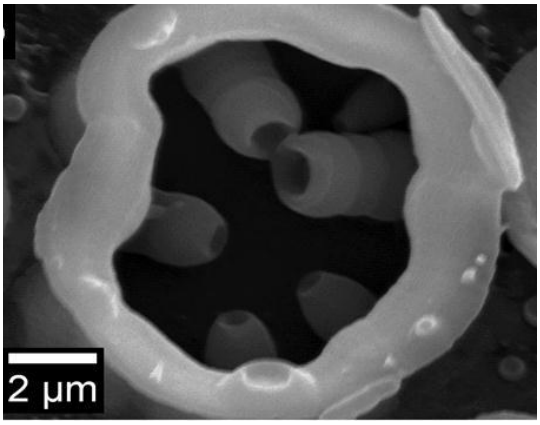

Figure 17. SEM micrographs of microstructures deposited at 0.95 V for 30 minutes.

TEM micrographs were recorded of individual tubes showing that the hollow cavity extends the entire length of the structure (Figure 18a). These micrographs also confirmed that the tube morphology remained intact despite being removed from the surface and sonicated, indicating high structural stability. High-magnification TEM analysis of the outer walls showed that there was dense packing of polymer surrounding the hollow interior (Figure 18b). The high density of the polymer in the tube walls most likely arises due to the combination of the slow rate of polymer propagation combined with the preferential polymerisation at the droplet surface. The inset image in Figure 18a shows the electron diffraction pattern, which was a diffusive ring, identifying the microtubes as having an amorphous structure.

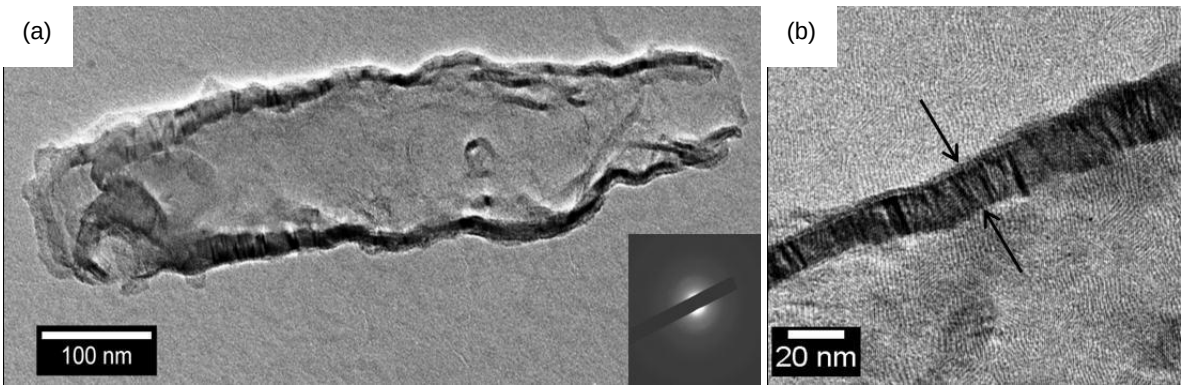

Figure 18. TEM micrograph of (a) individual PPyEtCN tube and (b) magnification of exterior wall area of tube.

2.2.4. Electrodeposition of Copper Micro/Nano Structures at Poly[N-(2-cyanoethyl)pyrrole] Polymers for the Electrochemical Detection of Nitrate

The PPyEtCN polymers previously discussed were a novel morphology of CP, therefore the electrochemical deposition of Cu on their surface was attempted to identify their ability to be effective supports for copper deposition. These materials could then also be tested for their ability to be used as a nitrate-sensing material. The lower electrical conductivity observed for the PPyEtCN nanowires is due to steric clashing from the substituted group and an over-oxidation process at the carbon β position. This produced a low $\pi-\pi$ overlap between the Py rings. However, in spite of this, having the C≡N moiety at the nitrogen position of the Py may have permitted a new interaction between the polymer and the electrodeposited copper. This possibility was investigated.

PPyEtCN bulk polymers were initially used as the substrate material followed by the nanowire/microtube polymers, with copper being deposited in 0.05 M $CuSO_4$ in 0.05 M Na_2SO_4. The low electrical conductivity was evident in the electrochemical deposition experiments, as the current recorded for the electrodeposition of Cu, at potentials of -0.135 and -0.200 V, was low, signifying a slow deposition rate. These were the same potentials which produced a complete coverage of large copper microdeposits on PPy films. While the current recorded did increase for experiments at -0.200 V, it was not a large increase. This was due to the more insulating PPyEtCN films requiring more energy to transfer electrons through the polymer layers, which resulted in a low reduction of Cu^{2+} across the electrode. Furthermore, when EDX and SEM analysis were obtained, neither displayed any indication of the presence of copper deposits. Deposition was observed only when extremely negative potentials, lower than -1.0 V, were applied. Inspection of the SEM micrographs obtained from the electrodeposition at -1.1 V displays some interesting nucleation of copper microstructures. At a low magnification, a large ring of copper was observed around the outside of the electrode (Figure 19a). These structures had grown significantly in size and extended their length over electrode without creating new nucleation sites (Figure 19b). Closer inspection of the original nucleation sites reveals that the copper was in fact nucleating down the side of the electrode, which was possibly not covered by insulating PPyEtCN (Figure 19c). The high energy barrier associated with depositing on the PPyEtCN film forced the copper to nucleate at these exposed areas of bare electrode. Once deposition sites had formed, fresh copper deposition continued at these copper deposit sites, rather than forming new nucleation sites on the insulating PPyEtCN surface. This produced the extremely large microstructures. Inspection of the centre of the electrode, which was covered in a uniform film of PPyEtCN, showed that a relatively small amount of copper was deposited. Small ~300 nm copper cubes were seen to form in a dispersed pattern (Figure 19d). It was clear that an applied potential of -1.1 V was not sufficiently negative to lower the deposition barrier, to allow formation of micro deposits on the PPyEtCN polymer surface.

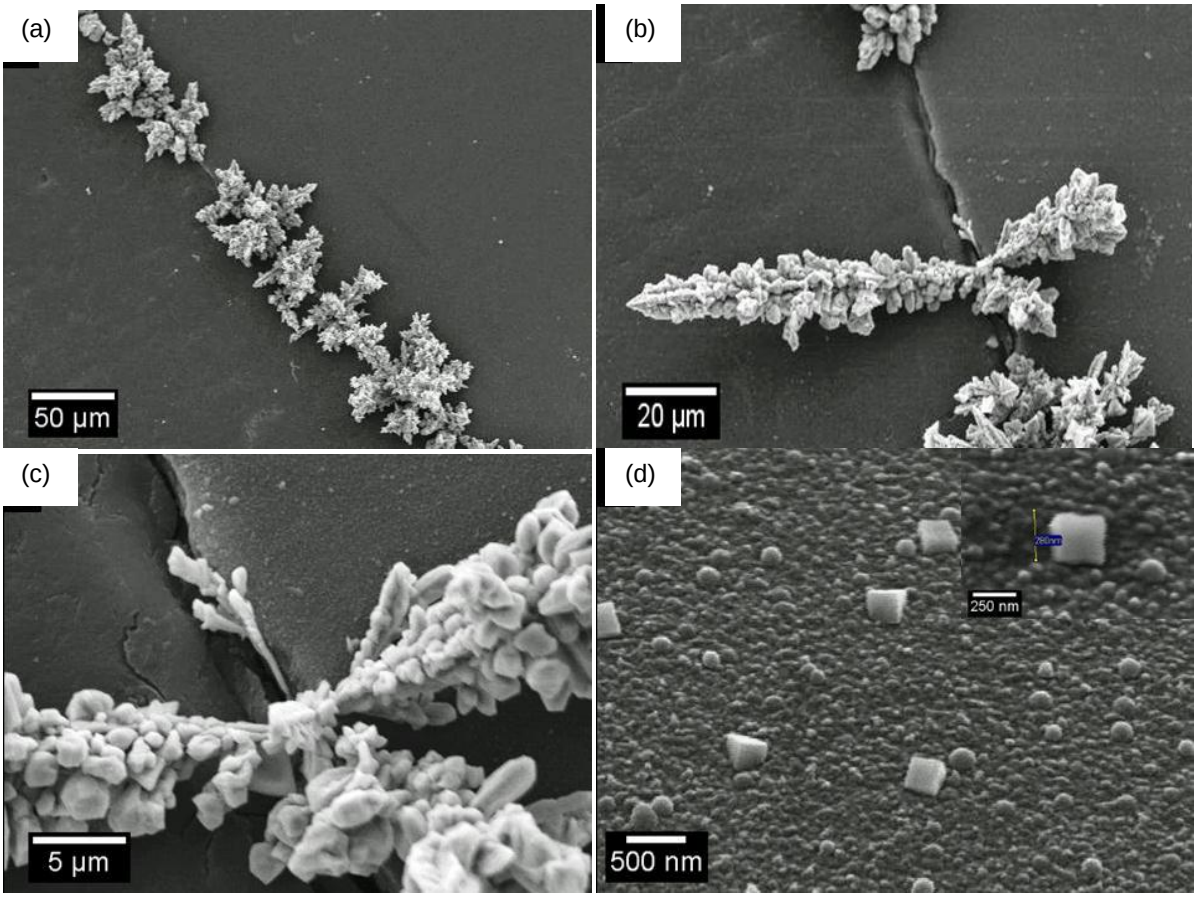

Figure 19. SEM micrographs of electrodeposited copper on PPyEtCN films from a 0.050 M $CuCl_2$ in 0.1 M Na_2SO_4 solution at 1.1 V for 700 s (a)-(c) various magnifications of edge of electrode and (d) centre of electrode.

Increasing the potential to -1.2 V led to a larger increase in the current recorded. Inspection of the centre of the electrode by SEM revealed large deposits of copper covering the entire electrode. Similar to the -1.1 V experiments, these deposits, once formed on the electrode, grew as very large microstructures. These copper structures grew to a large vertical height perpendicular from the electrode, as fresh copper growth only occurred from nucleation sites of already deposited copper. The deposits were very random in nature, with a range of structures forming including cube, triangle, branch and sheet type morphologies. These materials were verified as copper by EDX analysis. It was observed that the deposits were nucleating in a progressive manner, as there was a dramatic difference in the deposit size across the electrode surface. The same types of structures could also be seen at different growth stages on the same electrode. It was possible to electrodeposit large structures of hierarchical copper, using H_2SO_4 as a supporting electrolyte, onto PPyEtCN nanowires/microtube films. The deposition was not uniform, however, and only occurred towards the outer areas of the PPyEtCN films. It can be seen from Figure 20a that the copper structures deposited on both the nanowires and the semi-hollow microtubes. The copper was observed wrapped around the outside of the microtubes and grew outwards from them (Figure 20b). In other cases, the copper was observed in several sections along walls of the tubes (Figure 20c). Unexpectedly, it

was seen that even thick and potentially insulating microtubes, which were several microns from the electrode surface, had copper deposits at their extremities, as shown in Figure 20d. Further investigation found that, while it was possible to electrodeposit copper materials onto PPyEtCN polymers, the process was very slow due to the low electrical conductivity of the polymer. Therefore, as a substrate material, PPyEtCN was not an efficient material for electrodeposition of metallic structures due to its insulating properties compared to typically employed CPs.

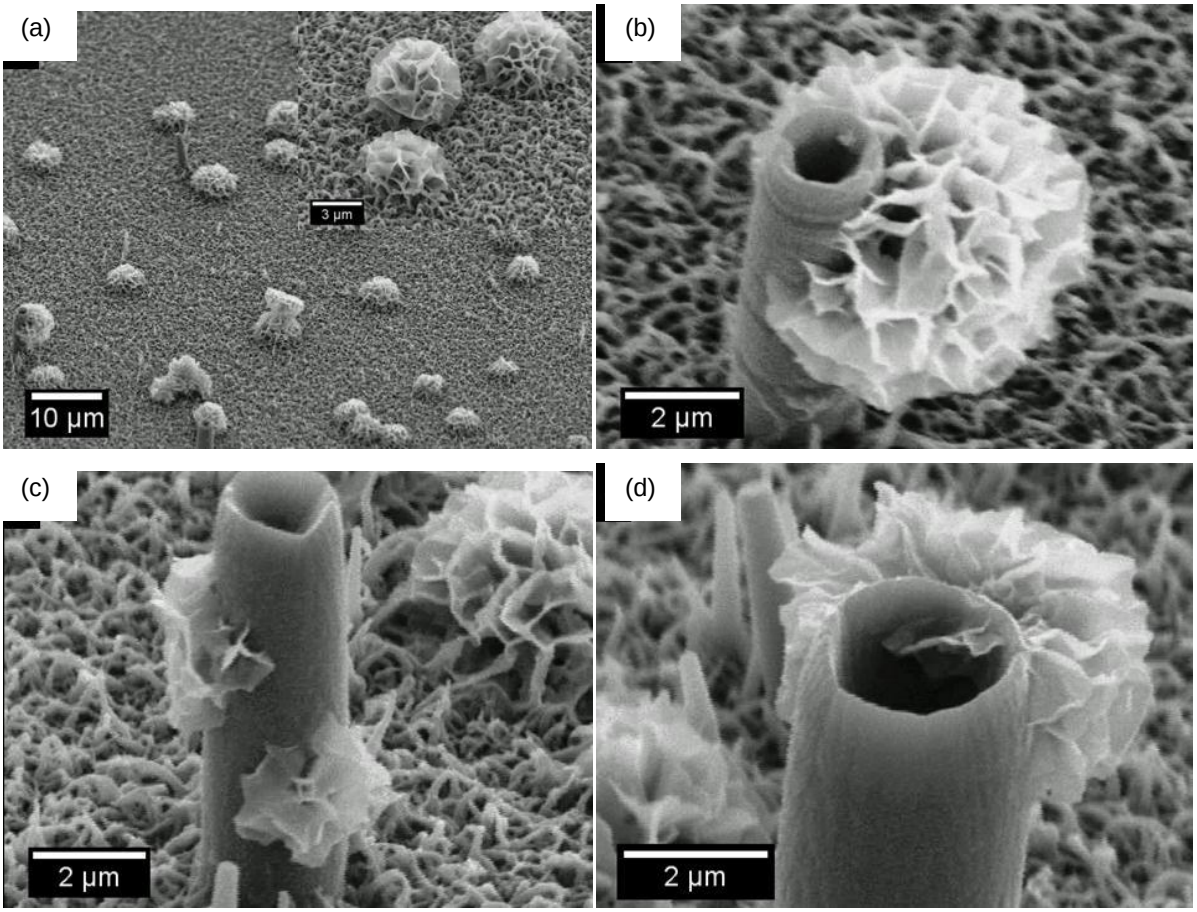

Figure 20. SEM micrographs of electrodeposited copper on PPyEtCN nanowires and microtubes from a solution of 0.05 M $CuCl_2$ in 0.05 M H_2SO_4 at -1.2 V for 700 s. (a) Distribution of copper particles on nanowires and (b) – (d) different nucleation points of copper structures on the microtubes.

To overcome the insulating nature of the PPyEtCN and still maintain the attractive properties of a nanowire polymer, experiments were performed using PPy nanowires as an alternate polymer substrate. This would utilise the larger surface area of the nanowires combined with the ability to easily electrodeposit copper at PPy substrates. PPy nanowires have been reported in the literature by various researchers using different methods. Ge et al. (2002) used a carbonate-based system which provided precise control over the resultant wires, by alterations in pH and applied potential. Employing PPy nanowires as a substrate for electrodeposition of copper takes advantage of the increased surface area of the wires. This provides enhanced electrochemical properties, which will benefit the composite material due to

the increased interaction with the electrolyte, leading to a faster electrochemical response. This stems from a shorter diffusion length of counter ions from the bulk solution to the surface of the nanomaterial (Huang et al., 2010). This carbonate system was used in conjunction with 0.1 M $LiClO_4$ and 0.1 M Py monomer. It was observed that the concentration of the carbonate in the polymerisation solution had a marked effect on the nanowire polymerisation rate and electrode coverage. The carbonate solution was comprised of Na_2CO_3 and $NaHCO_3$. The ratio of these salts in the electrolyte mixture affected the solution pH. Additions of 0.1 M Na_2CO_3 to 0.1 M $LiClO_4$ resulted in a pH of 10.5. At this pH, the growth of the polymer was very slow and resulted in patchy and uneven polymer deposits. In an attempt to reduce the electrolyte pH, the concentration of $NaHCO_3$ in the electrolyte was varied to 0.1, 0.2 and 0.3 M. This led to the decrease in the pH from 10.5 to 9.8, 9.5 and 9.3 respectively. The lower pH was more suitable for growing the PPy nanowires and significantly reduced the irregular growth issues previously described. The electrodeposition of copper onto PPy nanowires was achieved using cyclic voltammetry. The polymer was cycled between two set potentials of 0.1 and -0.4 V. The copper was electrodeposited at reductive potentials and then re-oxidised at anodic potentials. It was observed that once the copper became oxidised, it would dissolve back into solution at a very fast rate when the switching potential was more positive than 0.1 V. Similarly, applying reductive potentials below -0.400 V caused an excessive amount of copper to deposit on the electrode.

It is well known that copper has a catalytic response for the electrochemical reduction of nitrate. Therefore, the nanowire/copper composites produced were tested for their ability to electrochemically reduce nitrate. Firstly, the best parameters for studying the nitrate electroreduction were explored. A glassy carbon/copper electrode was used to optimise the scanning window and loading of copper, which favoured nitrate reduction. This removed problems associated with the irreproducibility of the nanowires, which were discussed previously. Once the optimised conditions were identified, they were applied to the PPy nanowire/copper composite.

Nitrate has been shown to undergo a reversible adsorption process, particularly on copper surfaces. To study this process for the copper nanomaterials employed in this work, a copper film was first deposited on a bare glassy carbon (GC) electrode using 100 mV/s for 10 cycles between 0.1 to -0.4 V in 0.05 M $CuCl_2$ (in 0.050 M H_2SO_4). This electrode was denoted as GC/Cu. A uniform copper layer with mixed nano and micro deposits was obtained under these conditions. This composite electrode showed almost ideal reproducibility between electrodes for the nitrate reduction reaction. Cyclic voltammetry produced a detection limit of 8.0 x 10^{-4} M. However, the nitrate electroreduction reaction at copper surfaces has been shown to be enhanced when cyclic voltammetry is employed. The sensitivity has been shown to increase, as copper dissolution/redeposition produces a fresh copper layer which promotes the electroreduction of nitrate. Employing the GC/Cu electrode and immersing it in 0.005 M $NaNO_3$ produced several reductive and oxidative signals (Figure 21). The signals more positive than -0.7 V are associated with the redox activity of the electrodeposited copper. The signals more negative than -0.7 V are due to the irreversible reduction of the nitrate ion to nitrite and other products. The processes associated with each are labelled and summarised in Table 1.

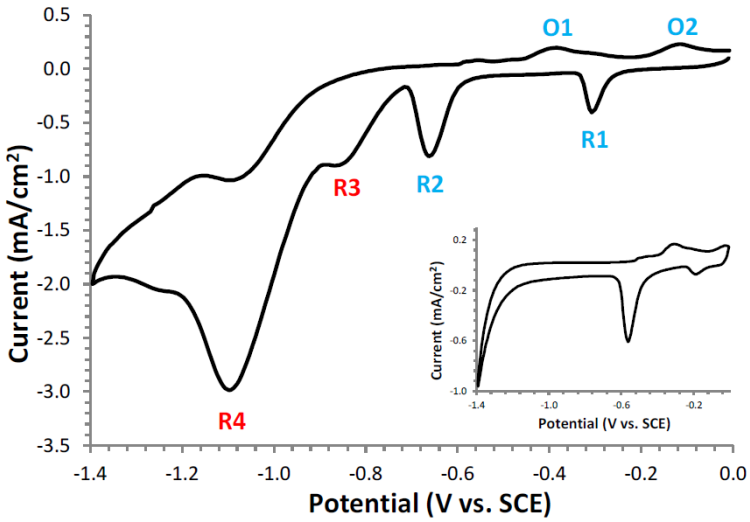

Figure 21. A GC/Cu electrode immersed in a 0.005 M $NaNO_3$ solution cycled between 0.0 and -1.4 V at 50 mV/s. Blue labels are associated with copper species and red labels are associated with the nitrate reduction. Cycles performed in 0.1 M Na_2SO_4 without 0.005 M $NaNO_3$ shown inset.

Table 1. The electrochemistry at a GC/Cu electrode in 0.005 M $NaNO_3$. Peak labels taken from Figure 20.

Peak Label	Potential (V)	Process
R1	-0.30	Cu(II) → Cu(I)
R2	-0.66	Cu(I) → Cu(0)
R3	-0.84	NO_3^- →NO_2^-
R4	-1.09	NO_2^- → NH_2OH/NH_3
O1	-0.39	Cu(0) → Cu(I)
O2	-0.11	Cu(I) → Cu(II)

The effect of increasing the copper loading on the GC/Cu composite electrode was measured using the optimised window (0.0 to -1.4 V). Increasing the amount of cycles in the copper deposition solution from 5 to 320 increased the current response for the peaks at R1, R2, O1 and O2. As shown in Figure 22a, the main copper peaks of R1 and R2 increase in current density as the copper deposition was increased from 5 to 320 cycles. This was expected, as increasing the number of cycles led to a greater amount of copper on the electrode surface. This increase in copper loading produced a greater response for the electrochemical reduction of nitrate. As shown in Figure 22b, the peak currents increase for the main nitrate peak and also shift towards lower overpotentials. The potential shifts from -1.10 to -1.01 V when the number of cycles in the copper solution increases from 5 to 320.

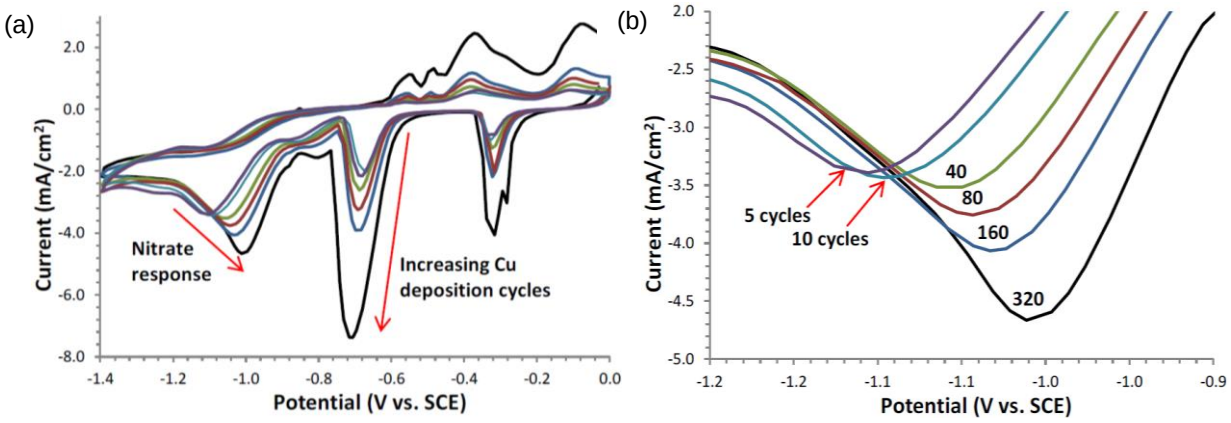

Figure 22. Cu deposited at a bare GC electrode using 5 to 320 cycles at 100 mV/s in 0.05 M $CuCl_2$ in 0.050 M H_2SO_4 then (a) cycled in 0.005 M $NaNO_3$ at 100 mV/s between the potentials -1.4 and 0.0 V and (b) magnification of nitrate response area.

When examining the relationship between increasing copper deposition and nitrate signal, it was found that as the copper signal increases, the nitrate response does not increase in a proportional manner. This may be due to the electrode being saturated in copper deposits forming a bulk-like layer, which does not increase the surface area of the active copper. However, with a greater copper loading, there is a possibility of the copper leaching or detaching from the surface. Therefore, to avoid such issues, which would reduce the sensor lifetime significantly, the larger loadings were avoided for use in the electroreduction reaction.

The optimised conditions for nitrate electroreduction employed with the GC/Cu nanocomposite were applied to the PPy nanowire/Cu nanocomposite, denoted PPy-NW/Cu. The speed at which the copper deposition was performed had a direct influence on the resultant copper morphology. It was also observed that increasing the number of copper deposition cycles produces a greater loading of copper at the electrode, which favourably increases the nitrate reduction reaction. In an attempt to obtain the maximum amount of copper at the nanowire morphology, a large number of cycles (160) were performed at an intermediate scan rate (300 mV/s). As can be seen from Figure 23a, the nitrate signal produced at this PPy-NW/Cu electrode was poor. The background cycle (black trace) and nitrate reduction (red trace) did not display the same reduction peaks, as shown in Figure 22. Furthermore, the current response was significantly lower. This would suggest that nitrate electroreduction was not catalysed at this PPy NW/Cu electrode. Examination of the SEM micrograph (Figure 23a) reveals that the entire electrode had been covered in a bulk copper deposit. This excessively large copper loading, combined with the semi-conducting nanowires, would significantly reduce the electron transfer across the PPy-NW/Cu surface. Furthermore, the high surface area property of the nanowires was not being exploited, since they were covered in a dense copper coating. It was apparent, even with the optimal 160 cycles, that the slow sweep rate was still encouraging the formation of a bulk copper layer. To reduce the amount of copper deposited at the PPy nanowires, the scan rate for the copper deposition was increased to 600 mV/s, while maintaining 160 cycles. This produced an increase in response for the nitrate reduction, as shown in Figure 23b, where a peak current (I_p) was observed at ~-1.07 V with a

magnitude of -0.38 mA/cm^2. The capacitive behaviour of the nanowires was also observed at -0.5 V, signifying that a proportion of the nanowires were exposed to the electrolyte. The copper redox chemistry, as seen in Figure 21 (R1 and R2), was also present. Examination of the SEM micrograph confirmed these observations, as the nanowire morphology was identified as having large copper triangles deposited on the surface. Clearly, these deposits were in the micro range and were similar to the copper morphology seen previously for slower scan rates using less cycles. The benefit of using faster scan rates with a greater number of cycles was that less bulk deposition was produced. However, the copper reductive peaks and the nitrate reduction were only marginally larger than the background signal. Employing a scan rate of 900 mV/s and maintaining 160 cycles produced the greatest response from the PPy-NW/Cu electrode (Figure 23c). Firstly, the copper redox chemistry peaks (R1 and R2) were significantly more pronounced, which was indicative of a greater exposed surface area of copper deposits. Secondly, the capacitive region of the nanowire polymer at ~-0.500 V reached 0.80 mA/cm^2 compared to 0.40 mA/cm^2 for the 600 mV/s deposition experiments. Most significantly, a large nitrate reduction peak was generated at -1.080 V with a magnitude of -1.39 mA/cm^2. This compares to -0.38 mA/cm^2 for the PPy-NW/Cu electrode produced at 600 mV/s. Inspection of the SEM micrograph reveals the copper deposits were present with an average diameter of ~500 nm dispersed in a homogeneous distribution. No bulk deposition was present and the nanowires were clearly exposed through the embedded copper. These results outline that the PPy-NW/Cu nanocomposite was more effective when the deposited copper was in nano dimensions. This allowed for a greater catalytic ability from the nanoparticles, which were combined with the increased surface area of the exposed polymer nanowires.

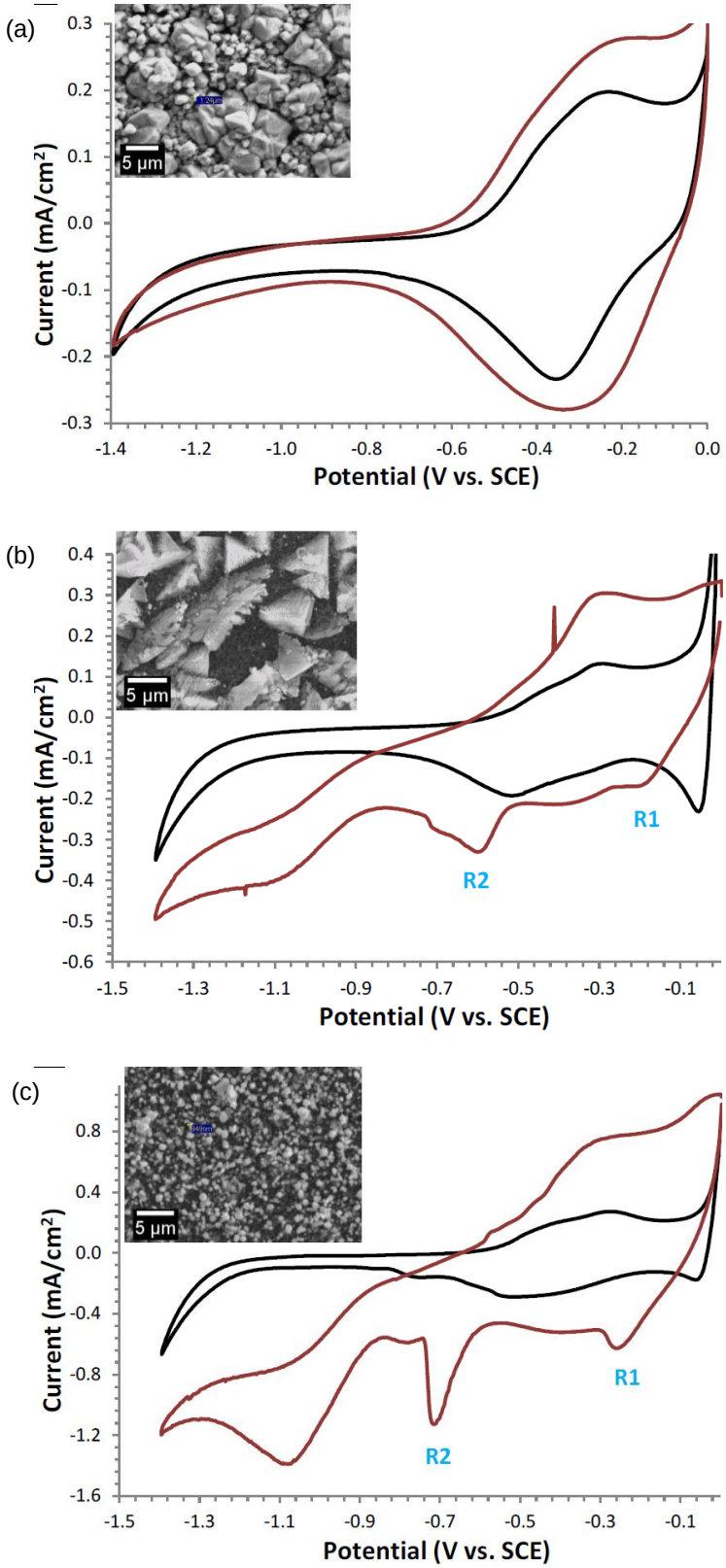

Figure 23. Cu deposited at PPy/Cu electrode for 160 cycles at (a) 300, (b) 600 and (c) 900 mV/s in 0.05 M $CuCl_2$ in 0.05 M H_2SO_4 then cycled in 0.005 M $NaNO_3$ at 20 mV/s between 0.0 - 1.4 V. Black trace is background cycle in 0.1 M Na_2SO_4 free of $NaNO_3$.

The reproducibility of this system using an n=3 produced a standard deviation of 5.08 $x10^{-5}$ mA/cm^{-2}, with a percentage error of 1.59%. However, the GC/Cu electrode was more sensitive than the PPy-NW/Cu electrode, as it recorded larger currents for the electroreduction of 0.005 M nitrate under the same conditions. In Figure 24, it can be seen that the GC/Cu electrode has a current magnitude of -2.3 mA/cm^2, almost double the -1.39 mA/cm^2 for the PPy-NW/Cu nanocomposite. Therefore, the PPy-NW/Cu electrode was not as effective at reducing the nitrate ion compared to the GC/Cu electrode. After several attempts to increase the sensitivity by altering the copper loading, it was apparent that the PPy nanowires were impeding the reduction reaction in some way. It was possible that the nanowires were more insulating than the GC/Cu substrate but if this was indeed the case, the nitrate peak would shift to larger overpotentials. While a slight shift was observed, it was not significant. The PPy-NW electrode, despite the large surface area compared to the bare GC, performed as if it had a lower amount of effective copper present. This was a contradictory observation, since SEM analysis shows nanoparticles of copper embedded on the PPy nanowires, suggesting a high surface area.

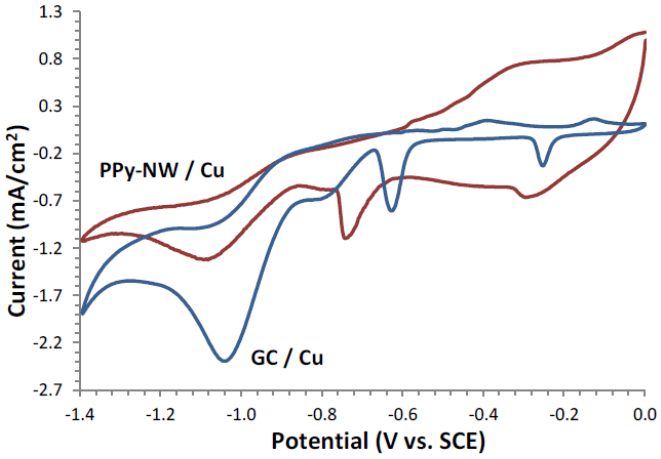

Figure 24. Cu deposited at electrodes for 160 cycles at 900 mV/s in 0.05 M $CuCl_2$ in 0.05 M H_2SO_4 at a GC/Cu electrode and a PPy-NW/Cu electrode, then cycled in 0.005 M $NaNO_3$ at 20 mV/s between 0.0 and -1.4 V.

It was concluded that the sensitivity of the PPy-NW/Cu electrode was not as high as the GC/Cu electrode due to the carbonate interference. However, despite this, the electrode did have an increased stability over a larger number of cycles compared to the GC/Cu electrode. This was possibly due to the GC/Cu electrode slowly dissolving the active copper from the electrode as it was cycled to oxidative potentials. This process would be reduced in the PPy system since PPy and Cu can form a charge transfer process, which would stabilise the Cu within the polymer matrix (Liu et al., 2002). This would suggest that the PPy nanowire composite would be suited to repetitive testing without as much degradation of the copper catalyst as compared to a GC electrode.

2.3 The Electrochemical Characterisation of Carbon-based Nanomaterials and their Applications in the Detection of Heavy Metal Ions

2.3.1 Introduction

The aim of this research was to produce new electrochemical sensors for the potential detection of two specific metal ion pollutants; chromium, in the form of Cr(VI), and copper in the form of Cu(II). The use of carbon-based nanomaterials in electrochemical sensors was investigated; namely multi-walled carbon nanotubes (MWCNTs) and graphene. The use of MWCNTs in the detection of both Cr(VI) and Cu(II) was explored and they are electrochemically characterised using a potassium ferricyanide probe. Many variations of a MWCNTs-based electrochemical sensor were explored in the detection of Cr(VI); namely the use of polymers and nanoparticles. In the detection of Cu(II), the use of ligand-metal complexation was investigated as a means of electrochemical detection and the use of MWCNTs to enhance the sensitivity of detection was explored.

2.3.2 The Electrochemical Characterisation of Electrodes Modified with Multi-walled Carbon Nanotubes

In the preparation of the modified electrodes, a glassy carbon electrode (GCE) was prepared for each experiment by polishing with diamond paste. The MWCNT samples were prepared by adding 10 mg MWCNTs to 1 mL DMF. The non-sonicated samples were inverted several times to mix the suspension and the sonicated samples were subjected to 30 minutes' sonication to disperse the nanotubes. The GCE was modified by drop-casting a specific volume of the MWCNT sample on the polished surface and the electrode was dried at room temperature or with the aid of an infra-red (IR) lamp.

The FTIR spectra of MWCNTs sonicated for 30 minutes in DMF and non-sonicated (pristine) are compared in Figure 25. Both samples were prepared as KBr disks and exhibit large O-H stretches with bands at 3433 cm^{-1} and 1632 cm^{-1} due to the absorbance of water, and a less intense peak at 1385 cm^{-1} that can be identified as a standard impurity in the KBr used in preparing the samples. The presence of DMF in both sonicated and non-sonicated samples was apparent by the absorbance bands representing $C\text{-}H_2$ between 2849 and 2959 cm^{-1}, and by the band representing an N-H vibration at 805 cm^{-1}. Surprisingly, the absorbance of the C=O component of DMF at 1680 cm^{-1} was absent. The DMF is known to adsorb on the nanotube surface via hydrophobic or π-π interactions, which could have caused this bond to weaken, leading it to be shifted and masked by the water absorbance in the same region. The bands between 2849 and 2959 cm^{-1} and at 805 cm^{-1}, however, provide an indication that some DMF had adsorbed onto the MWCNTs in both the sonicated and non-sonicated samples. The increase in oxygenated species on MWCNTs with sonication was identified by a small C=O band at 1723 cm^{-1}, which was not visible in the non-sonicated sample. As the band was of low intensity, it shows that sonication in DMF does not drastically increase the content of oxygenated moieties in the MWCNTs sample in comparison to modification of MWCNTs surfaces, for example, with -COOH groups using acid treatment.

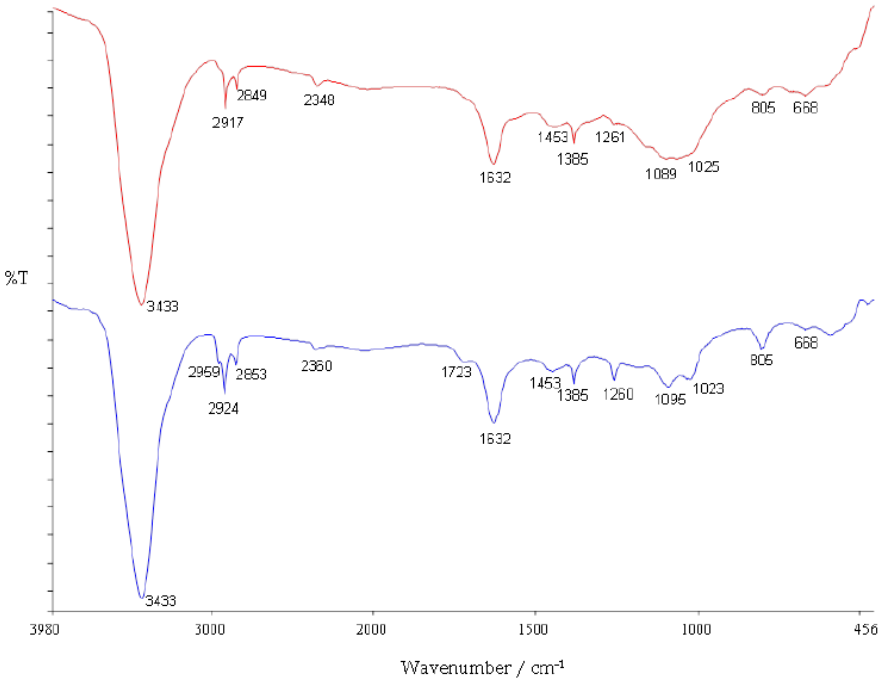

Figure 25. FTIR spectra of — non-sonicated MWCNTs and — MWCNTs sonicated for 30 minutes in DMF.

SEM imaging of the modified surfaces was used to highlight the effect of sonication on the morphology of the resultant castings. The images in Figures 26a and 26b compare the morphologies of GCEs modified with 20 µL non-sonicated and sonicated MWCNTs at a low magnification, showing the overall increased coverage obtained by sonication of the MWCNTs. The non-sonicated sample exhibited large agglomerations of MWCNTs on the GCE surface, whereas the sonicated sample showed more evidence of networking between the smaller agglomerations of MWCNTs. Increased magnification showed that the non-sonicated sample had a more compact structure in comparison to the loosely entangled sonicated MWCNTs. It was found that the structure of the sonicated MWCNTs had individual MWCNTs visible, indicating that reasonable dispersion was achieved with gentle shaking of the sample in DMF. The images suggest an increased surface area of the sonicated MWCNTs due to the separation of the large agglomerations, in comparison to the slightly more dense-packed structure of the non-sonicated MWCNTs.

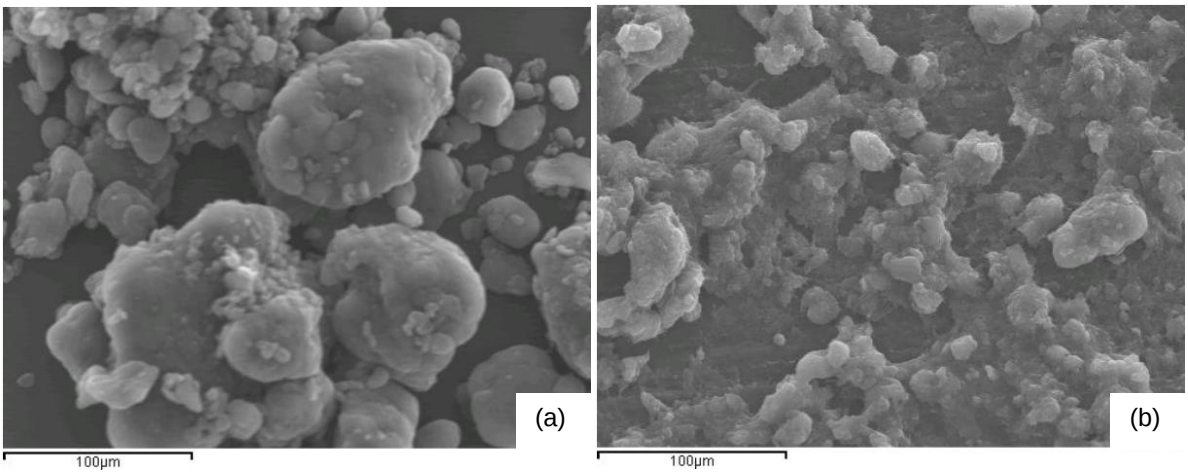

Figure 26. SEM micrographs of GCE modified with 20 µL 10 mg mL^{-1} MWCNTs in DMF. (a) non-sonicated MWCNTs and (b) sonicated samples.

EDX analysis was carried out on the modified electrode surface, and the recorded spectra showed evidence of cobalt and chlorine impurities which can arise from the metal catalysts used in the production of MWCNTs. The Au peaks observed in the spectra are due to the pre-treatment of the electrodes with Au sputter-coating to prevent charging of the surface. No differences were seen in comparing the non-sonicated sample to the sonicated sample.

To gain information about the electron transfer abilities of electrodes, redox reactions at the electrolyte interface are often analysed. The electrochemical probe used in this set of experiments was the redox couple $[Fe(CN)_6]^{3-}$ /$[Fe(CN)_6]^{4-}$. Cyclic voltammetry in 1.00×10^{-3} M $K_3Fe(CN)_6$ was performed on the electrodes prior to modification, to provide a comparison for the modified surfaces. The substrates were then replenished and cast with 5, 10, 15 or 20 µL of the 10 mg mL^{-1} MWCNTs/DMF samples. In both cases, the volume cast was used to give a rough estimation of the mass of MWCNTs on the GC surface. The reproducibility of the results using various casting volumes indicate that, in both cases, the MWCNTs were reasonably well dispersed throughout the solvent, and it was estimated that 5 µL of the MWCNTs sample would result in approximately 0.05 mg MWCNTs on the GC surface. This solution was also used to provide background currents for each voltammogram, ensuring that any peaks or waves observed were a result of the $[Fe(CN)_6]^{3-}$ /$[Fe(CN)_6]^{4-}$ couple. The peak potentials (Ep) and peak currents (Ip) of the redox probe were measured. Cyclic voltammograms illustrating the redox behaviour of $[Fe(CN)_6]^{3-}$/$[Fe(CN)_6]^{4-}$ at the modified electrodes can be seen in Figure 27, which compares GCEs modified with both non-sonicated and sonicated MWCNTs to the bare GCE. An increase in faradaic currents with both modifications of glassy carbon is apparent from these voltammograms, suggesting an increased surface area with enhanced electrochemical activity.

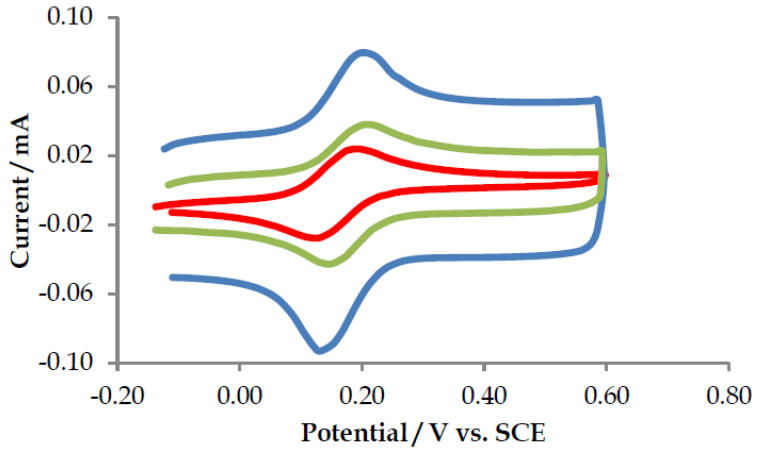

Figure 27. Cyclic voltammograms comparing GCE which is — unmodified, — modified with 5 µL non-sonicated MWCNTs (10 mg mL^{-1}) and — modified with 5 µL sonicated MWCNTs (10 mg mL^{-1}). All electrodes were cycled in 1.00 × 10^{-3} M $[Fe(CN)_6]^{3-}$/$[Fe(CN)_6]^{4-}$, with 0.05 M KCl and 0.05 M KH_2PO_4 as a supporting electrolyte system, at a scan rate of 100 mV/s.

In analysing the voltammograms of GCEs modified with various casting volumes (5, 10, 15 and 20 µL) of both samples, slight increases were observed in the faradaic currents of $[Fe(CN)_6]^{3-}$/$[Fe(CN)_6]^{4-}$ with additions of 5 to 15 µL of non-sonicated MWCNTs. In particular, the anodic peak currents increased steadily from 2.38 × 10^{-5} A at the bare electrode to 3.13 × 10^{-5} A at the GCE modified with 15 µL non-sonicated MWCNTs but did not further increase at the 20 µL casting. The slight enhancement of the peak current can possibly be attributed to a small increase in the electroactive surface area of the modified electrode. The diffusion process at the modified electrodes was investigated and it was found that a diffusional process is predominantly occurring for the redox couple of $[Fe(CN)_6]^{3-}$/$[Fe(CN)_6]^{4-}$. Confirmation of the diffusional nature of this process was further supported by the linearity observed in plotting the peak current (*Ip*) against the square root of the scan rate (√v). In monitoring the peak currents against cycle number, it was found that they were stable and did not steadily increase with time, which also discounted any significant adsorption at the electrodes modified with sonicated MWCNTs samples. These observations coincide with the observed diffusive tail seen in cyclic voltammograms, confirming that adsorption to the nanotube surface is unlikely. As the diffusional nature of this system appears to be prevalent, it is likely that the diffusion through bulk solution and thin films are dominant factors in electron transfer at these modified electrodes. In terms of electrodes modified with MWCNTs, it has been proposed that probe molecules or analytes can diffuse into “pockets” which form between networked nanotubes on the electrode surface. As the species is trapped at the electrode surface, it does not diffuse back into the bulk solution, as it would for semi-infinite diffusion, making electron transfer more efficient. Thin layer diffusion results in a small peak separation and is dependent on many factors, such as the thickness of the thin layer. The small peak separation observed under certain conditions can be due to the contribution of thin layer diffusion. Thin layer diffusion might be expected to have a bigger effect for the non-sonicated MWCNTS, as an increase in the size of the thin layer “pockets” should occur in the sonicated MWCNTs agglomerations. It has been reported that an increase in the thin layer size will shift the anodic potential to more oxidative

potentials as the electron transfer becomes more difficult (Streeter et al., 2008). By comparing the peak separations at each scan rate for the bare GCE to that modified with a sonicated sample of MWCNTs, the largest difference between the electrodes is seen at the slower scan rates. At higher scan rates, the modified and bare electrodes behaved similarly, showing the contribution from semi-infinite planar diffusion for the GCE modified with sonicated MWCNTs. This suggests that the thin layer diffusion process is an important contribution to fast electron transfer at MWCNTs used in this work, and that slow scan rates and low casting volume are required to allow for the diffusion to occur in the sonicated sample.

2.3.3 The Electrochemical Characterisation of Electrodes Modified with Graphene

Glassy carbon (GC) and Platinum (Pt) pencil-style working electrodes of three mm diameter were prepared for use by polishing with alumina slurry (1.00, 0.30 and 0.05 µm grades). Highly ordered pyrolytic graphite (HOPG) was used to construct a basal plane HOPG working electrode as a comparative substrate. The quality of the basal plane HOPG was ensured by stripping defected layers from the surface with adhesive tape, rinsing with EtOH and drying with N_2. Graphene samples were prepared from 10 mg mL^{-1} suspensions in DMF, whereby non-sonicated samples were inverted to achieve their maximum dispersion without the aid of sonication, and sonicated samples were dispersed using sonication for 30 minutes. The modified electrodes were prepared by drop-casting five or 10 µL aliquots of the sample on the surface of the prepared working electrode and drying in an oven at 45°C for 10 minutes. Cyclic voltammetry was carried out using the ferricyanide probe, as described in Section 2.3.2.

The cyclic voltammograms in Figure 28 compare results obtained at bare GC to the GC electrode modified with non-sonicated graphene in $[Fe(CN)_6]^{3-}/[Fe(CN)_6]^{4-}$ at 100 mV/s. There was a distinct decrease in the peak currents by modification of GCE with non-sonicated graphene, which can be seen in Figure 28a. The average anodic peak current measured at the bare GCE was 0.013 mA, which decreased to 0.004 mA (n=3) upon modification with 5 µL of the non-sonicated graphene sample. The significance of this decrease was confirmed using a t-test ($t=10.04$, d.f.=5, $P<0.001$) and suggested that poorly dispersed graphene resulted in a lower active surface area of the modified electrode. Contrastingly, Figure 28b shows an increase in faradaic currents at the GCE modified with sonicated graphene, with the average anodic peak current (n=4) increased to 0.016 mA. This slight increase was likely due to the increased surface area of the dispersed graphene sheets, as was similarly shown for sonicated MWCNTs samples. However, the difference observed between the GCE modified with non-sonicated and sonicated graphene was significant ($t=7.130$, d.f.=5, $P < 0.001$), highlighting the effect of sonication on the graphene sample. The volume of graphene cast on GCE was also varied. It was found that by increasing the volume of non-sonicated material, the peak current varied insignificantly ($t=1.077$, d.f.=4, $P > 0.05$). For modification of the GCE with sonicated graphene, the peak currents were increased from 1.56×10^{-5} A for 5 µL casting to 1.68×10^{-4} A upon modification with 10 µL. Statistical analysis of these data, however, again showed no significance in this increase ($t=0.6078$, d.f.=6, $P > 0.05$), indicating that the increased volume did not significantly increase the active surface area of the modified electrode.

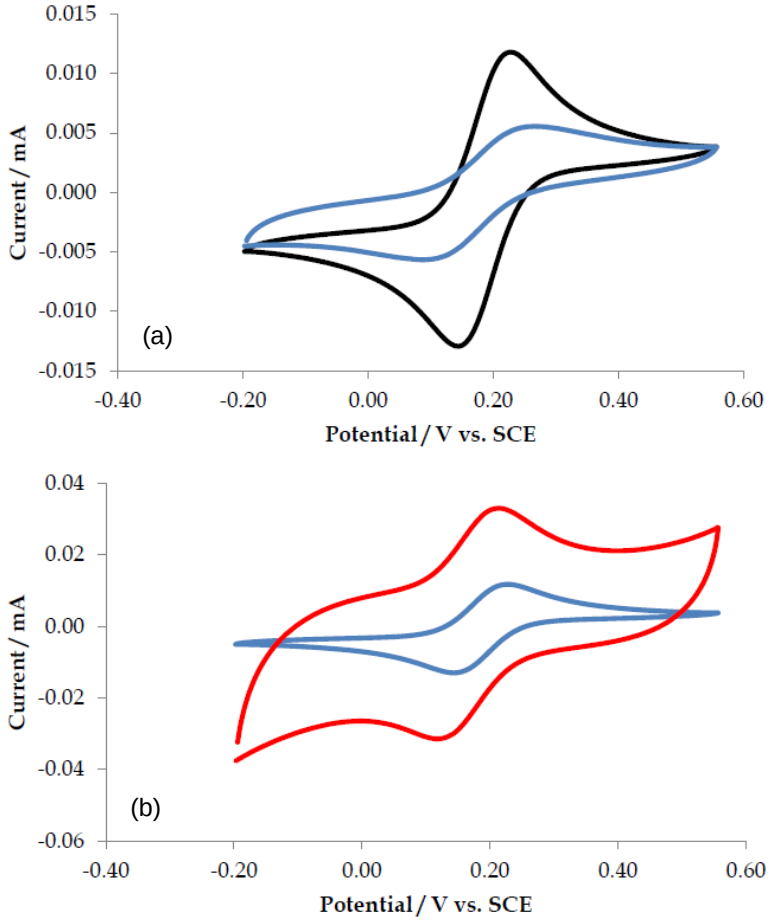

Figure 28. Cyclic voltammograms comparing 3 mm GCE (a) — bare to — modified with 5 µL non-sonicated graphene and (b) — bare to — modified with 5 µL sonicated graphene. All electrodes were cycled in 1.00 × 10^{-3} M $[Fe(CN)_6]^{3-}$/$[Fe(CN)_6]^{4-}$ with 0.05 M KCl and 0.05 M KH_2PO_4 as a supporting electrolyte system, at a scan rate of 100 mV/s.

High resolution micrographs obtained of the cast graphene samples can be seen in Figures 29a and 29b. The images show agglomeration of the carbon material without sonication (Figure 29a), and the image in Figure 29b highlights that some order was achieved in the sample by sonication.

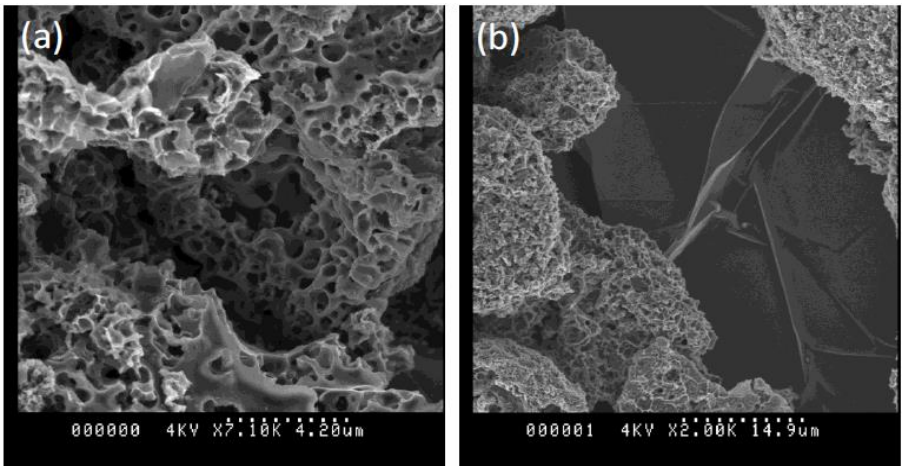

Figure 29. SEM images for (a) non-sonicated and (b) sonicated graphene samples.

2.3.4 The Electrochemical Detection of Cr(VI) using Electrodes Modified with Multi-walled Carbon Nanotubes

The electrochemical detection of Cr(VI) in this work was based on its reduction to the less toxic Cr(III) using cyclic voltammetry. As the reduction reaction is favoured in acidic solutions, it was initially carried out in an aqueous media of H_2SO_4 at pH 2.0. The detection of this reduction was compared at a bare glassy carbon electrode (GCE) and the MWCNTs modified GCE (GCE/MWCNTs). The electrodes were firstly cycled in the supporting electrolyte solution without Cr(VI) to obtain stable background readings and the voltammograms were recorded between -0.25 and +0.90 V, at 10 mV/s. The detection of 6.00×10^{-4} M Cr(VI) at both bare GCE and at GCE/MWCNTs is compared in Figure 30, and the average (n=4) peak position (E_p) and peak current (I_p) values are tabulated inset. The bare GCE showed a broad reduction peak at approximately. 0.25 V. Upon modification of the GCE with MWCNTs, a shift in peak position was observed to a more favourable position of 0.65 V, which could be attributed to the fast electron transfer properties of MWCNTs. In the reduction of Cr(VI) to Cr(III), many factors, such as the increased wettability of the surface and the presence of defects (Nugent et al., 2001), as well as the presence of oxygenated groups at defect sites on MWCNTs (Chou et al., 2005), may have contributed to this catalytic effect. Overall, the detection of Cr(VI) was enhanced at the MWCNTs surface in comparison to the bare GCE by the shift in peak potential of 0.40 V and the 5.7 fold increase in peak current. These results show that that the reduction of Cr(VI) to Cr(III) at the MWCNTs surface exhibited a more electrochemically reversible peak at a more favourable position in comparison to the bare GCE, therefore this modified electrode was promising for the detection of Cr(VI).

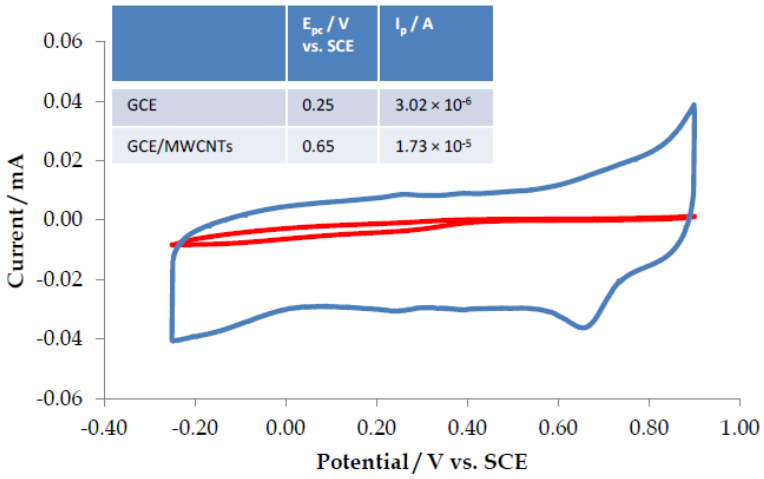

Figure 30. Cyclic voltammograms in 6.00×10^{-4} M Cr(VI) in H_2SO_4 pH 2.0, at 10 mV/s, of — bare GCE and — GCE modified with 20 µL 10 mg mL^{-1} MWCNTs in DMF. Average electrochemical properties are tabulated inset.

A study was conducted comparing the response at the GCE/MWCNTs electrode in electrolyte solutions of varying conductivities. To accurately compare the effects of such parameters on this reduction process, the data are compared from the 10th cycle in 1.00×10^{-3} M Cr(VI) with varying concentrations of Na_2SO_4 supporting electrolyte, and the pH was adjusted to 2.0 using

concentrated sulphuric acid. By altering the concentration of the supporting electrolyte, the conductivity of the solutions increased. However, this did not appear to affect the reduction peak potential of Cr(VI) at the modified electrode to the same extent. Statistical analysis showed, in this case, that the overall difference between the peak potentials was significant (F=11.33; $d.f.$=2,10; $P < 0.01$). However, it was calculated that the difference between the potentials recorded in 0.10 and 0.20 M solutions specifically was insignificant, using Bonferroni post-hoc analysis. As the changes in peak potential did not correlate with the changes in conductivity, it appears that they were not necessarily related and the changes observed could be an effect of slight changes in the pH of the solution.

The peak currents for the reduction of Cr(VI) surprisingly appeared to correlatively decrease with increasing conductivity of the supporting electrolyte solution, which was also calculated to be significant (F=32.48; $d.f.$=2,10; $P < 0.0001$). Bonferroni post-hoc analysis in this case showed significant differences, ($P < 0.0001$) between 0.1 and 0.2 M solutions and ($P < 0.05$) between 0.1 and 0.15 M solutions of Na2SO4. This decrease in peak current was unexpected, as it is generally observed that an increase in conductivity would enhance the electron transfer kinetics in a solution, thus increasing the peak current. It can therefore be assumed that increasing the concentration of Na_2SO_4 may have led to some SO_4^{2-} adsorption on the MWCNTs.

The effect of pH on the reduction of Cr(VI) was investigated specifically from pH 1.9 to 4.8 at a GCE/MWCNTs electrode using Na_2SO_4 as a supporting electrolyte modified with appropriate amounts of concentrated H_2SO_4. A shift in peak potential from 0.65 to 0.44 V by increasing the pH from 1.9 to 2.4 was observed, which is characteristic of the decrease in H^+ concentration. By further increasing the pH of the solution to 2.8, the reduction peak decreased to 0.39 V, however, a second peak also appeared at this pH at 0.13 V. While comparing the reduction of Cr(VI) to Cr(III) at pH 4.8, 3.6 and at 2.8, only the second reduction peak was observed at the higher pH values. It was further observed that the peak potential decreased slightly from 0.13 V at pH 2.8, to 0.10 V at pH 3.6. It is noted that no further decrease in peak potential was seen in further increasing the pH to 4.8, indicating that Nernstian behaviour was not being followed. A reduction mechanism of Cr(VI) to Cr(III) was proposed by Welch et al. (2005), whereby the initial reduction of Cr(VI) occurred via a rate determining one electron transfer step to form Cr(V), seen in Equation 4. They suggested that at low pH levels, this Cr(V) can rapidly form Cr(III) via a disproportionation reaction, illustrated in Equations 5 and 6. They observed a pre-shoulder wave for the reduction of Cr(VI) at a GCE, similar to that observed in this study, in a 0.010 M HCl solution that they did not observe in 0.100 or 0.001 M HCl solutions. They attributed this shoulder peak to the reduction of Cr(VI) to Cr(V) and found it to be more electrochemically reversible than the more dominant reduction peak.

$Cr(VI) + e^- \leftrightarrow Cr(V)$ Equation 4

$2Cr(V) \leftrightarrow Cr(IV) + Cr(VI)$ Equation 5

$Cr(IV) + Cr(V) \leftrightarrow Cr(III) + Cr(VI)$

or

$2Cr(IV) \leftrightarrow Cr(III) + Cr(V)$ Equation 6

In the work shown here; at pH 1.9, it can be assumed that the high concentration of protons enabled the fast electron transfer at the MWCNTs modified electrode, which produced a voltammogram with one intense sharp reduction peak. It is therefore possible, that by increasing the pH of the solution to 2.8, the rate of reduction of Cr(VI) to Cr(V) decreased and was observed

as a pre-shoulder peak at 0.40 V. The rate of disproportionation of Cr(V) to Cr(III) was therefore also decreased so that the direct reduction of Cr(V) to Cr(III) was observed at 0.13 V. In comparing the voltammogram at pH 2.8 to those at pH 3.6 and 4.8, the rapid reduction of Cr(VI) to Cr(III) was observed with a successive decrease in peak potential. However, the pre-shoulder peak representing Cr(VI) reduction to Cr(V) was not observed at higher pH values. This was most likely because the initial reduction of Cr(VI) to Cr(V) is a slow, proton-dependent step. In a less acidic medium, this reaction would be less favourable and also be of small magnitude. Therefore the peak representing the reduction of Cr(VI) to Cr(V) would have shifted to lower potentials and would possibly occur at the same potential as the reduction of Cr(V) to Cr(III), and appeared as one reduction peak representing the entire process at 0.10 V for pH 3.6 and 4.8.

To evaluate the use of MWCNTs modified electrodes for their use in the detection of Cr(VI), their stability, selectivity and sensitivity were evaluated. This was carried out using a GCE modified with 20 µL of a 10 mg mL^{-1} sonicated dispersion of MWCNTs in DMF, cast on a four mm diameter GCE (GCE/MWCNTs). The electrode was then dried under an IR lamp. The detection of Cr(VI) was evaluated at this electrode from a solution of $Na_2CrO_7.2H_2O$ in H_2SO_4 at pH 2.0. The stability of the peak current for Cr(VI) reduction was monitored as a function of cycle number at the GCE/MWCNTs electrode using cyclic voltammetry. The modified electrode was cycled in 6.00×10^{-4} M Cr(VI) at 10 mV/s for 100 cycles. It was found that the current dropped by approximately 50% over the first 10 cycles until it reached a steady state, as displayed in Figure 31. The currents remained relatively constant at this point over the remaining 90 cycles, showing reasonable stability in the acidic solution. This suggested that the electrode was not spoiled by adsorbing molecules under these conditions. All current responses were therefore recorded after 10 cycles, to ensure a stable, reliable value.

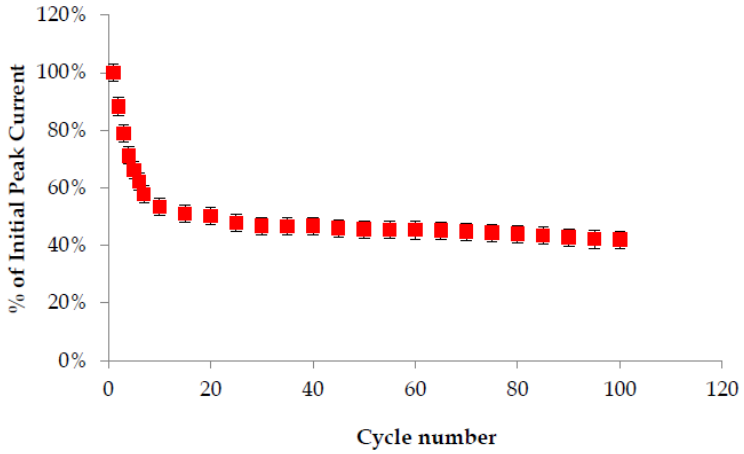

Figure 31. Plot representing the stability of the peak current for the reduction of 6.00×10^{-4} M Cr(VI) at 10 mV/s over 100 cycles (n=3) using GCE/MWCNTs. The currents are measured as a percentage of the initial magnitude of the peak and are plot as a function of cycle number.

The efficiency of the sensor in the presence of potentially interfering substances is very important, as the sensor response may be impaired or the electrode surface may be spoiled in real water samples. Nitrate (NO_3^-) pollution is widespread and therefore is very likely to be found in real water samples, according to recent reports from the EPA (Environmental Protection Agency, 2010), which show that, in Ireland, some exceedances of the NO_3^- mandatory limit were recorded in 2010. The presence of Cl^- in water is generally utilised as an indication of pollution from sewage or industrial effluent, therefore it is also likely to be present in contaminated water samples. The efficiency of the sensor in Cr(VI) reduction was also tested in the presence of Cu^{2+} ions, as both metal ions are known pollutants from similar industrial waste, for example electroplating and timber treatment facilities.

The GCE/MWCNTs modified electrodes were cycled in a solution containing 4.00×10^{-4} M Cr(VI) to provide an original reduction peak for comparison. The interferants were added to the sample solution in separate experiments and the concentration was increased gradually. The interferant solutions prepared were of relatively high concentration and contained both the supporting electrolyte and 4.00×10^{-4} M Cr(VI), to ensure the composition of the sample solution was not greatly altered. The stability of the sensor at the parametric concentration of each interfering substance was tested by continuous cycling, without further addition of the interfering solution. In all cases, the peak potential of Cr(VI) reduction to Cr(III) did not shift with varying concentrations of interferants, which indicated that the substances did not interfere with the reduction process. The peak currents were also investigated with varying concentrations of each interferant. The recorded data were analysed by comparing the peak current (*Ip*) measured after each addition of interferant and measuring it as a percentage of the original peak current (recorded prior to the addition of the interferant), according to Equation 7.

$$\%\ of\ original\ Ip = \frac{Ip\ (CrVI+Interferent)}{Ip\ (CrVI)} \times 100$$

Equation 7

The effect of Cl^- on the reduction of Cr(VI) can be seen in Figure 32a. As the sites of Cr(VI) contamination are generally inland, the concentration of Cl^- is not expected to exceed the parametric value specified by the EPA which takes into account areas of high Cl^-, such as coastal areas. The concentrations utilised in this study, however, ranged from 0.0 to 9.0×10^{-3} M Cl^- to take any exceeding values into account. There was a slight decrease observed in *Ip* to approximately 75% of the original value with the addition of 2.0×10^{-3} M Cl^-, however, the currents remained stable with further additions of Cl^-, which suggested that the modified electrode was not greatly affected by this ion. The interference of Cu^{2+} ions was tested from 0.0 to 4.2×10^{-5} M, as the parametric limit for copper in drinking water is approximately 3.20×10^{-5} M, as set by the EPA Drinking Water Regulations. The data obtained in this range are presented in Figure 32b, where it can be seen that the stability of the peak current was slightly increased by the presence of this substance until the parametric value was exceeded. Further statistical analysis found that the addition of 6.00×10^{-6} to 4.20×10^{-5} M concentrations of Cu^{2+} had no significant effect on the Cr(VI) reduction peak current with $P > 0.05$ in all cases. The addition of NO_3^- ion to the Cr(VI) solution was monitored over the concentration range 0.0 to 7.0×10^{-4} M. There was some increase in peak current in the case of this substance, suggesting it interfered with the detection of Cr(VI). As can be seen in Figure 32c, the currents increased to approximately 120% of the original peak current after addition of relatively low concentrations of nitrate. The

currents decreased with further increase in NO_3^- concentration and, at higher concentrations, the currents increased greatly, with large errors recorded between repeated experiments. This variable response can be explained by possible adsorption of NO_3^- to the electrode surface. This indicated that for this modified electrode to work efficiently in the detection of Cr(VI), any nitrate contamination of the sample should be firstly removed.

To assess the limits of detection for Cr(VI) at GCE/MWCNTs, a calibration curve was constructed by plotting the peak current response from cyclic voltammetry against Cr(VI) concentration. The calibration curve was constructed for Cr(VI) at pH 2.0 and a linear relationship was observed. The limit of detection (LOD) at this electrode was determined to be 2.07×10^{-4} M, which is significantly higher than the mandatory limit of 5.2×10^{-6} M set by the EPA. This high LOD can be explained by the poor linearity observed at lower concentrations of Cr(VI).

Real water samples were tested after modification with concentrated H_2SO_4 to obtain a pH level of 2.0, as this level provided the largest current response for the reduction of Cr(VI). Samples were tested with the addition of various concentrations of Cr(VI) and exhibited reduction peaks at 0.57 V, as was also seen in laboratory-prepared samples. However, poor reproducibility was observed in both cases, which signifies that the water samples were unsuitable for the electrochemical detection of Cr(VI), possibly due to the solid content which may have adsorbed some of the Cr(VI).

Further studies were carried out to investigate if the electrochemical response analysed in previously could be enhanced to improve the detection of Cr(VI). This was done by the preparation and characterisation of various electrode materials and a voltammetric study, to screen their ability to sense Cr(VI). The most promising of these materials were found to be a gold electrode modified with MWCNTs (i.e. the material of the base electrode was changed, Au/MWCNTs) and also a gold electrode modified with MWCNTs and gold nanoparticles (Au/MWCNTs/Au NPs).

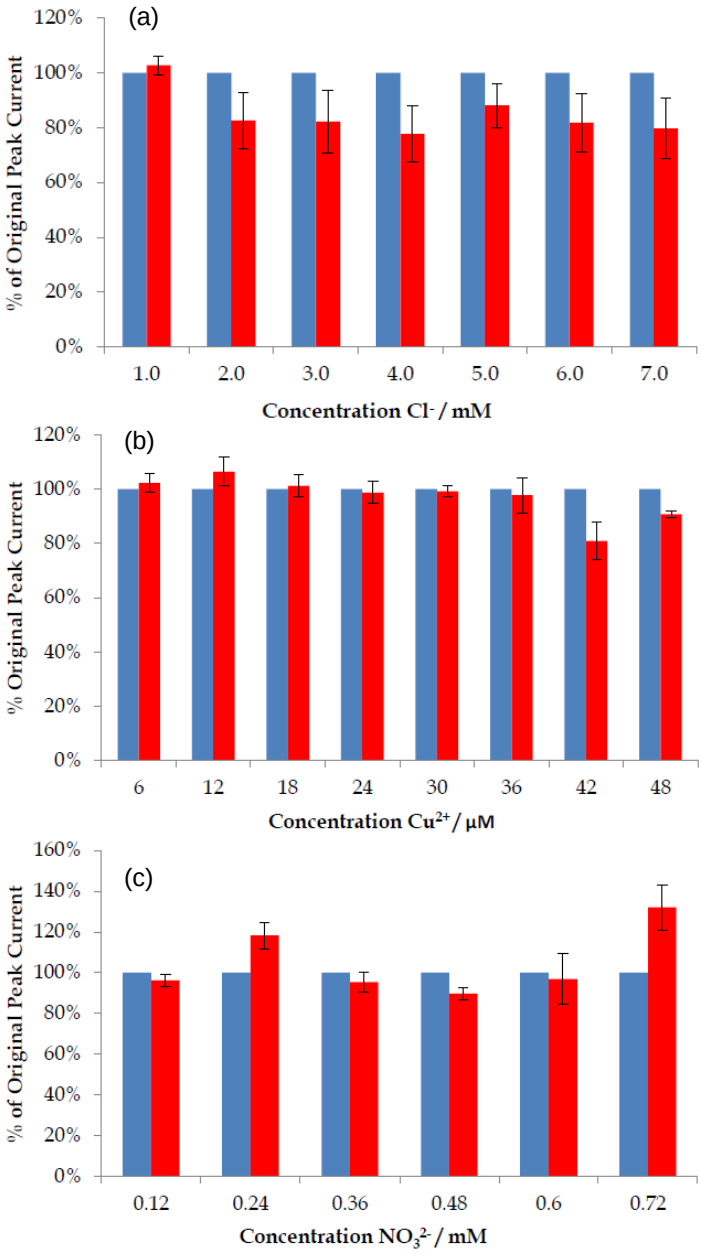

Figure 32. Stability of peak current for the reduction of 4.00×10^{-4} M Cr(VI) at 10 mV/s ■ with increasing concentration of interferant and ■ without interferant for (a) Cl^-, (b) Cu^{2+} and (c) NO_3^-.

The reduction of Cr(VI) at the Au/MWCNTs electrode is compared to that at a bare Au electrode in Figure 33, with the relevant properties tabulated inset. The reduction peak appears at 0.41 V at the bare Au electrode, which shows a more efficient reduction of Cr(VI) in comparison to that seen at the bare GCE, as it appears at a more favourable potential and appears to be more electrochemically reversible, with a more symmetrical and intense peak. The reduction peak at the Au/MWCNTs electrode appears at a more favourable potential of 0.57 V in comparison to that seen at the bare electrode, however, the peak currents in this case appear to be enhanced only by 1.6 fold at the electrode modified with MWCNTs. The reversible peaks at approximately 0.40 V are visible again at the Au/MWCNTs electrode due to the presence of oxygen containing molecules.

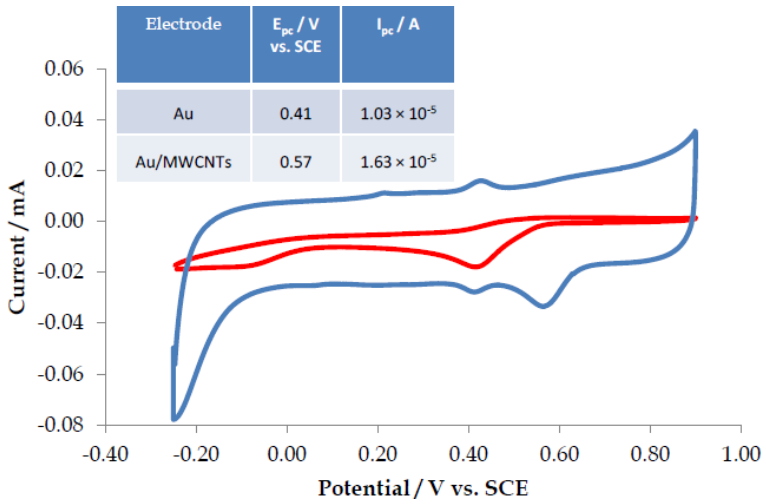

Figure 33. Cyclic voltammograms of — bare Au and — Au modified with 20 µL 10 mg mL^{-1} MWCNTs in DMF recorded in 5.0 × 10^{-4} M Cr(VI) in H_2SO_4 pH 2.0, at 10 mV/s. The relevant electrochemical properties are tabulated inset.

In the preparation of MWCNTs/AuNPs, the pristine MWCNTs were used as received and, in the case of MWCNTsOx/AuNPs, the MWCNTs were acid treated to modify any defect areas with oxygen containing functional groups. The MWCNTsOx and pristine MWCNTs were both firstly dispersed in SDS by sonication in highly concentrated solutions (1% w/v). This step provided well-dispersed suspensions and is likely to have provided nucleation sites for the AuNPs to form. The AuNPs were formed by the addition of an aqueous solution of HAuCl4 to the MWCNTs suspension under vigorous stirring, and the subsequent slow addition of $NaBH_4$ aqueous solution. The modified suspension was then filtered and rinsed with copious amounts of H_2O. The MWCNTsOx/AuNPs were characterised physically using transmission electron microscopy (TEM) and both the MWCNTs/AuNPs and MWCNTsOx/AuNPs were characterised using atomic absorption (A.A.) spectroscopy. It was found using A.A. spectroscopy that the MWCNTsOx/AuNPs samples used in this work consisted of 2% wt. Au and the MWCNTs/AuNPs samples consisted of 1% wt. The TEM images taken at various magnifications can be seen in Figure 34. It was found using this sensitive imaging, coupled with EDX analysis, that the MWCNTsOx were indeed decorated with AuNPs. The distribution of the particle sizes (diameter) was analysed, and it was found that the majority of the particles measured were 7.5 nm in diameter; and the range of sizes was 5.5 to 12.5 nm. This analysis is direct evidence that the Au particles used to modify the MWCNTs were nanoparticulate.

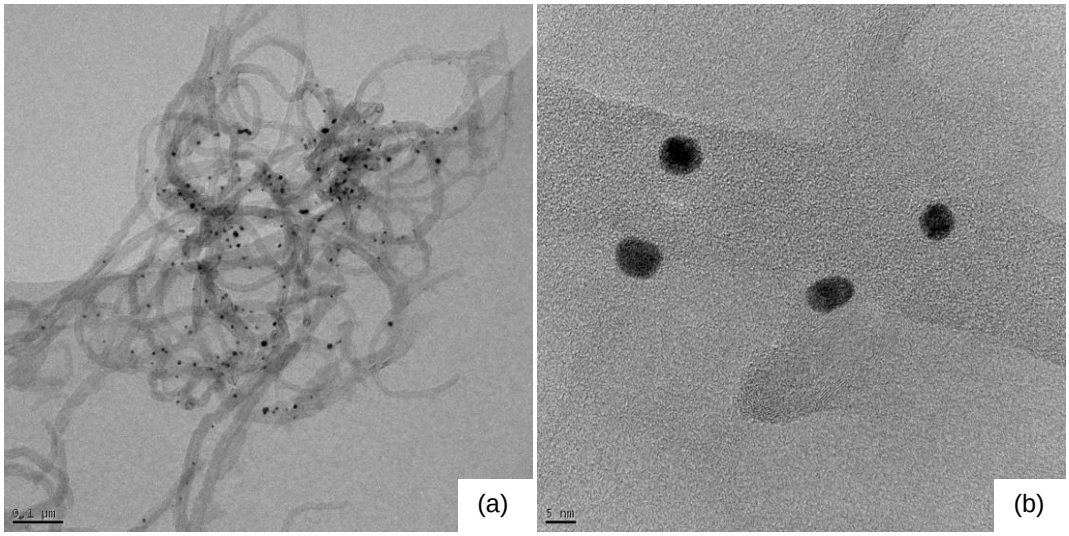

Figure 34. (a) and (b) TEM images of MWCNTsOx/AuNPs at various magnifications.

The MWCNTsOx/AuNPs and MWCNTs/AuNPs suspensions were prepared by dispersing 10 mg mL^{-1} modified MWCNTs in DMF via sonication for 30 minutes. The Au electrodes were then drop-cast with 20 µL MWCNTsOx/AuNPs or MWCNTs/AuNPs and dried under an IR lamp. The voltammetric response of MWCNTsOx/AuNPs and MWCNTs/AuNPs is compared in Figure 35 in the reduction of 5.00×10^{-4} M Cr(VI) in H_2SO_4 at pH 2.0, with the peak potentials and currents tabulated inset. The broad redox pair at 0.20/0.30 V, seen at the MWCNTsOx/AuNPs modified electrode, most probably arose from the oxygen functionalities on the oxidised MWCNTs, as has previously been reported in the literature (Welch et al., 2005). There was no clear reduction peak observed at this modified electrode, likely as a result of this redox pair masking the peak. However, rough estimates of both peak potential and peak current were made from the voltammogram. The approximate peak position of 0.52 V and peak current of 8.11×10^{-6} A appear to be lower than those seen at the MWCNTs/AuNPs. It would appear, however, that cyclic voltammetry was unsuitable for the detection of Cr(VI) at the MWCNTsOx/AuNPs modified electrode.

A clear reduction peak was observed at the electrode modified with MWCNTs/AuNPs, where it is of note that there was a shift in peak position from 0.56 V at bare MWCNTs to 0.60 V at MWCNTs/AuNPs. This indicates that some sensing occurred at both the AuNPs surface and the MWCNTs, which resulted in a lower over-potential than for the MWCNTs alone. The peak currents in this case were 8.92×10^{-6} A for the reduction of 5.0×10^{-4} M Cr(VI).

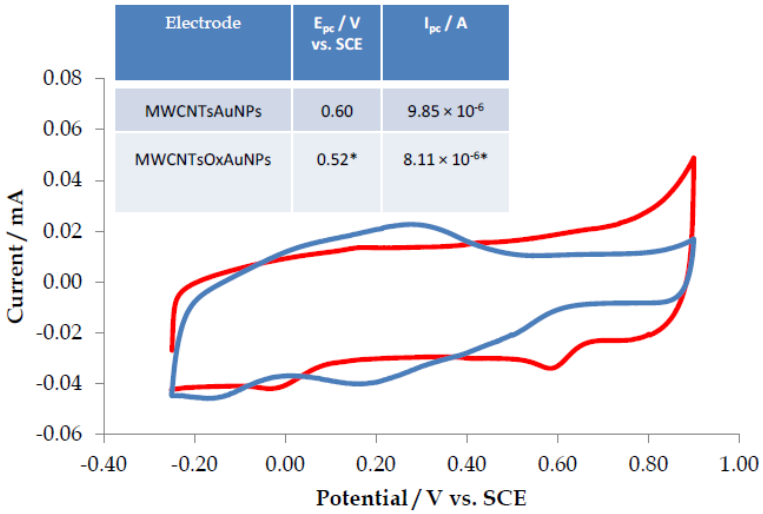

Figure 35. Cyclic voltammograms of modified gold electrodes in a 5.0 × 10^{-4} M Cr(VI) in H_2SO_4 (pH 2.0) at 10 mV/s. Plot shows gold electrode modified with — MWCNTsOx/AuNPs compared to — MWCNTs/AuNPs. The relevant electrochemical properties are tabulated inset. *Approximate peak position and current values were determined from cyclic voltammetry.

In order to further investigate this system and overcome the limitations presented by cyclic voltammetry, various other electrochemical techniques were considered. Other electrochemical techniques were also investigated in order to improve the LODs of the MWCNTs modified electrode.

The use of rotating disc voltammetry and constant potential amperometry are shown in this section, to lower the limit of Cr(VI) detection at the various electrodes. The use of rotating disc electrodes in electrochemical detection is often implemented to aid in the transport of the analyte to the electrode surface, by removing diffusion limitations by means of convection. This technique could therefore possibly be utilised to enhance diffusion of an analyte through the mesoporous MWCNTs layer. This technique is generally coupled with constant potential amperometry, as the sufficient transport of the analyte to the surface ensures a consistent supply from the bulk solution, which therefore can provide sensitive detection. A calibration curve was constructed of the bare Au rotating disc electrode at the rotation speed of 1900 rpm. It was found that the bare electrode exhibited poor reproducibility, causing the plot to deviate from linearity at lower concentrations. A LOD of 5.07 × 10^{-5} M was calculated from the linear region of the plot at the bare Au substrate, using this technique. A gold rotating disc electrode, modified with MWCNTs (20 µL 10 mg mL^{-1} MWCNTs/DMF), was also tested using constant potential amperometry to introduce convection in the electrochemical cell. A constant potential of 0.40 V was applied to the Au/MWCNTs electrode, to ensure a sufficient over-potential was applied to achieve complete conversion of Cr(VI) to Cr(III), based on the previous cyclic voltammetry experiments. A calibration curve was then constructed for the Au/MWCNTs electrode using constant potential amperometry at 0.40 V on a rotating disc at 1900 rpm. A linear response with good reproducibility was produced using this technique and lower LOD of 2.22 × 10^{-6} M Cr(VI) was achieved. The physical characterisation of the modified MWCNTs showed that MWCNTsOx/AuNPs had a higher loading of Au than the pristine MWCNT/AuNPs, therefore the MWCNTsOx/AuNPs were solely

investigated in this case. A calibration curve was constructed of the Au/MWCNTsOx/AuNPs electrode and a LOD of 1.20 × 10^{-6} M was calculated, at a constant potential of 0.40 V and a rotation speed of 1900 rpm, which is in the region of the mandatory limits set by the EPA. The excellent reproducibility of this modified electrode is highlighted by the small error bars and linear current response. The lower limit of detection can be attributed to the increased amount of AuNPs (2% wt.), which are known to act as electron antennae in electrochemical sensing.

2.3.5 The Electrochemical Detection of Cu(II) in Aqueous Solutions using N,N-Diethyldithiocarbamate

Copper is a transition metal that is found naturally in some rock sediments and forms monovalent and divalent cations in solution. Copper pollution generally stems from anthropogenic uses, such as copper piping and wiring, where it can be leached into drinking water. Although it is an essential dietary requirement, it can cause organoleptic (taste) problems when ingested at levels above 1 mg L^{-1}. At lower doses, it can cause symptoms typical of food poisoning, and the acute lethal dose for adults lies between 1 and 400 mg of copper (II) per kg of body weight (Clenaghan and O'Neill, 2005). As copper is found naturally in the environment at low concentrations, its sensitive detection is very important. The EPA has thus imposed a parametric value, i.e. a mandatory limit, of 3.15 × 10^{-5} M Cu(II) in drinking water in Ireland. For the most part, copper is detected using techniques such as ICP-MS, which are expensive, time-consuming and do not provide real-time analysis. The development of electrochemical sensors for metal ion detection would allow for simple, on-site detection with remote access to data, potentially making it a very attractive technique for environmental monitoring.

Herein, both a glassy carbon electrode (GCE) and platinum (Pt) mesh electrode were modified with a diethyl-dithiocarbamate (DDC) ligand. Dithiocarbamates are simple analogues of carbamates, whereby both oxygen atoms are replaced by sulphur atoms. They have been investigated for several decades in the detection of copper, as the sulphur atoms are known to co-ordinate with transition metal cations (Kamata et al., 1989). They are known to form highly stable complexes with copper, in particular copper diethyl-dithiocarbamate ($Cu(DDC)_2$). The complex is poorly soluble in water (log *ksp*=-31), which was beneficial in this work, as the complex formed on the electrode surface and was not easily leached into the aqueous sample solution. The detection of Cu(II) in this work is based on the formation of the $Cu(DDC)_2$ complex at the electrode surface, using cyclic voltammetry to detect the presence of copper. The $Cu(DDC)_2$ complex is generally studied in organic solvents, as it is insoluble in aqueous media. In this work, the researchers discuss the use of a Nafion perfluorinated ionomer film as a structured support for the formation of the copper complex. Nafion is chemically and thermally inert, non-electroactive and insoluble in water, and is therefore particularly suitable for the modification of electrodes. It has been shown particularly by Chen et al. (1999) that electrodes modified with DDC and Nafion can be used for the detection of metal ions in stripping voltammetry, a technique that involves the deposition of the metal on the electrode surface.

2.3.5.1 The Electrochemical Analysis of DDC/Nafion on a Pt mesh Electrode

A Pt mesh working electrode was investigated as a substrate for modification with DDC/Nafion due to its small apertures allowing for its possible use

in UV-vis spectroscopy, as well as electrochemical experiments. The DDC/Nafion solution was electrodeposited onto the mesh from a solution consisting of 0.240 g DDC dispersed in 6.00 mL 5% wt. Nafion (in lower aliphatic alcohols and 15-20% water) was prepared, giving a 0.2 M solution of DDC at a constant potential of 1.0 V. The electrochemical characterisation of the modified electrode (Pt/DDC/Nafion) was carried out by cycling the modified mesh in 0.10 M NaCl at 50 mV/s for 10 cycles. As can be seen in Figure 36, the oxidation peak potential, for the oxidation of DDC to its radical, was observed at 0.20 V. The complete oxidation of DDC to DDC$^{\cdot}$ after 10 cycles can also be seen, as well as the hysteresis loop indicating the dimerisation of the radicals to form DSF. After DDC was electrochemically converted to DSF within the Nafion film, the stability of Pt/DDC/Nafion was investigated. The modified electrode was placed in a fresh solution of 0.1 M NaCl and scanned for 100 cycles at 50 mV/s between -0.5 and 0.9 V. A small reduction peak appeared at -0.50 V in the initial cycle, the current diminished over the first 40 cycles, and then reached a steady state. The stability of the modified Pt mesh was therefore investigated in a smaller potential window by repeating the experiment but scanning the potential from -0.1 to 0.6 V. No redox process was observed to occur in 0.1 M NaCl within this potential window. The electrode remained stable throughout the 100 cycles tested, indicating a more controlled and reliable background for further experiments.

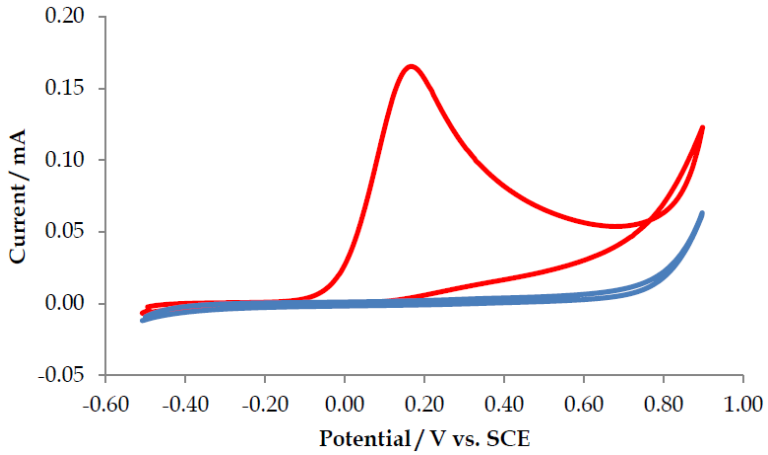

Figure 36. Cyclic voltammograms showing cycles — 1 and — 10 of the oxidation of DDC/Nafion coating on a Pt mesh in 0.1 M NaCl at 50 mV/s.

2.3.5.2 Copper Detection at a DDC/Nafion Modified Pt mesh Electrode

It has been shown that the oxidation of a Pt mesh electrode modified with DDC/Nafion film results in the formation of a DSF/Nafion modified electrode. Tonkin et al. (2004) propose that the formation of $Cu(DDC)_2$ from DSF occurs via the two electron reduction of DSF to DDC, and Victoriano (2000) describes the oxidising properties of DSF, with the reduction of the ligand breaking the S-S bond. In particular, Burkitt et al. (1998) have demonstrated the formation of $Cu(DDC)_2$ from DSF in the presence of Cu(II), using electron paramagnetic resonance

(EPR). They propose a mechanism whereby, with the oxidation of either Cu(I) to Cu(II) or Cu(II) to Cu(III), DSF can undergo a one electron reduction to form the DDC anion and one thiyl radical, as illustrated in Scheme 1. Two DDC anions are reported to co-ordinate with Cu(II) to form the square planar Cu(DDC)2 complex.

Although in this instance, Cu(II) was added to the sample solution, the redox cycling would enable the production of Cu(I), which in turn would facilitate the formation of the $Cu(DDC)_2$ complex.

The further oxidation of DSF to Bitt-4^{2+} has also been discussed as a possible reaction, depending on the upper limit of the potential window, and Cen et al. (2004) have shown that it is possible for Bitt-4^{2+} to react with Cu(I) to make the $Cu(DDC)_2$ complex. They synthesised the complex shown in Scheme 2, and showed that under hydrolysis it can form $Cu(DDC)_2$. Accordingly, it is possible that DDC, DSF and Bitt-4^{2+} all form the $Cu(DDC)_2$ complex in the presence of Cu(II) or Cu(I).

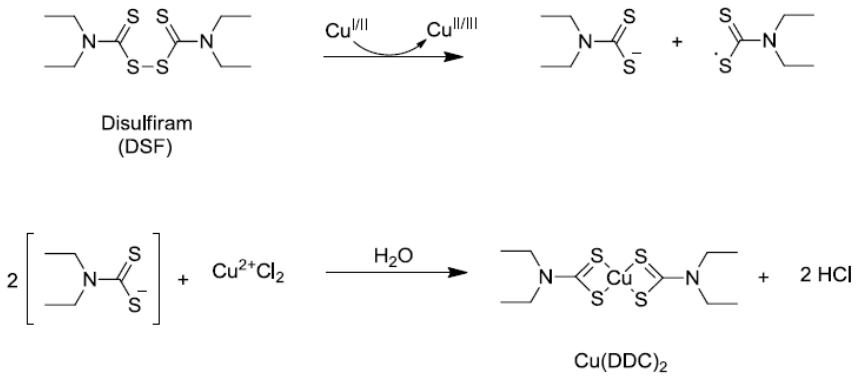

Scheme 1. Schematic representation of the complexation of DSF to Cu(II) *via* the chemical reduction of DSF to DDC and DDC˙.

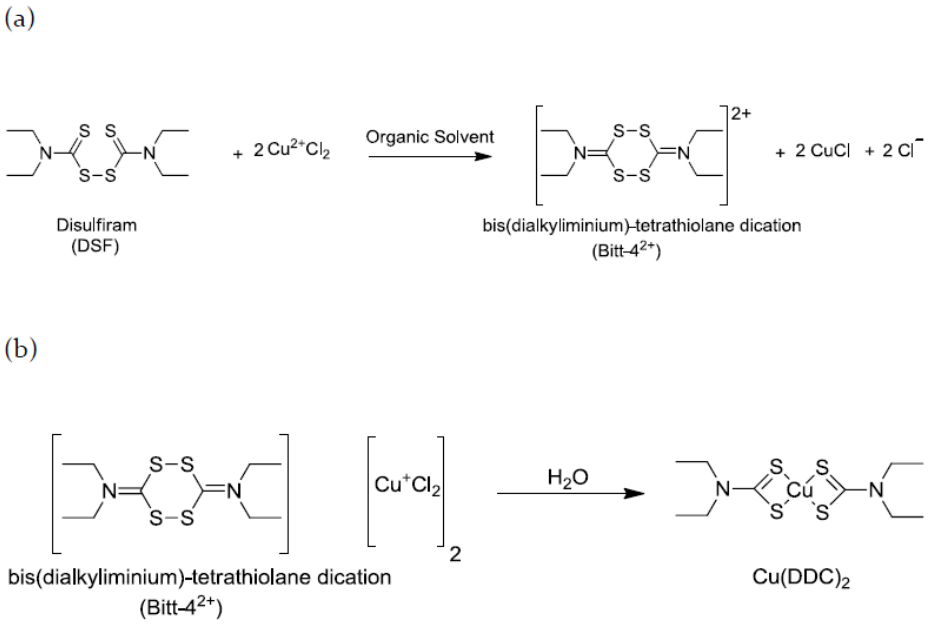

Scheme 2. Schematic representation of (a) oxidation of DSF to Bitt-4^{2+} in the presence of Cu(II), and (b) the hydrolysis of [Bitt-4][$CuCl_2$] forming $Cu(DDC)_2$. (Cen et al., 2004).

Figure 37 shows the electrochemical response of the modified electrode to 2.44 × 10^{-5} M $CuCl_2$ in comparison to the background of 0.10 M NaCl. The reduction peak at 0.08 V is indicative of the reduction of Cu(II) to Cu(I), and the coupled oxidation peak at 0.32 V is most likely the oxidation of Cu(I) to Cu(II). The peak separation for the redox couple is 0.24 V, which is larger than the values of 0.06 V and 0.15 V reported in TBAB and EtOH respectively (Dunbar et al., 2006) for the Cu(DDC)2 complex. This is possibly due to the immobilisation of the complex in the Nafion film which is poorly conducting, thus making electron transfer less efficient. The E1/2 value in this case is 0.22 V which is lower than the values reported of 0.57 V and 0.51 V in TBAB and EtOH respectively (Dunbar et al., 2006), indicating a more thermodynamically favoured reaction, which can be attributed to the immobilisation of the complex on the electrode surface. In restricting the lower potential to -0.10 V, and thus probably inhibiting the reduction of Cu(I) to Cu(0), the majority of Cu(I) was oxidised to Cu(II), resulting in good electrochemical reversibility, indicated by the ratio of the peak currents of 1.28.

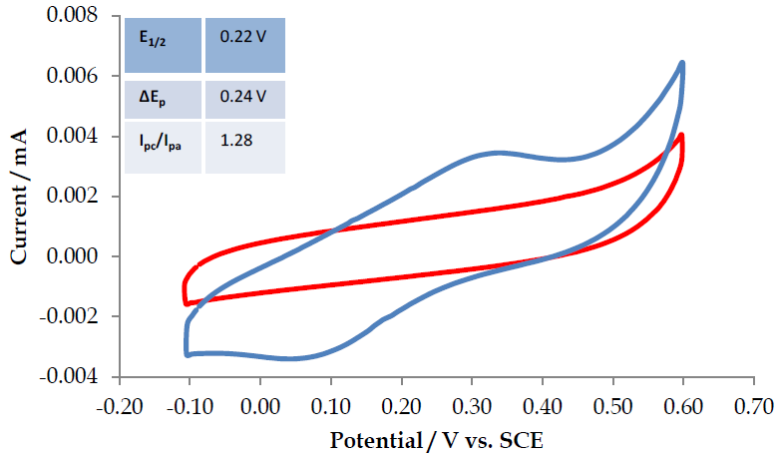

Figure 37. Cyclic voltammogram of Pt mesh modified with DDC/Nafion cycled at 50 mV/s in — 0.1 M NaCl and — 0.1 M NaCl with 2.44 × 10^{-5} M $CuCl_2$. Electrochemical properties of the redox couple are tabulated inset.

It was observed that the peak currents increased linearly with increasing concentration of Cu(II). The modified electrode showed good stability, as both the peak potentials and currents remained stable over 50 cycles. A calibration curve was constructed relating the peak current to increasing Cu(II) concentration, and the standard deviation of the background signal and the slope of the calibration curve were used to calculate the limit of detection of 5.40 × 10^{-5} M at Pt/DDC/Nafion. This is close to the recommended limit of 3.15 × 10^{-5} M set by the EPA for drinking water (Environmental Protection Agency 2010).

Electrochemical data indicated that the detection occurred as a result of $Cu(DDC)_2$ formation. UV-vis spectroscopy was therefore used in this section to help confirm that the complex formed on the electrode surface was in fact $Cu(DDC)_2$. To investigate the formation of $Cu(DDC)_2$ at the modified Pt mesh electrode, the absorbance spectra of the ligand, DDC and commercially

available $Cu(DDC)_2$ were compared to the absorption spectra of the modified electrodes used in the detection of Cu(II). As can be seen in Figures 38a and 38b respectively, the absorbance spectrum of 1.70×10^{-5} M DDC was recorded in 0.1 M NaCl and shows absorbance bands at 257 and 282 nm, representing electronic transitions associated with the S-C=S and the N-C=S moieties respectively. The linear correlation between the absorbance of the peaks with increasing concentration was used to calculate the extinction co-efficients (ε) for DDC as 9941 and 10078 M cm^{-1}, giving absorptions bands of log ε = 4.0 in both cases. According to Dunbar et al. (2006), the complex exhibits absorbance bands at 269, 289 and 433 nm in EtOH, with respective extinction co-efficients of 11,900, 6,400 and 5,100 M^{-1} cm^{-1}. The spectrum of 4.20 × 10-6 M Cu(DDC)2 was recorded in EtOH, which can be seen in Figure 36(b). The spectrum shows absorbance bands at 434, 270 and 290 nm with absorbance ratios of 2.6:1.8:1, which agree reasonably well with the literature values reported by Dunbar et al. (2006).

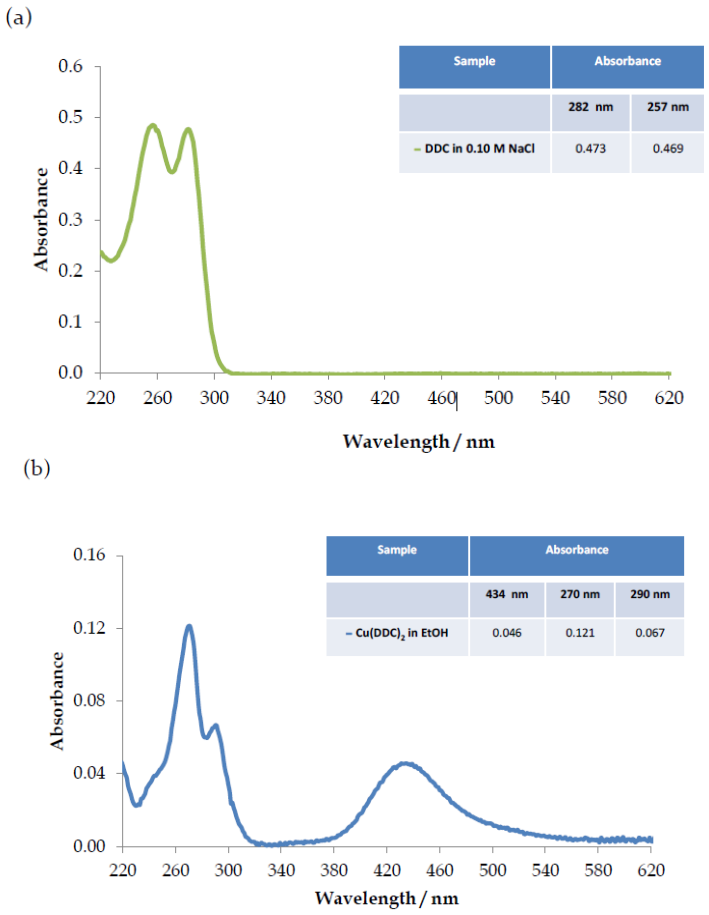

Figure 38. UV-vis absorbance spectra of (a) 1.70×10^{-5} M DDC in 0.1 M NaCl and (b) 4.20×10^{-6} M $Cu(DDC)_2$ in EtOH with absorbance data for relevant peaks tabulated inset.

To confirm that the complex formed at the DDC/Nafion modified electrode was $Cu(DDC)_2$, the UV-vis spectra of the modified electrodes were obtained by dissolving the Nafion films in EtOH. This was carried out for the mesh modified with DDC/Nafion oxidised and used to detect Cu(II) and for the Pt mesh modified with $Cu(DDC)_2$/Nafion. The resulting spectra can be

seen in Figure 37, where absorbance peaks at 434, 290 and 270 nm can be seen in both cases. The ratio of the absorbance of the peaks (434 nm: 290 nm: 270 nm) were calculated for each sample, and it was found that the ratios were 2.4:1.9:1 and 2.3:2.0:1, which agree reasonably well with the extinction co-efficients reported in the literature (Dunbar et al., 2006), This further indicates that the complex formed at the electrode surface was most likely to be $Cu(DDC)_2$. Pt mesh was used as a working electrode (WE) to allow for the characterisation of the modified electrode using UV-vis spectroscopy. Spectra were therefore obtained from the electrode modified with DDC/Nafion that had been cycled in Cu(II) and the Pt mesh modified with Nafion/$Cu(DDC)_2$ by suspending the electrodes in cuvettes containing H_2O. Absorbance peaks at 261 nm were observed in both spectra, however, the absorbance bands in the visible region of the spectra were slightly different at each electrode. At the Pt mesh modified with $Cu(DDC)_2$, the absorbance shows a λmax at 416 nm, however, for the complexed DDC/Nafion modified electrode, the absorbance appears to have a λmax of 406 nm. This is likely due to the poor signal to noise ratio, causing asymmetry of the latter peak and poor accuracy in the determination of λmax, as a much lower concentration of the complex was formed at this electrode. However, it is noteworthy that the absorbance peaks occur in the same region (480 – 360 nm) in both cases. This further supports that the complex formed at the electrode surface was $Cu(DDC)_2$, however, further use of the modified mesh electrode in spectrophotometric analysis was not recommended due to its poor sensitivity under these conditions. It is noteworthy, however, that the peaks observed at the modified electrode, did not coincide with those observed from solution-based samples in Figure 39, therefore, the film used was dissolved in EtOH to ensure that the peaks were in fact characteristic of the $Cu(DDC)_2$ complex. It can be seen here that the peak in the visible region has shifted from 434 to 416 nm, confirming that the absorbance band observed was that of $Cu(DDC)_2$, and indicates that the immobilisation of the complex on the electrode caused the shift in wavelength.

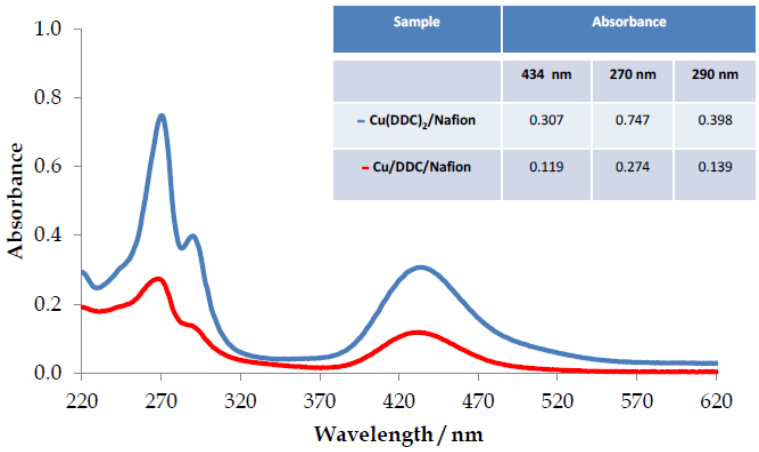

Figure 39. UV-vis spectra of Nafion films containing — $Cu(DDC)_2$ and —DDC and Cu(II) dissolved in EtOH.

2.3.5.3 Investigating the use of MWCNTs to Enhance the Detection of Cu(II) at a DDC/Nafion Modified Pt Mesh Electrode

There are many variations reported in the literature for the preparation of nanotube composites, including the modification of MWCNTs, and generally it is found that acid-treated MWCNTs provide a well dispersed matrix (Xu et al., 2008). However, during the course of this work, it has been found that acid-treated MWCNTs exhibit a large, broad redox couple at 0.20/0.30 V, which is very close to the redox couple of Cu(II) monitored in this work (0.08/0.32 V), therefore large amounts of interference was expected from their use. Pristine MWCNTs were therefore used in the formation of Nafion/MWCNTs composites, with note taken that some agglomerations would be present. In this preliminary testing, a 1.0 mg mL^{-1} solution of pristine MWCNTs in 5% wt. Nafion (in lower aliphatic alcohols and 15-20% water) was prepared using sonication for 30 minutes. The ligand (0.20 M DDC) was added to the Nafion/MWCNTs solution and stirred for 10 minutes. The Pt mesh electrode was modified with DDC/Nafion/MWCNTs by electrodeposition, as before, by applying 1.00 V to the WE for 120 s. The composite was then dried under an IR lamp for 10 minutes. The oxidation of DDC to its radical was observed by cycling the modified electrode in 0.10 M NaCl at 50 mV/s for 10 cycles. Figure 40a shows the initial and final cycles of this oxidation step, where it can be seen that the oxidation peak at 0.03 V had diminished by the 10th cycle. In this case, however, unlike the DDC/Nafion modified electrode, a reduction peak was observed at 0.06 V. With continued cycling, the reduction peak increased and an oxidation peak appeared at 0.38 V. This could indicate the oxidation of DSF to Bitt-4^{2+} and its reduction back to DSF, possibly facilitated by the fast electron transfer properties of the MWCNTs. The redox couple reached stable currents, and in Figure 40b, it can be seen that a stable background voltammogram was obtained in a fresh solution of NaCl.

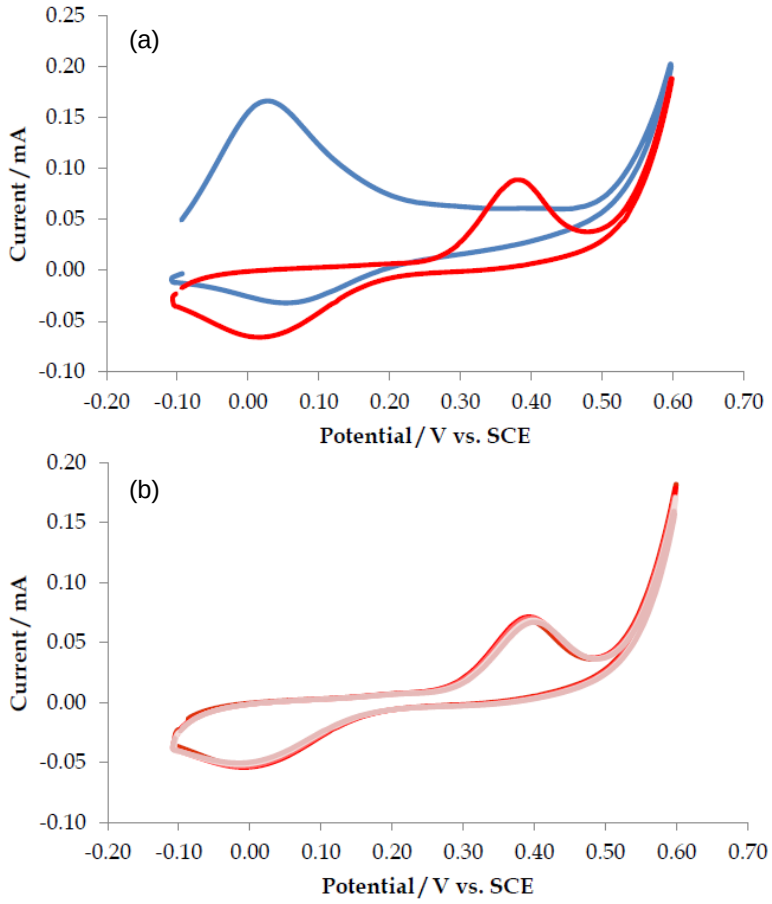

Figure 40. Cyclic voltammograms in 0.10 M NaCl at 50 mV/ s of a Pt mesh electrode modified with DDC/Nafion/MWCNTs from 0.20 M DDC and 1.0 mg mL^{-1} MWCNTs in 5% wt. Nafion via electrodeposition at 1.00 V for 120 s (a) cycles — 1 and — 10 showing oxidation of DDC and (b) 10 subsequent overlaying cycles showing the stability of the background.

The detection of Cu(II) was investigated at the oxidised DDC/Nafion/MWCNTs modified Pt mesh electrode. It can be seen from these voltammograms, shown in Figure 41a, that upon addition of Cu(II), the redox couple seen in the background (at 0.06/0.38 V) gradually diminished, and a redox pair similar to that seen at the DDC/Nafion modified electrode gradually appeared. This is indicative that the detection mechanism was similar in both cases, however, further work would be required to identify the significance of the background peaks. The voltammograms in Figure 41b compare the detection of Cu(II) at Pt/DDC/Nafion to that at Pt/DDC/Nafion/MWCNTs, and the calculated electrochemical properties are tabulated inset. The peak positions of this redox couple recorded at Pt/DDC/Nafion/MWCNTs were 0.14/0.24 V, giving an E1/2 value of 0.19 V with a ΔEp of 0.10 V in this case. These values are lower than the E1/2 = 0.22 and ΔEp = 0.24 V seen at Pt/DDC/Nafion, which can be explained by the conductivity and the fast electron transfer properties of the MWCNTs. The peak currents were also dramatically enhanced (2.6 fold) by the incorporation of MWCNTs into the DDC/Nafion film, and the electrochemical reversibility at the DDC/Nafion modified Pt mesh electrode was improved with the incorporation of MWCNTs; from Ipc/Ipa = 1.28, to Ipc/Ipa = 1.10. This is also a good indication that the incorporation of MWCNTs into the DDC/Nafion film would lead to

more sensitive detection of Cu(II). To preliminarily screen the sensitivity of Pt/DDC/Nafion/MWCNTs in comparison to Pt/DDC/Nafion, the current response at each electrode was compared at the same concentration. The current response for the reduction of 3.45 × 10^{-5} M Cu(II) at Pt/DDC/Nafion was 1.16 × 10^{-6} A. The current response under the same conditions at Pt/DDC/Nafion/MWCNTs was recorded as 4.71 × 10^{-5} A, which is an increase of over 40 fold.

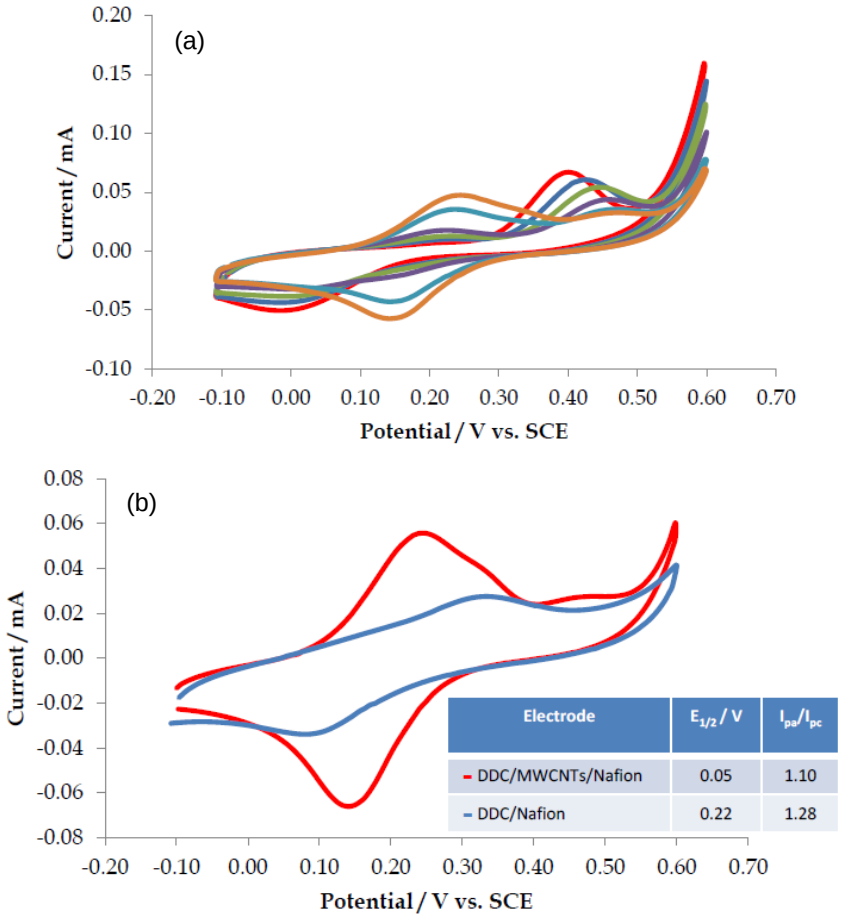

Figure 41. Cyclic voltammograms of Pt mesh electrode modified with (a) —DDC/Nafion/MWCNTs from 0.20 M DDC and 1.0 mg mL^{-1} MWCNTs in 5% wt. Nafion via electrodeposition at 1.00 V for 120 s; cycled in 0.10 M NaCl with additions of — 0.00, — 7.09 × 10^{-6}, — 1.40 × 10^{-5}, — 2.10 × 10^{-5},— 2.78 × 10^{-5} and — 3.45 × 10^{-5} M $CuCl_2$ and (b) — DDC/Nafion/MWCNTs and —DDC/Nafion from 0.20 M DDC in 5% wt. Nafion, both in 0.10 M NaCl containing 3.45 × 10^{-5} M $CuCl_2$ with relevant data tabulated inset.

To confirm that the detection of Cu(II) at the DDC/Nafion/MWCNTs modified electrode was via the formation of the $Cu(DDC)_2$ complex, the detection of Cu(II) was compared to that at a Pt mesh modified with Nafion/MWCNTs. The Pt mesh was modified via electrodeposition as before, from a solution of 1.0 mg mL^{-1} MWCNTs in 5% wt. Nafion (in lower aliphatic alcohols and 15-20% water) at 1.00 V for 120 s. The modified electrode was dried under an IR lamp for 10 minutes and cycled in the background electrolyte of 0.10 M NaCl to obtain a steady background current. Cyclic voltammogrammetry measurements showed that the detection at both electrodes is very different, with the Nafion/MWCNTs modified mesh showing similar

peak positions to the Nafion modified mesh, but with enhanced peak currents. This indicates that the detection of Cu(II) at the DDC/Nafion/MWCNTs modified electrode occurred via the complexation of Cu(II) to DDC results in the formation of $Cu(DDC)_2$ complex.

The reproducibility of the DDC/Nafion/MWCNTs modified Pt mesh was investigated in the detection of Cu(II) and three repeated experiments can be seen in Figure 42. The voltammograms highlight the poor reproducibility of the sensor, which is most likely due to poor reproducibility in the incorporation of MWCNTs into the Nafion film. The electrodeposition of Nafion and DDC is based on the attraction of their negatively charged moieties to the positive potential applied to the WE. As the MWCNTs used in this investigation were not modified and, thus, were expected to contain very few negatively charged sites, their incorporation into the Nafion film is likely to be predominantly due to physical entrapment. It is therefore suggested that the reported method of preparation is unsuitable for the modification of an electrode with MWCNTs. As the electrochemical response of the DDC/Nafion/MWCNTs modified electrode was clearly enhanced as a result of the incorporation of MWCNTs, the experimental design should be revised to optimise its use for further work.

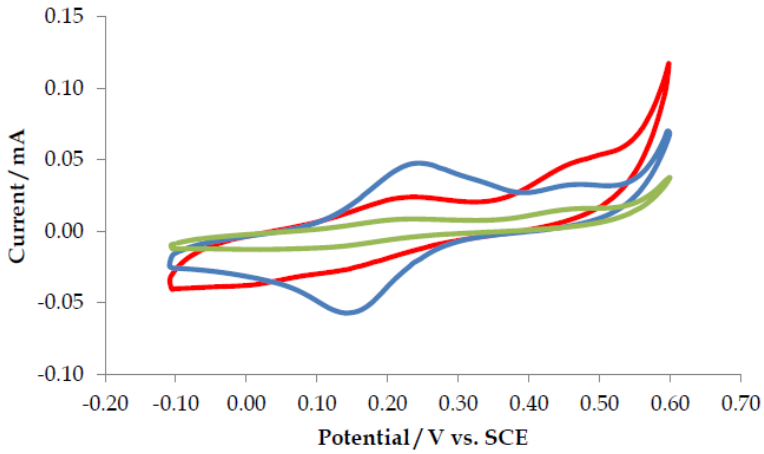

Figure 42. Cyclic voltammograms of Pt mesh modified with DDC/Nafion/MWCNTs from 0.20 M DDC and 1.0 mg mL^{-1} MWCNTs in 5% wt. Nafion in 2.44 × 10^{-5} M $CuCl_2$ in 0.10 M NaCl for repeated experiments — n=1, — n=2 and — n=3 showing poor reproducibility.

Conclusions and Recommendations

The investigation and development of an electrochemical system to monitor organic contaminants was carried out. Initial experiments were carried out to observe if the chosen electrode modification could be used to detect these contaminants, and if this was successful, then remediation studies would be carried out. The electrode material consisted of polypyrrole (PPy) doped with sulfonated β-cyclodextrin (sβ-CD). Polypyrrole was chosen due to its ease of preparation by electropolymerisation, relative stability compared to other conducting polymers, and the ready commercial availability of many of its derivatives. Cyclodextrins are naturally occurring macrocyclic oligosaccharides built from α-1,4-linked D-glucopyranose units. The most common and readily available cyclodextrins are the α, β and γ-cyclodextrins. These cyclodextrins are composed of six, seven and eight glucopyranose units respectively. Cyclodextrins are well known to bind with suitable guest molecules in aqueous solutions to form inclusion complexes. SEM measurements showed that the PPy-sβCD film exhibits a 'cauliflower' morphology, typically seen in PPy films. However, its morphology seems to be more structured and organised and this is not normally observed with a characteristic PPy film. EDX measurements confirmed the presence of sulphur in the polymer film. This proves that both the anionic β-cyclodextrin and the chloride anions from the NaCl supporting electrolyte are incorporated into the polymer film. The surface coverage of electroactive centres was estimated at 2×10^{-9} mol cm^{-2}., while the capacitance of the PPy-sβCD film was found to be 1.84×10^{-3} F cm^{-2} compared to 1.3×10^{-4} F cm^{-4} for PPy-Cl. The high value calculated for the PPy-sβCD film indicates that considerably more negative charge is being stored in the film and, as a result, more cations will be attracted to the film surface.

Initial studies were carried out on phenol and chlorophenols. Initially, detection of phenol and 3-chlorophenol at PPy-sβCD was shown to be promising. Unfortunately, when the influence of phenol or 3-chlorophenol concentration was investigated, it was found that there was no clear linear relationship between concentration and the oxidation peak current. This may be due to the fact that higher phenol concentrations allows for the formation of greater amounts of phenoxy radicals, which polymerise and cause faster passivation of the electrode surface. When the influence of dopant was investigated, it was found the phenol or 3-chlorophenol were only oxidised in the presence of the sβ-CD dopant. This would suggest that there was some interaction between the phenol or 3-chlorophenol and the sβ-CD. ^{1}H nmr was carried out in order to determine if an inclusion complex is being formed, and to investigate the manner in which the phenol or 3-chlorophenol was including inside the cavity of the sβ-CD. Results showed that while there is some interaction between the phenols and the β-CD, there is no evidence of a strong inclusion complex being formed. Due to the poor reproducibility of these results and no evidence of an inclusion complex being formed, further investigation into the possible use of PPy-sβCD in the remediation of phenol and phenol derivatives was not carried out.

Atrazine is a triazine herbicide used to stop pre- and post-emergence broadleaf and grassy weeds in major crops by binding to the plastoquinone-binding protein in photosystem II, inhibiting electron transport. While it was banned in the EU in 2004, it is still widely used in the US and Australia and is strongly persistent in the aqueous environment, and was therefore chosen

as a model herbicide for this study. A polypyrrole film doped with sβ-CD was polymerised and employed to detect atrazine. Several different acidic electrolytes were used, including Britton-Robinson buffer and sulphuric acid, however, atrazine was not successfully detected using the polypyrrole encapsulated cyclodextrin. Cyclic voltammograms in a cathodic direction and in an anionic direction, showed no significant difference in voltammogram shape between the background scan (without atrazine) and those in the presence of atrazine. Again, due to no evidence of detection of atrazine, and therefore it being unlikely that an inclusion complex is being formed, further investigation into the possible use of PPy-sβCD in the remediation of atrazine and atrazine derivatives was not carried out.

Acetaminophen or paracetamol is a widely used, over-the-counter analgesic and antipyretic. It is most commonly used for the relief of headaches and other minor aches and pains, as well as being a major ingredient of numerous cold and flu remedies. Cyclic voltammetry measurements of acetaminophen at PPy-sβCD showed a redox couple centred on 0.40 V could be seen, indicating some interaction between the cyclodextrin and the acetaminophen. These peaks (I and II) were observed at scan rates of both 50 and 100 mV/s. Both peak I and II maintained current over several cycles, indicating good stability of both the film and the interaction of the acetaminophen and cyclodextrin. Complexation between acetaminophen and sβ-CD was determined using UV-vis spectroscopy and cyclic voltammetry, while the Job's method was employed to distinguish the stoichiometric value of the complex. A series of solutions, where the sum of the guest (acetaminophen) and host (sβ-CD) concentrations was kept constant while changing the mole fraction, were prepared. These solutions were then analysed using UV-vis spectroscopy and cyclic voltammetry. The data for the Job's plot was generated by taking the product of the mole fraction with the change of the property from that of an equal concentration of free guest (ΔA). This product was then plotted as a function of the mole fraction. The stoichiometry was determined from the x-co-ordinate at a maximum value of the Job's curve. The maximum absorbance value was achieved at the 0.5 mole fraction and this is evidence that there exists a 1:1 acetaminophen:sβ-CD complex stoichiometry. To generate the Job's plot for the CV analysis, the changes in the peak current of acetaminophen in the presence and absence of CD (ΔI_p) was monitored. The Job's plot generated from the data reached a maximum value at 0.5 mole fraction, confirming the formation of a 1:1 acetaminophen:sβ-CD complex. When the influence of concentration of acetaminophen was investigated, it was found that there was no clear linear relationship between concentration and the oxidation peak current, especially at higher concentrations. This may be due to the formation of phenoxy radicals during oxidation of acetaminophen. These radicals can then polymerise and cause faster passivation of the electrode surface. At higher concentrations of acetaminophen, this passivation is more pronounced. Concentrations below 0.05 M were not investigated, as there was no clear resolution of oxidation peak I below this value. Due to no poor reproducibility, further investigation into the possible use of PPy-sβCD in the remediation of acetaminophen was not carried out. Studies to investigate alternative membrane materials and its use in real water samples would be recommended.

Nitrate contamination is a significant problem in countries with a large agricultural land usage, including Ireland. Therefore, the accurate and up-to-date monitoring of this pollutant is of utmost importance. Research in this area focussed on the use of polypyrrole (PPy) and

poly[N-2-(cyanoethyl)pyrrole] (PPyEtCN) polymers, as they have successfully been applied in sensor applications. To increase the sensitivity of these materials, they were developed into a nanowire morphology; during this process the authors also developed a new methodology to fabricate hollow microtubes. As copper is known for its catalytic ability to electro-reduce nitrate, the authors were eager to incorporate copper, again as a nanostructure, within these polymer nano/micro materials. The investigation of the *N*-substituted PPyEtCN monomer was undertaken, as it had shown promising application in sensor technology. This was mainly due to its ability to hydrogen bond and dipole-dipole interacts with other molecules. This monomer is typically polymerised in organic media, such as acetonitrile. However, to grow nanowires, an aqueous solvent must be employed, as the morphology directing salts have a limited solubility in organic media. This leads to solubility problems with the PyEtCN monomer, as it has a low solubility in water. These solubility problems were overcome by using a mixed solvent system comprised of water and ethanol in a 7:3 ratio. This allowed for a minimum solubility of the monomer and morphology directing salts to be maintained in sufficient concentrations to allow polymerisation. It was hoped that these polymers could be utilised in application as a nitrate sensor. However, the resistive nature of these nanowire films made the electrodeposition of copper onto their surfaces quite difficult. Discrete particles could not be obtained in a controllable fashion covering the electrode. Therefore, based on these results, the nitrate sensing abilities of these PPyEtCN nanowires were not pursued.

During the electrodeposition of the PPyEtCN nanowires, a second morphology developed in certain experiments. The structures were composed of randomly formed microtubes. These new materials possessed unique properties for application in entrapment and drug delivery systems due to their exposed hollow centre. Using the solubility of the monomer to control the occurrence of the microtubes revealed that they developed by a 'droplet guided' mechanism. They formed because large insoluble monomer droplets were present in the polymerisation electrolyte, as identified by microscopy analysis. Electrochemical characterisation indicated that the PPyEtCN microtube morphology had an increased electrochemical response compared to its bulk counterpart. They also increased the hydrophilicity of the polymer by trapping air within the tubes. As the PPyEtCN microtubes were subject to the same low conductivity limitations as the PPyEtCN nanowires, their nitrate-sensing abilities were not explored. However, using them in another manner may allow for new materials to be developed to construct a cheap and reliable copper electrochemical sensor.

Electrochemically polymerised PPy nanowire films were proven to be a reproducible substrate for the nucleation and growth of copper crystals. These nanocomposites were tested as a surface for the electroreduction of the nitrate ion, which was shown to begin with an adsorption step. The addition of a greater copper loading was seen to generate a greater response for the nitrate electroreduction. However, overloading the electrode was possible at deposition cycles greater than 160, at 100 mV/s. The PPy nanowire/copper composite was observed to generate a larger current for nitrate electroreduction when smaller copper particles were deposited. However, the optimised nanowire/copper hybrid had a lower sensitivity compared to a glassy carbon/copper composite. This was due to residual carbonate remaining within the polymer matrix, which formed a complex with the copper ions and interfered with

the nitrate reaction. In spite of this, the PPy nanowires were shown to have a stabilising interaction with the copper through a charge transfer complex, which resulted in a better stability of the sensor over time. The catalytic ability of copper for increasing the electroreduction of the nitrate ion in aqueous solutions has been highlighted. The nanowires were seen as reproducible substrates for copper electrodeposition. While the sensitivity of the nanowire/copper hybrid was not as sufficient as hoped, the formation of a stable PPy/copper charge transfer complex allowed for a slower degradation of the nitrate reduction signal. This would suggest these electrodes would be applicable in long-term sensing systems, where longevity rather than lowest sensitivity is necessary. If required, overcoming the drawbacks associated with the reduced sensitivity may be achieved by employing nanowires which are synthesised without the use of buffer solutions, possibly using a biomolecule approach.

Chromium (VI) is a toxic metal ion which is found in many parts of the environment due to its ability to leach great distances in groundwater. The Environmental Protection Agency (EPA) has set a mandatory limit of 9.61×10^{-7} M (50 μg L^{-1}) Cr(VI) in drinking water. It is therefore crucial to enable its specific detection at low levels by a simple and fast method. There are many benefits to the use of electrochemical sensors in environmental monitoring of toxic species, such as Cr(VI), including real-time analysis and on-site monitoring. The electrochemistry at GCEs modified with MWCNTs and graphene has been evaluated. Overall, it was found that GCEs modified with MWCNTs exhibited faster electron transfer kinetics than GCEs modified with graphene, which has been explained by the mesoporous structure of MWCNTs providing superior electrochemical properties to the modified electrodes in this study, most likely due to thin layer diffusion processes. The electroactive surface areas of the modified electrodes were calculated from the peak currents using the Randles Sevcik Equation, and it was found that modification of the GCE with sonicated MWCNTs provided a larger increase in surface area in comparison to that of graphene modified electrodes. In comparing the electrochemistry at MWCNTs modified electrodes to graphene modified electrodes, the rate constants and electroactive surface areas are greater for the GCEs modified with MWCNTs. It was found that a MWCNTs modified glassy carbon electrode could be used to detect the electrochemical reduction of Cr(VI). The reduction peak was monitored at 0.65 V using cyclic voltammetry and a LOD of 1.95×10^{-4} M was determined. A reasonably stable peak current was monitored over 30 cycles, which was not influenced by the potential interferants Cl^- and Cu^{2+}. Some interference was noted in the presence of NO_3^-, however, and poor reproducibility was seen in real water samples. As expected, the peak potential for the reduction of Cr(VI) to Cr(III) was influenced greatly by the pH of the sample solution, however, it did not follow simple Nernstian behaviour. Surprisingly, the peak current did not increase with an increase in the conductivity of the sample solution, perhaps due to adsorption of SO_4^{2-} on the MWCNTs surface. Different modifications were explored in the construction of the Cr(VI) sensor in an attempt to enhance the limits of detection, the most promising of which was the modification of the electrode with MWCNTs incorporating AuNPs. Samples of MWCNTs, both pristine and oxidised, were modified with AuNPs and it was found, using atomic absorption spectroscopy, that the MWCNTsOx contained substantially more AuNPs than the pristine MWCNTs after modification. A LOD of 1.55 ×

10^{-4} M was achieved at the Au/MWCNTs/AuNPs. Constant potential amperometry at a rotating disc electrode was therefore investigated, as a means of decreasing the limit of Cr(VI) detection. The lowest LOD achieved using this technique was 1.20×10^{-6} M at the Au/MWCNTsOx/AuNPs electrode. Although it would appear that simple modification of an electrode with MWCNTs can be used to detect Cr(VI), there are problems with its LOD. The AuNPs modified MWCNTs, however, show enhanced detection of Cr(VI). Future recommendations for this work would include optimising the modification of the MWCNTs with AuNPs to maximise the %wt. of AuNPs on the modified surface. Studies to investigate the selectivity of the optimised electrode and its use in real water samples would also be recommended.

Copper is a transition metal that is found naturally in some rock sediments and forms monovalent and divalent cations in solution. Copper pollution generally stems from anthropogenic uses, such as copper piping and wiring, where it can be leached into drinking water. Although it is an essential dietary requirement, it can cause organoleptic (taste) problems when ingested at levels above 1 mg L^{-1}. At lower doses, it can cause symptoms typical of food poisoning, and the acute lethal dose for adults lies between 1 and 400 mg of copper (II) per kg of body weight (Clenaghan and O'Neill, 2005). As copper is found naturally in the environment at low concentrations, its sensitive detection is very important. The EPA has thus imposed a parametric value, i.e. a mandatory limit, of 3.15×10^{-5} M Cu(II) in drinking water in Ireland. For the most part, copper is detected using techniques such as ICP-MS, which are expensive, time-consuming and do not provide real-time analysis. The development of electrochemical sensors for metal ion detection would allow for simple, on-site detection with remote access to data, making it a very attractive technique for environmental monitoring.

The modification of a Pt mesh electrode with the ligand DDC immobilised in a Nafion film, and its subsequent oxidation to DSF, was investigated as a possible Cu sensor. It has been shown that this resulting modified electrode can be used as a simple sensor for the detection of Cu(II) ions in solution, and a detection limit of 5.40×10^{-5} M was determined using cyclic voltammetry. The electrodeposition of the ligand, DDC, in Nafion on the Pt mesh and its electrochemical oxidation has been monitored using cyclic voltammetry. The oxidation of DDC was consistent with the formation of DSF. Control studies involving Pt/DSF/Nafion, Pt/Nafion and bare Pt were also carried out to confirm that the sensing of Cu(II) occurred at the oxidised DDC/Nafion film. It was evident from these studies that the interactions of DSF/Nafion and oxidised DDC/Nafion with Cu(II) were very similar, however, it was found that due to its solubility and electroactivity, DDC was the favoured ligand for use in the preparation of the modified electrode. Studies were also carried out to identify the complexation of Cu(II) at the modified electrode with the formation of $Cu(DDC)_2$. In order to confirm the formation of the complex, cyclic voltammetry was carried out on a $Cu(DDC)_2$/Nafion modified electrode and compared to the oxidised DDC/Nafion modified electrode cycled in Cu(II). A similar redox couple was observed at both electrodes. UV-vis spectroscopy of the Pt mesh was also utilised as a means of confirming the complexation of Cu(II) at the modified electrode. It was found, however, that the poor signal to noise ratio at the Pt mesh electrode, due to the short path length, decreased the sensitivity of the absorbance spectra, and a definitive characterisation could not be made at the oxidised DDC/Nafion modified electrode. The spectra were obtained for the films deposited on both electrodes by

dissolving the Nafion films in EtOH, and it was found that both films exhibited very similar absorbance spectra, giving good evidence that $Cu(DDC)_2$ was formed at the oxidised DDC/Nafion modified electrode cycled in Cu(II). An attempt was made to enhance the sensitivity of the oxidised DDC/Nafion modified electrode towards the detection of Cu(II) by introducing MWCNTs into the film. Preliminary investigations suggested that the MWCNTs enhanced the electrochemical response of the modified electrode and a larger current response was observed, which would signify greater sensitivity. Problems arose with the reproducibility of this modified electrode, however, with variable amounts of MWCNTs incorporated into each DDC/Nafion film formed.

These preliminary studies would indicate that an oxidised DDC/Nafion modified electrode could form the basis of a simple sensor for the detection of Cu(II) using cyclic voltammetry. Further studies would be recommended, however, to optimise the loading of DDC in the Nafion film and to optimise the film thickness. There is also the possibility of altering the morphology and, thus, the physical properties of the film using heat treatments. Studies would also be required to determine the effects of interferants such as Pb(II) and Fe(III) which form well known complexes with DDC on the electrochemical detection of Cu(II).

References

Asami, R., Atobe, M. and Fuchigami, T. (2005). "Electropolymerization of an Immiscible Monomer in Aqueous Electrolytes Using Acoustic Emulsification." Journal of the American Chemical Society **127**(38): 13160-13161.

Asami, R., Fuchigami, T. and Atobe, M. (2006). "Development of a Novel Environmentally Friendly Electropolymerization of Water-Insoluble Monomers in Aqueous Electrolytes Using Acoustic Emulsification." Langmuir **22**(24): 10258-10263.

Asavapiriyanont, S., Chandler, G. K., Gunawardena, G. A. and Pletcher, D. (1984). "The electrodeposition of polypyrrole films from aqueous solutions." Journal of Electroanalytical Chemistry **177**: 229-244.

Bedioui, F., Nyokong, T. and Zagal, J. H. (2012). "Surface electrochemistry: structured electrode, synthesis and characterization." Int. J. Electrochem.: 405825.

Bernini, A., Spiga, O., Ciutti, A., Scarselli, M., Bottoni, G., Mascagni, P. and Niccolai, N. (2004). "NMR studies of the inclusion complex between β-cyclodextrin and paroxetine." European Journal of Pharmaceutical Sciences **22**(5): 445-450.

Burkitt, M. J., Bishop, H. S., Milne, L., Tsang, S. Y., Provan, G. J., Nobel, C. S. I., Orrenius, S. and Slater, A. F. G. (1998). "Dithiocarbamate toxicity toward thymocytes involves their copper-catalyzed conversion to thiuram disulfides, which oxidize glutathione in a redox cycle without the release of reactive oxygen species." Archives of Biochemistry and Biophysics **353**(1): 73-84.

Cen, D. Z., Brayton, D., Shahandeh, B., Meyskens, F. L. and Farmer, P. J. (2004). "Disulfiram facilitates intracellular Cu uptake and induces apoptosis in human melanoma cells." Journal of Medicinal Chemistry **47**(27): 6914-6920.

Chen, L. Z., Pourabedi, Z. and Hibbert B. D. (1999). "Stripping voltammetry of Pb(II), Cu(II), and Hg(II) at a nafion-coated glassy carbon electrode modified by neutral ionophores." Electroanalysis **11**(13): 964-968.

Chou, A., Bocking, T., Singh, K.N. and Gooding J.J. (2005). "Demonstration of the importance of oxygenated species at the ends of carbon nanotubes for their favourable electrochemical properties." Chemical Communications(7): 842-844.

Clenaghan, C. and O'Neill, N. (2005). Dangerous Substances Regulations National Implementation Report 2005.

Coutouli-Argyropoulou, E., Kelaidopoulou, A., Sideris, C. and Kokkinidis, G. (1999). "Electrochemical studies of ferrocene derivatives and their complexation by [beta]-cyclodextrin." Journal of Electroanalytical Chemistry **477**(2): 130-139.

Dang, X.-J., Nie, M.-Y., Jian, T. and Li, H.-L. (1998). "Inclusion of the parent molecules of some drugs with [beta]-cyclodextrin studied by electrochemical and spectrometric methods." Journal of Electroanalytical Chemistry **448**(1): 61-67.

Debiemme-Chouvy, C. (2009). "Template-free one-step electrochemical formation of polypyrrole nanowire array." Electrochemistry Communications **11**(2): 298-301.

Dong, S., Chen, X., Zhang, X. and Cui, G. (2013). "Nanostructured transition metal nitrides for energy storage and fuel cells." Coord. Chem. Rev. **257**: 1946-1950.

Dunbar, A., Omiatek, D. M., Thai, S. D., Kendrex, C. E., Grotzinger, L. L., Boyko, W. J., Weinstein, R. D., Skaf, D. W., Bessel, C. A., Denison, G. M. and DeSimone, J. M. (2006). "Use of substituted bis(acetylacetone) ethylenediimine and dialkyldithiocarbamate ligands for copper chelation in supercritical carbon dioxide." Industrial & Engineering Chemistry Research **45**(26): 8779-8787.

Dziewonski, P. M. and Grzeszczuk, M. (2010). "Impact of the Electrochemical Porosity and Chemical Composition on the Lithium Ion Exchange Behavior of Polypyrroles (ClO4-, TOS-, TFSI-) Prepared Electrochemically in Propylene Carbonate. Comparative EQCM, EIS and CV Studies." J. Phys. Chem. B **114**: 7158-7171.

Environmental Protection Agency. (2010). The Provision and Quality of Drinking Water in Ireland: A Report for the Year 2010.

EPA (2000). Protecting and Improving Ireland's Environment (Vision 2020). Wexford: Environmental Protection Agency.

EPA (2013). Strategic Plan 2013–2015., Wexford:Environmental Protection Agency.

European Commision. (2011). Communication From The Commission To The European Parliament, The Council, The European Economic And Social Committee And The Committee Of The Regions: A Resource-efficient Europe., Brussels: European Commission.

Forfás (2010). Ireland's Nanotechnology Commercialisation Framework 2010–2014., Dublin: Forfás.

Gattrell, M. and Kirk, D. W. (1993). "A Study of Electrode Passivation During Aqueous Phenol Electrolysis." Journal of the Electrochemical Society **140**(4): 903-911.

Ge, D., Wang, J., Wang, Z. and Wang, S. (2002). "Electrochemical synthesis of polypyrrole nanowires on composite electrode." Synthetic Metals **132**(1): 93-95.

George, P. M., Lyckman, A. W., LaVan, D. A., Hegde, A., Leung, Y., Avasare, R., Testa, C., Alexander, P. M., Langer, R. and Sur, M. (2005). "Fabrication and biocompatibility of polypyrrole implants suitable for neural prosthetics." Biomaterials **26**(17): 3511-3519.

Gibaud, S., Zirar, S. B., Mutzenhardt, P., Fries, I. and Astier, A. (2005). "Melarsoprol–cyclodextrins inclusion complexes." International Journal of Pharmaceutics **306**(1–2): 107-121.

Gupta, S. (2008). "Hydrogen bubble-assisted syntheses of polypyrrole micro/nanostructures using electrochemistry: structural and physical property characterization." Journal of Raman Spectroscopy **39**(10): 1343-1355.

Hafaid, I., Chebil, S., Korri-Youssoufi, H., Bessueille, F. O., Errachid, A., Sassi, Z., Ali, Z., Abdelghani, A. and Jaffrezic-Renault, N. (2010). "Effect of electrical conditions on an impedimetric immunosensor based on a modified conducting polypyrrole." Sensors and Actuators B: Chemical **144**(1): 323-331.

Huang, J., Quan, B., Liu, M., Wei, Z., and Jiang, L. (2008). "Conducting Polypyrrole Conical Nanocontainers: Formation Mechanism and Voltage Switchable Property." Macromolecular Rapid Communications **29**(15): 1335-1340.

Huang, J., Wang, K. and Wei, Z. (2010). "Conducting polymer nanowire arrays with enhanced electrochemical performance." J. Mater. Chem. **20**(Copyright (C) 2013 American Chemical Society (ACS). All Rights Reserved.): 1117-1121.

Ibrahim, M. S., Shehatta, I. S. and Al-Nayeli, A. A. (2002). "Voltammetric studies of the interaction of lumazine with cyclodextrins and DNA." Journal of Pharmaceutical and Biomedical Analysis **28**(2): 217-225.

Jiao, S.-H., Xu, D.-S., Xu, L.-F. and Zhang, X.-G. (2012). "Recent progress in electrochemical synthesis and morphological control of metal oxide nanostructures." Wuli Huaxue Xuebao **28**: 2436-2446.

Johanson, U., Marandi, M., Tamm, T. and Tamm, J. (2005). "Comparative study of the behavior of anions in polypyrrole films." Electrochim. Acta **50**: 1523-1528.

Kamata, S., Murata, H., Kubo, Y. and Bhale, A. (1989). "Copper(II)-selective membrane electrodes based on ortho-xylylene bis(dithiocarbamates) as neutral carriers. " Analyst **114**(9): 1029-1031.

Kois, J., Bereznev, S., Gurevits, J. and Volobujeva, O. (2013). "Electrochemically synthesised CdSe nanofibers and pearl-chain nanostructures for photovoltaic applications." Material Letters **95**: 110-113.

Kumar, H., Rajan, S. and Shukla, A. K. (2012). "Development of lithium-ion batteries from micro-structured to nanostructured materials: its issues and challenges." Sci. Prog. **95**: 283-314.

Liu, Y.-C., Yang, K.-H. and Ger, M.-D. (2002). "Mechanism of underpotential deposition of metal on conducting polymers." Synth. Met. **126**: 337-345.

Long, Y.-Z., Li, M.-M., Gu, C., Wan, M., Duvail, J.-L., Liu, Z. and Fan, Z. (2011). "Recent advances in synthesis, physical properties and applications of conducting polymer nanotubes and nanofibers." Progress in Polymer Science **36**(10): 1415-1442.

Maksymiuk, K. (2006). "Chemical reactivity of polypyrrole and its relevance to polypyrrole based electrochemical sensors." Electroanalysis **18**(16): 1537-1551.

Mazur, M. (2008). "Polypyrrole Containers Grown on Oil Microdroplets: Encapsulation of Fluorescent Dyes." Langmuir **24**(18): 10414-10420.

Monk, P. M. S. (2001). Fundamentals of Electroanalytical Chemistry, John Wiley & Sons.

Nie, G., Zhang, Y., Guo, Q. and Zhang, S. (2009). "Label-free DNA detection based on a novel nanostructured conducting poly(indole-6-carboxylic acid) films." Sensors and Actuators B: Chemical **139**(2): 592-597.

Nugent, J. M., Santhanam, K. S. V., Rubio, A. and Ajayan, P. M. (2001). "Fast electron transfer kinetics on multiwalled carbon nanotube microbundle electrodes." Nano Letters **1**(2): 87-91.

O'Lehane, M. and O'Leary, B. (2012). Ireland's Environment 2012: An Assessment., Wexford: Environmental Protection Agency.

Oja, S. M., Wood, M. and Zhang, B. (2013). "Nanoscale Electrochemistry." Anal. Chem. **85**: 473-486.

Patake, V. D., Joshi, S. S., Lokhande, C. D. and Joo, O.-S. (2009). "Electrodeposited porous and amorphous copper oxide film for application in supercapacitor." Materials Chemistry and Physics **114**(1): 6-9.

Paunovic, M. and Schlesinger, M. (2006). Fundamentals of Electrochemical Deposition, Wiley.

Pospísil, L., Trsková, R., Fuoco, R. and Colombini, M. P. (1995). "Electrochemistry of s-triazine herbicides: Reduction of atrazine and terbutylazine in aqueous solutions." Journal of Electroanalytical Chemistry **395**(1-2): 189-193.

Roy, C. J., Leprince, L., Boulard, A. D., Landoulsi, J., Callegari, V., Jonas, A. M. and Demoustier-Champagne, S. (2011). "Electrosynthesis of pyrrole 3-carboxylic acid copolymer films and nanotubes with tunable degree of functionalization for biomedical applications." Electrochimica Acta **56**(10): 3641-3648.

Scharifker, B. and Hills, G. (1983). "Theoretical and experimental studies of multiple nucleation." Electrochimica Acta **28**(7): 879-889.

Singh, T., Pandya, D. K. and Singh, R. (2013). "Concentration dependent structural and optical properties of electrochemically grown ZnO thin films and nanostructures." Appl. Surf. Sci. **270**: 578-583.

Streeter, I., Wildgoose, G. G., Shao, L. and Compton, R. G. (2008). "Cyclic voltammetry on electrode surfaces covered with porous layers: An analysis of electron transfer kinetics at single-walled carbon nanotube modified electrodes." Sensors and Actuators B: Chemical **133**(2): 462-466.

Teixeira-Dias, B., Aleman, C., Estrany, F., Azambuja, D. S. and Armelin, E. (2011). "Microstructures of poly(N-methylpyrrole) and their interaction with morphine." Electrochimica Acta **56**: 5836-5843.

Tonkin, E. G., Valentine, H. L., Milatovic, D. M. and Valentine, M. W. (2004). "N,N-diethyldithiocarbamate produces copper accumulation, lipid peroxidation, and myelin injury in rat peripheral nerve." Toxicological Sciences **81**(1): 160-171.

Valle, E. M. M. D. (2004). "Cyclodextrins and their uses: a review." Process Biochemistry **39**(9): 1033-1046.

Veloso, A. J., Cheng, X. R. and Kerman, K. (2012). "Electrochemical biosensors for medical applications." Woodhead Publ. Ser. Biomater. **45**: 3-40.

Victoriano, L. I. (2000). "The reactivity of metal species towards thiuram sulfides: an alternative route to the syntheses of metal dithiocarbamates." Coordination Chemistry Reviews **196**: 383-398.

Wang, J., Xu, Y., Yan, F., Zhu, J. and Wang, J. (2011). "Template-free prepared micro/nanostructured polypyrrole with ultrafast charging/discharging rate and long cycle life." Journal of Power Sources **196**(4): 2373-2379.

Welch, C. M., Nekrassova, O. and Compton, R. G. (2005). "Reduction of hexavalent chromium at solid electrodes in acidic media: reaction mechanism and analytical applications." Talanta **65**(1): 74-80.

Xu, H., Zeng, L., Xing, S., Xian, Y. and Shi, G. (2008). "Ultrasensitive Voltammetric Detection of Trace Lead(II) and Cadmium(II) Using MWCNTs-Nafion/Bismuth Composite Electrodes." Electroanalysis **20**(24): 2655-2662.

Zang, J., Li, C. M., Bao, S.-J., Cui, X., Bao, Q. and Sun, C. Q. (2008). "Template-Free Electrochemical Synthesis of Superhydrophilic Polypyrrole Nanofiber Network." Macromolecules **41**(19): 7053-7057.

Acronyms and Annotations

AA - Atomic Absorption

Au – Gold

AuNPs - Gold nanoparticles

CD – Cyclodextrin

CP - Conducting Polymers

Cr – Chromium

Cu – Copper

CV - Cyclic voltammetry

D – Guest molecule

DDC – Diethyl-dithiocarbamate

DMF - Dimethylformamide

DSF – Disulfide disulfiram

EDX - Energy dispersive X-ray

Ep - Peak potentials

EPA - Environmental Protection Agency

EPR - Electron paramagnetic resonance

EtOH - Ethanol

EU – European Union

FE-SEM - Field emission scanning electron microscopy

FTIR - Fourier transformation infra-red spectroscopy

GC – Glassy carbon

GCE – Glassy carbon electrode

HOPG – Highly ordered pyrolytic graphite

Ip – Peak current

IR – Infra-red

KCl – Potassium chloride

LOD – Limit of detection

MWCNTs - Multi-walled carbon nanotubes

N_2 - Nitrogen

NMR - Nuclear magnetic resonance

NO_3^- - Nitrate

NSAID - Non-steroidal anti-inflammatory drug

PBS - Phosphate buffer solution

PPy - Polypyrrole

PPyEtCN - Poly[N-(2-cyanoethyl)pyrrole]

PPy-sβCD - polypyrrole doped with sulfonated β-cyclodextrin

Pt – Platinum

Py - Pyrrole

PyEtCN - [N-(2-cyanoethyl)pyrrole]

SDS – Sodium dodecylsulfate

SEM - Scanning electron microscopy

sβCD - Sulfonated β-cyclodextrin

TBAB – Tetra-n-butylammonium bromide

TEM - Transition electron microscopy

UV-vis - UV-vis spectroscopy

WE - Working electrode

Appendix

Conference Presentations and Publications

Peer-reviewed Journals

Conor P. McCarthy, Niall B. McGuinness, Patrick B. Carolan, Catherine M. Fox, Bernadette E. Alcock-Earley, Carmel B. Breslin, A. Denise Rooney. (2013). Electrochemical Deposition of Hollow N-substituted Polypyrrole Microtubes from an Acoustic Emulsion, *Macromolecules*, **46 (3)**, 1008–1016.

Conor P. McCarthy, Niall B. McGuinness, Carmel B. Breslin, Bernadette Alcock-Earley, A. Denise Rooney. (2012). Facile Template-Free Electrochemical Preparation of Poly[N-(2-cyanoethyl)pyrrole] Nanowires *Electrochemistry Communications* **20**, 79–82.

Lynn M. Garry, Bernadette E. Alcock and Carmel B. Breslin. (2013). Investigation of the Electrochemical Behaviour of MWCNTs in the detection of Cr (VI) *ECS Transactions*, **41 (27)** 1-7 (2012).

Conference Oral Presentations

Lynn Garry, Bernadette Alcock-Earley, Carmel Breslin. (2011). Electrochemical characterisation and application of carbon-based nanomaterials. 220th meeting of the Electrochemical Society, Boston, MA, USA. October 9th - 14th.

Conor McCarthy, Bernadette Alcock-Earley, Carmel Breslin. (2011). Formation of a polypyrrole/copper nano-composite for nitrate detection. 220th meeting of the Electrochemical Society, Boston, MA, USA. October 9th - 14th.

Conor McCarthy, Bernadette Alcock-Earley, Carmel Breslin. (2011). Development of a nitrate sensor using nanomaterials. ENVIRON 2011, UCC Cork, April 6th - 8th.

Lynn Garry, Bernadette Alcock-Earley, Carmel Breslin. (2011). Electrochemical Characterisation and Application of Carbon-Based Materials. Conference on Analytical Sciences Ireland 2011 - 6th CASi, The Helix, DCU, February 21st – 22nd.

Bernadette Alcock-Earley. (2010). The role of electroanalytical chemistry in water analysis. DRHEA Environmental Chemistry Masterclass, NUI Maynooth, June 24th - 25th.

Bernadette Alcock-Earley. (2010). Using nanotechnology to develop better pollution sensors EPA National Research AGM, Croke Park Conference Centre, June 23rd.

Lynn Garry, Bernadette Alcock-Earley and Carmel Breslin. (2010). Using carbon nanotubes to detect Cr(VI) in aqueous media, ENVIRON 2010, Limerick Institute of Technology, February 17-19th.

Bernadette E. Alcock. (2008). Removal of Organic Contaminants using Macrocyclic Cages Encapsulated in Conducting Polymer Matrices. 214th Meeting of the Electrochemical Society, Honolulu, Hawaii, USA, 12th-17th October.

Conference Posters

Conor McCarthy, Bernadette Alcock-Earley, Carmel Breslin. (2010). Characterisation of a polypyrrole/copper nano-composite for nitrate detection. The 61st Annual Meeting of the International Society of Electrochemistry, September 26th - October 1st 2010, Nice, France.

Conor McCarthy, Bernadette Alcock-Earley, Carmel Breslin. (2010). Reduction of nitrate at polypyrrole nanowires modified with copper nanoparticles. 62nd Irish Universities Chemistry Research Colloquium, Queens' University Belfast, July 1st – 2nd.

Conor McCarthy, Bernadette Alcock-Earley, Carmel Breslin. (2009). Reduction of nitrate at polypyrrole nanowires modified with copper nanoparticles. EPA postgraduate and postdoctoral research conference, November 2009.

Lynn Garry, Bernadette E. Alcock and Carmel B. Breslin. (2009). Electrochemical Detection of Chromium VI Using a Sensor Modified with Carbon Nanotubes. 216th meeting of the Electrochemical Society in Vienna, Austria, October 4th – 9th.

Conor P. McCarthy, Bernadette E. Alcock and Carmel B. Breslin. (2009). 216th meeting of the Electrochemical Society in Vienna, Austria, October 4th – 9th.

Lynn Garry, Bernadette E. Alcock and Carmel B. Breslin. (2009). Detection of Chromium(VI) using a Polypyrrole Films Modified with Carbon-Nanotubes. 12th EuCheMS International Conference on Chemistry and the Environment, ICCE2009, Stockholm, Sweden, June 14th – 17th.

Conor P. McCarthy, Bernadette E. Alcock and Carmel B. Breslin. (2009). Sensing of nitrates at polypyrrole nanowires modified with copper nanoparticles. 12th EuCheMS International Conference on Chemistry and the Environment, ICCE2009, Stockholm, Sweden, June 14th – 17th.

Lynn Garry and Bernadette E. Alcock. (2009). Detection of Heavy Metals using a Novel Electrochemical Based Sensor. The 19th Annual Irish Environmental Researchers Colloquium, WIT, 18th-20th February.

Conor P. McCarthy and Bernadette E. Alcock. (2009). Sensing of nitrates at nanowires modified with metal nanoparticles. The 19th Annual Irish Environmental Researchers Colloquium, WIT, 18th-20th February.

EPA Research Report 144

The Protection of Water Resources: Developing Novel Sensor Materials

Authors: Bernadette Alcock-Earley, Lynn Garry, Conor McCarthy, Carmel Breslin

epaResearch
Climate - Water - Sustainability
Identifying pressures • Informing policy • Developing solutions

One of the more pressing challenges in the 21st Century is the provision of an adequate clean water supply that is free from pollutants and suitable for a diversity of uses. Although the quality of water in Ireland is generally good, the protection of water resources in Ireland is becoming increasingly important and will be a major challenge in the next few years and into the future, as an ever-increasing population will need a continuous supply of clean drinking water. The protection of the quality of water resources and the sustainability of these resources are key environmental goals in the Environmental Protection Agency 2020 Vision (EPA, 2000) strategy document, and are also in line with the Flagship initiative of the Europe Union Commission (European Commission, 2011) strategy for a resource-efficient Europe. The research described herein sets out to develop polymer-coated membrane-based technologies that could be used to detect organic contaminants, nitrates or heavy metals, namely chromium and copper, in aqueous systems. The membranes were modified so as to investigate their potential in the required sensing capacity.

Identifying Pressures

Although the quality of water in Ireland is generally good, the protection of water resources in Ireland is becoming increasingly important and will be a major challenge in the next few years and into the future, as an ever-increasing population will need a continuous supply of clean drinking water.

Developing Solutions

The three projects involved in this research were concerned with the formation of novel materials that could be used in the detection of nitrates, heavy metals and organic contaminants in an aqueous environment. These novel materials consisted of modified conducting polymer films, with the modifications were carefully selected to ensure that the final materials will have the required sensing capacity. This research has indicated some potential for the development of new materials for environmental sensors. There is a need for further research and development to optimise the potential use of these sensors in the monitoring of contaminants in the aqueous environment. Support for research into developing innovative technologies that deal with current water challenges is important as there are significant economic opportunities for Ireland in a growing world market in this sector.

Comhshaol, Pobal agus Rialtas Áitiúil
Environment, Community and Local Government

EPA Research: McCumiskey House, Richiew, Clonskeagh, Dublin 14.
Phone: 01 268 0100
Twitter: @EPAResearchNews
Email: research@epa.ie

www.epa.ie
EPA Research Webpages
www.epa.ie/researchandeducation/research/